The Role of Microtubule-Associated Proteins during Microtubule Nucleation and Organization

Brianna Rose King

A dissertation

submitted in partial fulfillment of the

requirements for the degree of

Doctor of Philosophy

University of Washington

2020

Reading Committee:

Trisha N. Davis, Chair

Justin M. Kollman

Linda Wordeman

Program Authorized to Offer Degree:

Biochemistry

University of Washington

Abstract

The Role of Microtubule-Associated Proteins during Microtubule Nucleation and Organization

Brianna Rose King

Chair of the Supervisory Committee:
Trisha N. Davis, Professor and Chair
Department of Biochemistry

Successful mitotic division is fundamental to life. During mitosis, the cytoskeletal network is reorganized to form the bipolar spindle: microtubules extend from microtubule-organizing centers to attach to and separate chromosomes. The mitotic spindle is formed by 1) transport of existing microtubules and 2) targeted nucleation of new microtubules. These processes are governed by the microtubule-organizing center and proteins associated with the microtubule. Here I investigate how the MTOCs and the microtubule associated proteins work together to nucleate microtubules. Using a turbidity assay, I find that XMAP215 is a classically defined microtubule nucleator, as it reduces the nucleation lag seen in bulk tubulin assembly. I further characterize the role of XMAP215 in nucleation, finding its ability to nucleate correlates with its ability to elongate existing microtubules and this is true in both the presence and absence of γ-tubulin. Then using a novel tool, I define the role of three microtubule associated proteins (Stu2, Bim1 and Bik1) and two motors (Kip3 and Vik1) during assembly of microtubule arrays from an ectopic microtubule nucleation site expressed *in vivo*. I found that Stu2 and Bim1 are

required for microtubule nucleation from the ectopic site, whereas Bik1, Kip3 and Vik1 are required for organization of the microtubule arrays.

TABLE OF CONTENTS

LIST OF FIGURES

LIST OF TABLES

ACKNOWLEDGEMENTS

Getting here, to this side of graduate school, was the hardest thing I've ever done, and in the words of Matt and Kim, "I know I didn't get here on my own."

Part of getting here was finding the right scientific terrain to explore. I found that in my studies of mitosis with Trisha Davis and her lab. Thank you to Trisha for transforming potential into productivity. Her lab is well known for its enthusiastic and lengthy constructive criticism; but I never felt stronger than after my weaknesses were really stretched out and examined during those sessions. Thank you to Tamira, Kim, King, Gabby, Luke, James, Emily, Mike, Dan, Alex, and to my other mentor, Eric Muller, and to my best lab girlfriends, Grace and Evie.

I was also lucky enough to find some guides along the way that were outside of the lab. Thank you to all the others who "contributed to meaningful discussions:" Chip Asbury, David Agard, Michelle Moritz, Haein Kim, Justin Kollman, and Linda Wordeman.

Lastly, I will say that I came into grad school pretty well-prepared to travel. Thank you to Judi Davis for being a lifelong advocate, and to Dave Gillespie for sparking the light of research in my eyes. Thank you to my sisters, my cousin, and my aunt for grounding me in reality when grad school seemed so abstract. Thank you to my grandparents, Tom and Barbara, for being the solid ground under my microscope. And thank you finally to my parents, Brian and Cathy, for giving me these genes, for reading to me (constantly), for asking me questions, for letting me win, for letting me lose, and for making me feel I was important.

DEDICATION

There was never a question of whom I would dedicate this work to-

To my dad. His name was Brian Curtis Mock. He died in police custody three weeks after I moved cross-country for graduate school.

I have learned so much about addiction, and mental health, and our criminal justice system, and I only want to learn more forever.

The person I am now doesn't seem to resemble who I was before graduate school. I am not sure if it's because complex grief changes you, or because graduate school changes you, or because anyone in their twenties just changes. But to you, Dad, I think you would have liked to meet me now.

Chapter 1. INTRODUCTION

1.1 MITOSIS

As an undergraduate student majoring in biology, the first thing I learned were the key characteristics scientists use to define life. In order to be alive, an organism must be organized into cells, use energy, maintain homeostasis, respond to stimuli, grow, reproduce, and evolve. What do the latter three, growth, reproduction, and evolution, have in common? They each depend on successful cell division.

The macromolecular mechanisms of cell division have been remarkably well-characterized since the recorded observations of Walther Flemming in the late 19th century [1]. Flemming, renowned for his scientific rigor and his striking ability to visualize cellular anatomy, coined the term “mitosis,” from the Greek word for thread. Our terms for the events of mitosis have not changed much; DNA condenses intro threadlike structures called chromosomes, chromosomes attach to smaller threads called microtubules to align at the metaphase plate, poles and chromosome sets separate using the mitotic spindle (of many threads), and the cellular membrane divides to give two identical daughter cells.

While understanding cell division at a basic level is thrilling, the translational potential of mitotic research is equally so. Errors in mitosis early in human development are often lethal, with all but a handful of chromosomal segregation errors causing fetal death [2]. Later in development, healthy cells generally respond to mitotic errors by inhibiting cellular proliferation via mechanisms such as cell cycle arrest [3], [4] and apoptosis [5]–[8]. However, some cells do not respond to mitotic errors with inhibition,

but rather are able to grow and proliferate despite genetic aberrations. The resulting aneuploidy of these cells is associated with cancer [9].[1]

Understanding the mechanisms of the mitotic spindle and mitotic regulators is therefore critical to human health. The mitotic spindle is composed of chromosomes, kinetochores, microtubules (MTs), MT organizing centers (MTOCs), and MT-associated proteins (MAPs). Here I focus on the components of the mitotic spindle that I investigated during my doctoral work: MTOCs, MTs, and MAPs.

1.2 MICROTUBULE-ORGANIZING CENTERS

I will begin my discussion at the "beginning" of the mitotic spindle: the MTOC. Although MTs can form at places other than the MTOC, the MTOC serves as the main hub for MT nucleation throughout the cell cycle. In higher eukaryotes, the main MTOCs of the cell are known as centrosomes, while in fission and budding yeast this organelle is known as the spindle pole body (SPB). SPBs are more structurally organized than the relatively amorphous centrosome, but notably, the proteins that make up the SPB are functionally conserved across eukaryotes [10]–[12]. For my thesis work, *Saccharomyces cerevisiae* provided an ideal model organism in which to study MT nucleation and organization, because of its relatively simple mitotic spindle and genetic tractability.

[1] Aneuploidy seems to be more tolerated in brain tissue of human [185] and mice [186]. The authors describe aneuploidy as "normal."

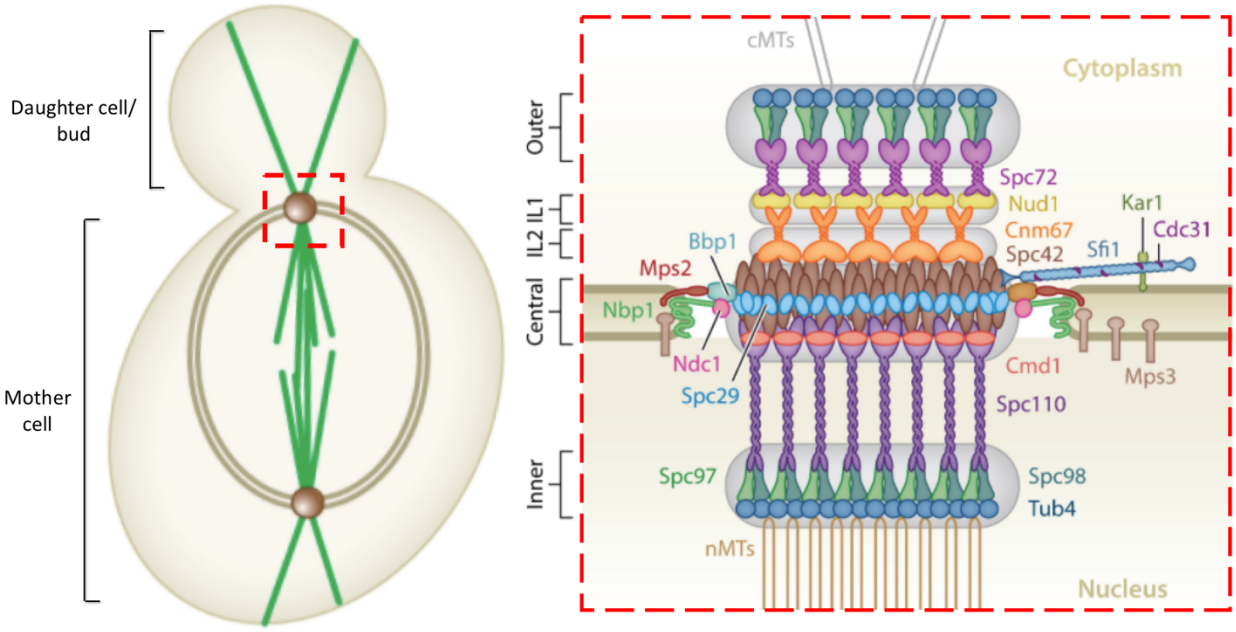

Figure 1.1. Organization of the budding yeast SPB.

(Left) Depiction of a S. cerevisiae cell, following SPB duplication, bud formation, and initiation of the mitotic spindle. MTs (green strands), SPBs (brown spheres), and the nuclear envelope (tan rings). Not shown are chromosomes, kinetochores, and microtubule-associated proteins. (Right) Inset of left, showing SPB proteins are organized into plaques. Abbreviations: cMTs, cytoplasmic microtubules; IL1, intermediate layer 1; IL2, intermediate layer 2; nMTs, nuclear microtubules. Figure used with permission from Annual Review of Genetics [13].

Spindle pole body structure

Composed of 18 proteins, the budding yeast SPB is embedded in the nuclear envelope and organized into plaques (Figure 1.1). The central plaque interacts with the nuclear envelope to anchor the SPB, while the inner and outer plaques are composed of γ-tubulin complexes that nucleate MTs. On the cytoplasmic face of the SPB, intermediate layers 1 (IL1) and 2 (IL2) bridge the central plaque to the outer plaque. On the nuclear side of the SPB, Spc110 anchors the γ-tubulin complex to the central plaque.

Spc110 and the γ-tubulin complex

Spc110 is a coiled coil protein that bridges the inner plaque and the central plaque via distinct domains: the N-terminal domain of Spc110 interacts with Spc97 and Spc98 of the γ-tubulin complex, and the C-terminal domain interacts with SPB core proteins Spc29, Spc42, and calmodulin [14]–[18]. Spc110 promotes oligomerization of γ-tubulin complexes, which in turn promotes MT nucleation [19], [20]. Spc110 is also phosphorylated by mitotic kinases [21]–[26]. For these reasons, Spc110 is thought to participate in the regulation of MT nucleation.

On the nuclear side of the SPB, Spc110 anchors the γ-tubulin complex, which is the generally accepted MT nucleator of the cell. In budding yeast, the γ-tubulin small complex consists of two copies of γ-tubulin and the proteins Spc97 and Spc98 (GCP2 and GCP3 in other eukaryotes) [27], [28]; the small complex oligomerizes to form a ring known as the γ-tubulin ring complex (γ-TuRC) [19], [28], [29]. The full γ-TuRC presents a ring of 13 γ-tubulins to match the symmetry of the 13-protofilament MT.

The γ-TuRC is thought to function as a template for MT nucleation. First, γ-tubulin is found at MTOCs and is required for spindle assembly across *A. nidulans*, *S. pombe*, *S. cerevisiae*, *D. melanogaster*, *X. laevis*, and *H. sapiens* [30]–[37]. Second, γ-tubulin is similar in structure and sequence to the α- and β-tubulin proteins that make up the MT [30]. Furthermore, the γ-TuRC was shown to localize specifically to the MT minus end, rather than associating with the MT as a protofilament, even early during MT formation [38]–[40].

In theory, the γ-TuRC provides an interface onto which αβ-tubulin dimers assemble longitudinally, which may help to overcome the kinetic barrier associated with MT nucleation by promoting early lateral αβ-tubulin interactions. However, purified γ-TuRCs do not nucleate well in vitro [19], [41]–[43], so the question of whether the γ-TuRC provides an accurate template geometrically for the early assembly of a MT is still open. While the γ-TuRC matches the 13-fold symmetry of the MT, the helical pitch of the γ-TuRC is not a perfect match for that of the 12.2 nm pitch of the MT. Cryo-EM reconstructions of γ-TuSC helical filaments[2] from budding yeast showed that the pitch was larger, around 14.7 nm, and that engineering disulfide bonds between γ-tubulin proteins reduces the pitch of the γ-TuRC to match the MT perfectly [29]. This has provided evidence that the γ-TuRC requires a conformational change in order to be "activated" for nucleation. The mechanisms of γ-TuRC activation may vary across organisms and may include the association of other factors. In fission yeast and metazoans, the γ-TuRC includes other core proteins outside of γ-tubulin and GCP2 and GCP3. These include the γ-tubulin related proteins (known as GCP4-6), and the conserved proteins MZT1, MZT2, and actin [42], [44]–[51]. MZT1 and MZT2 are critical for γ-TuRC localization, while actin is suspected to play a structural role. Importantly, even purified γ-TuRCs containing these additional core proteins do not perfectly match the helical pitch of the MT, with recent cryo-EM reconstructions of human and *X. laevis* γ-TuRCs having a pitch of around 11 nm [42], [49], [51].

[2] Efforts to purify γ-TuRC from budding yeast have failed; however γ-tubulin small complexes (γ-TuSCs) are thought to exist as rings in budding yeast. The filament formation of the γ-TuSCs provides evidence for this.

In my studies of MT nucleation, I have heavily considered the role of and interactions with γ-tubulin and/or Spc110. For my studies *in vitro*, I examined the interplay between a microtubule-associated protein and γ-tubulin; for my studies *in vivo*, I examined the interplay between microtubule-associated proteins, γ-tubulin complexes, and the N-terminal portion of Spc110 that binds the γ-tubulin complex.

1.3 MICROTUBULES OF THE MITOTIC SPINDLE

Throughout the cell cycle, MTs are primarily anchored at the MTOC via the MT minus end. During interphase, MTs radiate from the MTOC, dispersing their distal plus ends throughout the cytoplasm. As cells transition into mitosis, this disperse network is reorganized into the mitotic spindle.

Roles of microtubules during mitosis

MTs of the mitotic spindle serve three different purposes: attach to chromosomes, fortify the spindle, and position the MTOCs. Kinetochore MTs attach to chromosomes via the kinetochore protein complex. Interpolar MTs help to fortify the spindle by extending toward the opposite MTOC and overlapping in the spindle midzone. Finally, astral MTs position the MTOC by extending toward the cell cortex to interact with proteins there [52].

Microtubule dynamic instability

MTs are complex macromolecules: longitudinally associated αβ-tubulin dimers are organized into protofilaments, and 13 protofilaments associate laterally to form a

hollow tube.[3] The end that presents α-tubulin is known as the minus end. The minus end of the MT is the less dynamic end, and often stably interacts with γ-tubulin. The end that presents β-tubulin is known as the plus end. Plus ends form dynamic interactions with many proteins, including those of the kinetochore and those associated with cellular cortex interactions. Plus ends undergo rounds of polymerization and depolymerization, and catastrophe and rescue, in a process characterized as dynamic instability [53] (Figure 1.2). Dynamic instability is governed by GTP hydrolysis: αβ-tubulin dimers that are incorporated into a growing MT are bound to GTP, and over time the GTP is spontaneously hydrolyzed [53], [54]. When GTP hydrolysis "catches up" to the distal plus end, MTs rapidly depolymerize, or catastrophe.

[3] Microtubules can form in vitro with 11-16 protofilaments [187].

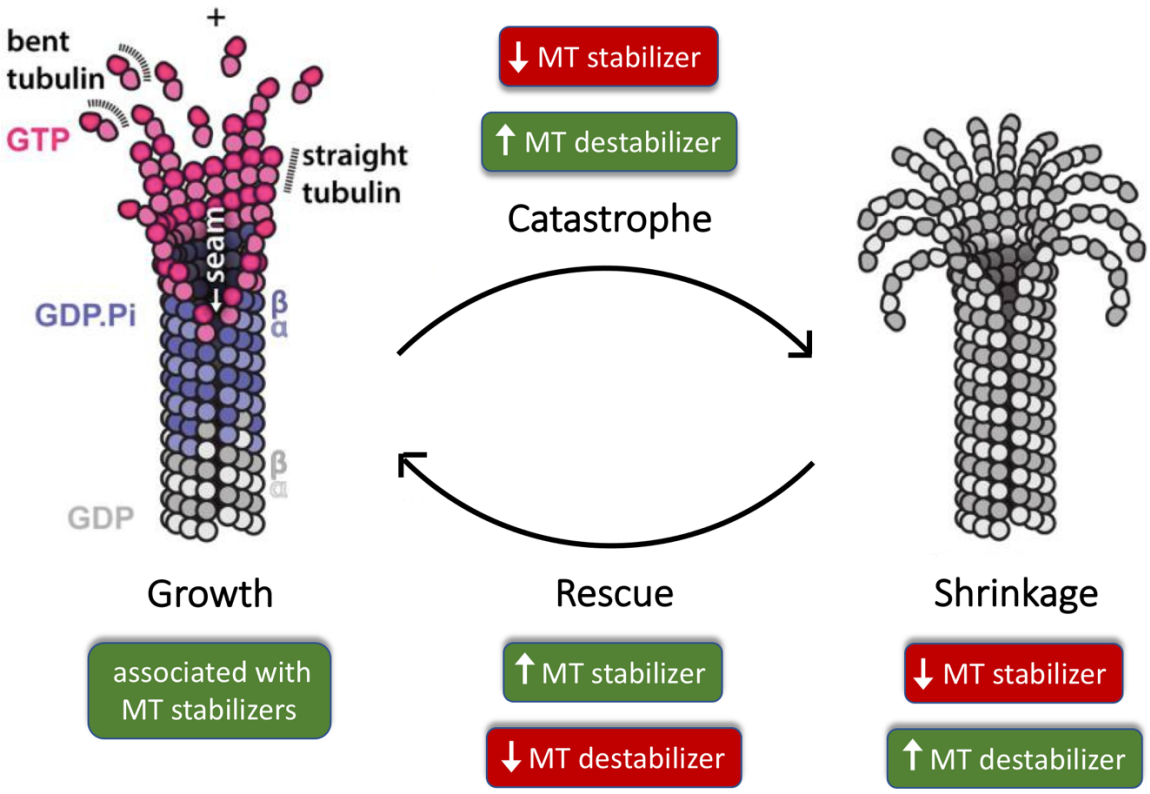

Figure 1.2. Dynamic instability of MTs.

MTs undergo periods of growth and shrinkage, with frequent switching between the two states. GTP-tubulin is incorporated into a growing MT and over time the GTP is hydrolyzed, resulting in GDP-tubulin. As GTP hydrolysis outpaces the rate of growth of the MT, αβ-tubulin dimers at the plus end hydrolyze their GTP. This results in a conformational change of the αβ-tubulin dimers that induces strain on the MT lattice and promotes MT depolymerization. Factors that stabilize MTs inhibit shrinkage rate and catastrophe, promote rescue, and are associated with promotion of growth rate. Images of polymerizing and depolymerizing MTs used in this figure are used with permission from Essays in Biochemistry [55].

Microtubule nucleation

While the dynamic instability of MTs has been well-characterized, MT nucleation from soluble tubulin dimers is significantly less well understood. MT nucleation must overcome unique kinetic barriers, as αβ-tubulin dimers must not only oligomerize, but must also form the hollow tube of the MT. Models of MT nucleation attempt to parameterize these kinetic barriers [56]–[59].

While the γ-TuRC is expected to help overcome some kinetic barriers, it is thought that additional cellular factors are required for MT nucleation. This is supported by the fact that purified MTOCs and γ-TuRCs do not nucleate well *in vitro* [19], [41]–[43] unless supplemented with cellular extract [60], [61]. One of the emerging hypotheses is that MT-associated proteins (MAPs) regulate MT nucleation.

1.4 MOTORS AND OTHER MICROTUBULE-ASSOCIATED PROTEINS

The formation of the mitotic spindle relies on the large-scale action of MT-associated proteins (MAPs), which include motors and other proteins that bind the MT lattice. The effect of these proteins on MT dynamic instability and on spindle assembly have been well-characterized. Importantly the function of MAPs is based on their correct localization, which is made possible through the inherent polarity of the MT polymer composed of heterodimers.

Localization of MAPs

All MAPs bind the MT lattice, and most localize to/move toward a specific end of the MT. Motors largely accomplish end specificity by utilizing ATP to “walk” along the MT, with the notable exception of the kinesin-13 MCAK, which exhibits lateral diffusion [62]. Nonmotor MAPs accomplish end specificity through a variety of ways: lateral diffusion, as seen for the chTOG/XMAP215 family of polymerases [63]; preferential binding to plus-end bound GTP-tubulin as seen for the end-binding (EB) family [64], [65]; or interactions with other end-specific proteins, specifically with EB proteins [66]–[69].

Effects on dynamic instability

MAPs largely function to regulate the mechanisms of dynamic instability, such as polymerization, depolymerization, catastrophe, and rescue. Using these measures, the activity of MAPs can be characterized as either “stabilizing” or “destabilizing.” Stabilizing properties include inhibition of shrinkage rate and catastrophe, promotion of rescue, and potentially promotion of polymerization rate (Figure 1.2).

The effect of a MAP on MT dynamic instability may be location-dependent, and therefore can be categorized as stabilizing or destabilizing only in specific cellular contexts. The kinesin-8 family of motors is known to destabilize/stabilize MTs in a length-dependent manner: they promote catastrophe of long MTs yet promote rescue of short MTs [70]–[77]. This is thought to be due to the accumulation of plus-end directed kinesin-8 motors at plus-ends [72]–[74], [76]–[80], and to be necessary for their differential function at different cellular locations [73], [77]. Local rescue activity is seen for other MAPs with the cytoplasmic linker protein (CLIP) family functioning as cytosolic rescue factors [68], [81] and the CLIP-associated protein (CLASP) family functioning as cortical rescue factors [68].

The chTOG/XMAP215 family of MT polymerases eludes easy classification as a MT stabilizer or MT destabilizer. The XMAP215 family promotes MT growth rate ~10-fold [63], [82]–[84], which is associated with MT stabilization. However, as catalysts, XMAP215 family members can promote either growth, when the concentration of free tubulin is sufficiently high, or shrinkage, when the concentration of free tubulin is sufficiently low [85], [86]. Further, factors that promote rapid growth of MTs can give rise to catastrophe as MTs reach the cellular cortex more quickly.

1.5 STUDYING THE EFFECT OF MICROTUBULE-ASSOCIATED PROTEINS DURING MICROTUBULE NUCLEATION AND ORGANIZATION

The γ-TuRC is a MT nucleator, but must function in concert in other factors, which may include MAPs. Which MAPs assist in nucleation, and the role of those MAPs, is controversial. For my thesis, I used techniques that specifically measure the effect of MAPs during the early stages of MT nucleation. Here I first use a classical light scattering assay to classify XMAP215 as a bona fide MT nucleator, as it reduces the nucleation lag associated with tubulin assembly. Then by measuring the combined effect of XMAP215 and γ-tubulin in the light scattering assay, I find their relationship to be functionally additive. Next I use a novel tool to measure the effect of five MAPs on *de novo* MT formation *in vivo*. When a Spc110 truncation mutant (a.a.1-220) is expressed *in vivo*, it is able to recruit the γ-tubulin complex and forms MTs distinctly from the SPB. This tool allowed me to 1) probe the role of Stu2 (the chTOG/XMAP215 homolog in budding yeast) in MT nucleation using principles learned from XMAP215, 2) define a role for Bim1, of the EB family of proteins, in MT nucleation, and 3) report roles for Bik1, Kip3, and Vik1 in MT organization.

Chapter 2. XMAP215 AND γ-TUBULIN ADDITIVELY PROMOTE MICROTUBULE NUCLEATION IN PURIFIED SOLUTIONS[4]

2.1 INTRODUCTION

Spontaneous nucleation of a new microtubule from nanometer-sized soluble αβ-tubulin dimers is an event that is currently impossible to observe directly. Tubulin dimers must associate longitudinally and laterally in order to form the final product: a hollow tube of side-by-side protofilaments. Models of the spontaneous microtubule nucleation pathway have disagreed on the number of rate-determining steps and key intermediates in the nucleation pathway [56]–[58].

More recently, studies of nucleation have centered on the γ-tubulin ring complex (γ-TuRC), which is essential for microtubule formation across organisms [30]–[33], [36], [37]. The γ-TuRC stably binds the microtubule minus end and is thought to act as a template onto which αβ-tubulin dimers associate [38], [39], [87], theoretically promoting lateral interactions between adjacent αβ -tubulin dimers [88]. However, increasingly higher resolution structures of purified γ-TuRC show that the template is not perfect—the 13-member γ-tubulin ring presented by the complex does not perfectly match the geometry of the microtubule [29], [42], [49]. Further, the fraction of purified γ-TuRC that nucleates *in vitro* is consistently low [19], [41]–[43]. It is hypothesized that, in order to

[4] This section is adapted from the manuscript in submission (King, et al., 2020).

nucleate well, γ-TuRC must be activated *in vivo* through interactions with other proteins [60], [61], [89].

There is a rapidly growing body of evidence that at least one of the crucial co-factors for the γ-TuRC is the XMAP215 family of microtubule polymerases. The XMAP215 family promotes microtubule growth from various templates, including the γ-TuRC, isolated centrosomes, and GMPCPP-stabilized seeds [42], [43], [90]–[93], and it also promotes microtubule nucleation in reactions without any template [90], [94]–[97]. Across these studies, the role of XMAP215 in nucleation was generally thought to be due to its polymerase activity. Recently, however, it was reported that XMAP215 and the γ-TuRC promote microtubule nucleation in a manner that is greater than the sum of their individual effects [42], [92], [93]. The mechanism underlying this reported synergy is unknown, although Thawani, et al. [92] hypothesized it is due to a direct binding interaction between the unstructured C-terminal tail of XMAP215 and γ-tubulin.

Here, we sought to characterize the mode of action of XMAP215 in a simplified system, using recombinantly expressed and purified protein in the classical turbidity assay. We first show that γ-tubulin alone forms laterally associated arrays that reduce the nucleation lag associated with αβ-tubulin assembly. We also confirm that XMAP215 alone reduces the nucleation lag and probe its mechanism of action using domain analysis, finding that nucleation activity strongly correlates with polymerase activity. We then explore the nucleation activity of the γ-tubulin arrays together with XMAP215. Across a range of concentrations of XMAP215 and across XMAP215 deletion constructs, we find additive action with γ-tubulin. These results provide evidence for two

distinct rate-limiting processes during microtubule nucleation that are independently promoted by XMAP215 and γ-tubulin.

2.2 Results and Discussion

γ-tubulin and XMAP215 each promote microtubule nucleation in the classical turbidity assay

Nucleation of a new microtubule is impossible to observe directly. Fluorescence microscopy can visualize dynamics of individual microtubule formation events, but it is complicated by the requirement of fluorophore-labeled αβ-tubulin heterodimers. In order for αβ-tubulin to assemble, only a small fraction of αβ-tubulin may carry a fluorophore; this not only makes early nucleation intermediates impossible to visualize, but it also indicates that unlabeled and labeled αβ-tubulin assemble differently.

Light scattering, on the other hand, uses unlabeled αβ-tubulin heterodimers to monitor formation of small nucleation intermediates. This assay, performed in bulk, is classically used in the study of polymerization dynamics [98], [99]. The initial delay or lag between the start of the reaction and when the turbidity reaches one-tenth of its maximum provides a sensitive measure of polymer nucleation efficiency [56], [57].

To establish the light scattering assay in our hands, we first tested an accepted αβ-tubulin nucleator, γ-tubulin. At higher concentrations (~250 nM and above), purified γ-tubulin oligomerizes, forming laterally associated arrays with plus-ends of γ-tubulin

oriented outward, as revealed by negative stain electron microscopy (Figure 2.1), and as seen previously in γ-tubulin crystals [88].

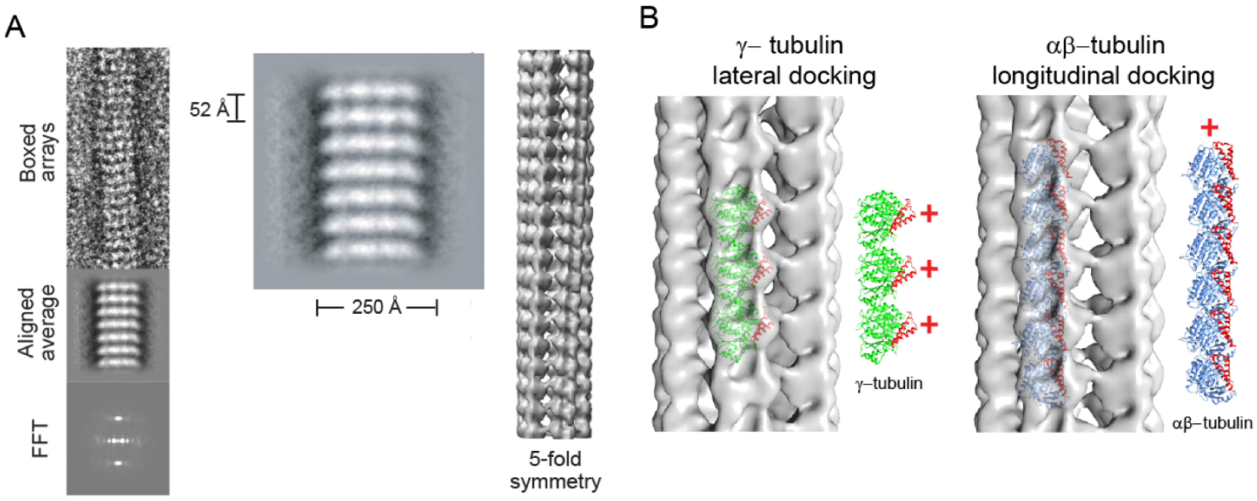

Figure 2.1. Negative-stain electron microscopy reveals that γ-tubulin forms arrays that are distinct from microtubules.
(A) γ-tubulin arrays were boxed and averaged for helical reconstruction. 2D averages of the arrays showed a ~52 Å repeat unit and ~250 Å width. Helical reconstruction reveals 5-fold symmetry in the array, with a hollow center. (B) Left: Docking of the human γ-tubulin crystal structure (1Z5W) into the 3D reconstruction revealed that γ-tubulins are laterally associated along the long axis of the arrays. The lateral packing of γ-tubulins is similar to that observed in crystals [88]. γ-Tubulins in the arrays are oriented with their plus-ends outward (red +). Helices 3 and 4 are red in the models to illustrate the orientation of the plus-end of the γ- or αβ-tubulins. Right: Docking of αβ-tubulins (1JFF) as a proxy for a hypothetical longitudinal assembly of αβ-tubulins. The periodicity of the longitudinal model does not match that of the EM map.

We first confirmed that these arrays alone do not scatter light and that they promoted formation of microtubules rather than other non-canonical tubulin polymers (Figure 2.2). We monitored the effect of γ-tubulin arrays on αβ-tubulin assembly, finding that they strongly decreased the nucleation lag compared to αβ-tubulin alone; in contrast, lower concentrations of γ-tubulin that failed to form laterally associated arrays only weakly promoted nucleation (Figure 2.3).

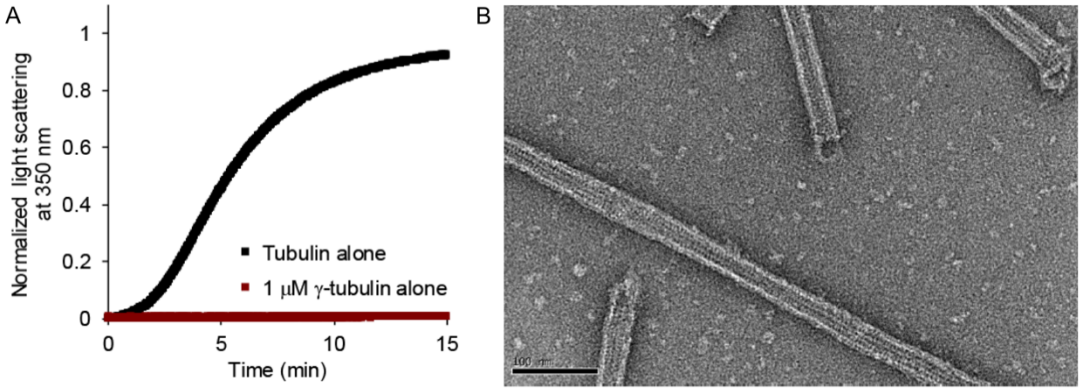

Figure 2.2. γ-tubulin arrays promote microtubule formation in a light scattering assay.

(A) Turbidity assay at 12 μM free αβ-tubulin or 1 μM γ-tubulin, showing that γ-tubulin arrays alone do not scatter light under our experimental conditions. (B) Negative-stain electron microscopy image of a sample from a light scattering assay using 1 μM γ-tubulin and 5 μM αβ-tubulin, showing that γ-tubulin arrays support the formation of microtubules, as opposed to other types of tubulin polymers.

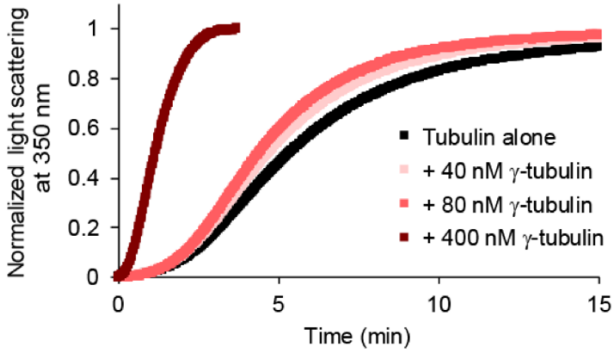

Figure 2.3. γ-tubulin arrays promote microtubule nucleation, while free γ-tubulin does not.

Characterization of 40, 80, or 400 nM γ-tubulin in the turbidity assay with 12 μM αβ-tubulin.

To quantify the nucleation activity of γ-tubulin for our comparisons with XMAP215, we used 300 nM γ-tubulin, a sufficiently high concentration for array formation. At this concentration, the γ-tubulin arrays decreased the time to reach 10% polymer formation, hereafter known as the nucleation lag, by approximately 50% (Figure 2.4A).

We then tested the nucleation activity of XMAP215, finding significant effects. The nucleation lag decreased monotonically with increasing concentrations of XMAP215, with a decrease of 75% at the highest concentration (60 nM, Figure 2.4B). This provided independent confirmation that XMAP215 is a nucleator, with similar potency to γ-tubulin arrays.

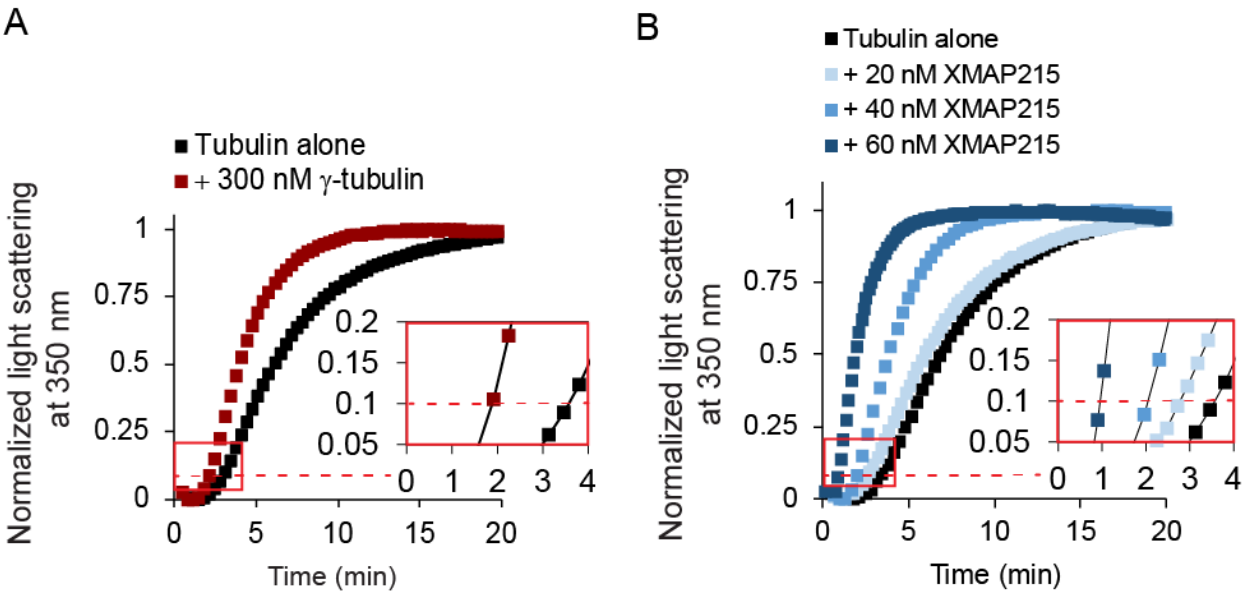

Figure 2.4. Laterally associated γ-tubulin arrays and XMAP215 are classically defined nucleators.

(A) Representative turbidity assay at 15 μM free αβ-tubulin, with γ-tubulin added at 300 nM. Red dashed line represents 10% of the maximum light scattering. Inset shows same data from red box plotted on larger scale for clarity. (B) Representative tubulin assembly assay for 20 nM, 40 nM, or 60 nM XMAP215 with 15 μM free tubulin. XMAP215 promotes spontaneous tubulin assembly in a concentration-dependent manner. Red dashed line represents 10% of the normalized maximum light scattering. Inset shows same data from red box plotted on larger scale for clarity.

XMAP215 functions as a microtubule polymerase during microtubule nucleation

XMAP215 has five TOG domains as well as a basic region referred to as the microtubule binding domain (MTbd). Previous domain analyses of XMAP215 have shown that two separate types of domains are required for polymerase activity: 1) TOGs 1 and 2, which bind free αβ-tubulin dimers with high affinity, and 2) a microtubule-lattice binding region, which can be provided by either the MTbd or by TOGs 3 and 4 [50], [93], [97], [100]. To test if the XMAP215 domain requirements for nucleation activity are the same as those for polymerase activity, we created an array of constructs with varying polymerase activities. In our constructs, we maintained the presence of TOGs 1 and 2, which are essential for polymerase activity, and varied the domains required for localization to the microtubule lattice (Figure 2.5A).

To examine the polymerase activities of the XMAP215 constructs, we measured microtubule elongation rates for individual microtubule plus-end tips assembling continuously from GMPCPP-stabilized seeds (Figure 2.5, B and C). As seen in previous studies, addition of full-length XMAP215 strongly accelerated microtubule elongation, increasing the plus-end growth rate by up to 10-fold over αβ-tubulin alone. Addition of TOG1-4MTbd, TOG12MTbd, or TOG1-4 at identical concentrations also accelerated growth, but increased the rate more modestly, by 2.5- to 3.3-fold. Addition of TOG12 had no significant effect. The necessity of TOGs 1 and 2 plus either the MTbd or TOGs 3 and 4 for polymerase activity confirms previous findings [50], [93], [100].

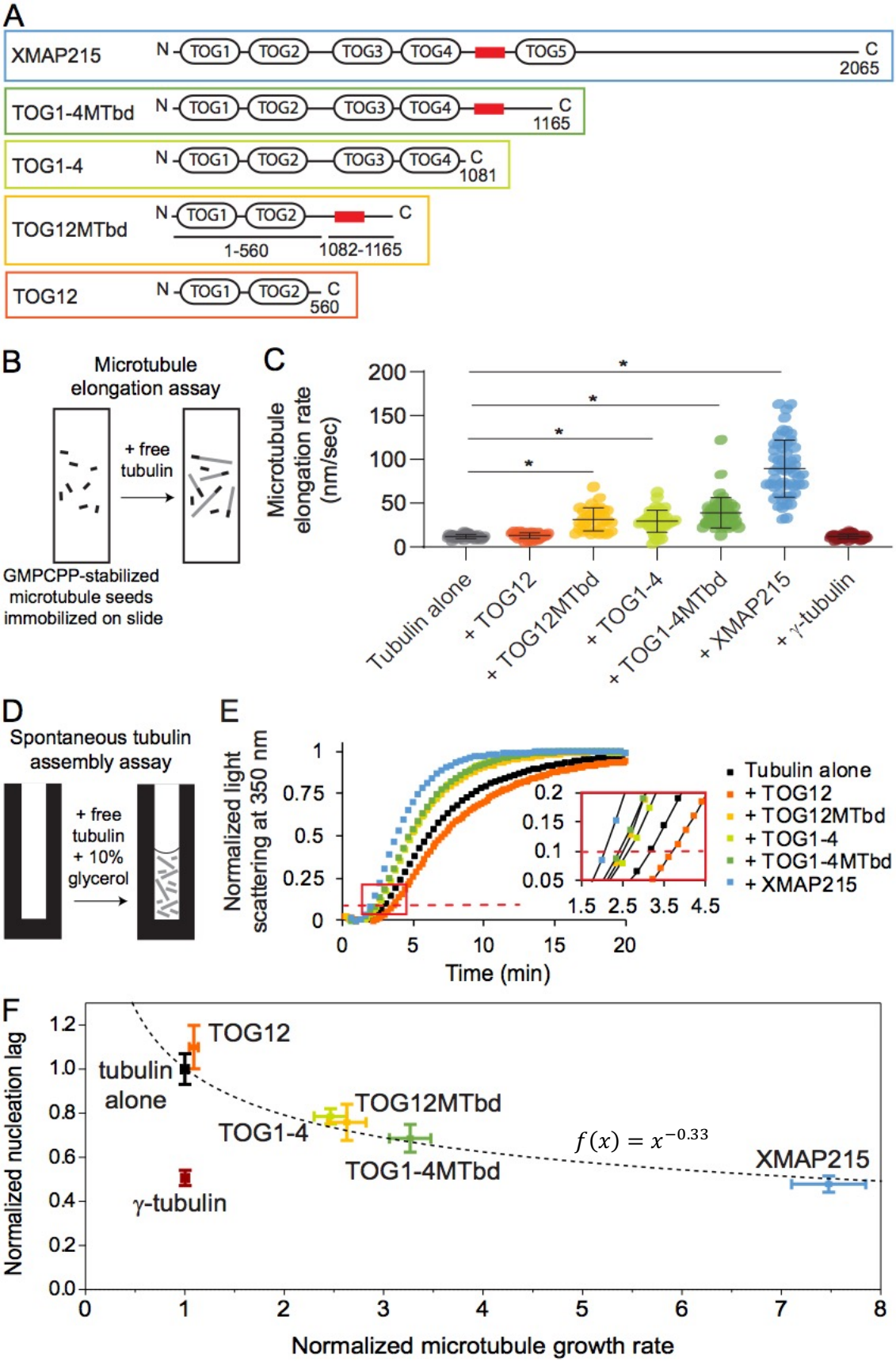
A
XMAP215
N
TOG1
TOG2
TOG3
TOG4
TOG5
C
2065
TOG1-4MTbd
1165
TOG1-4
1081
TOG12MTbd
1-560
1082-1165
TOG12
560
B
Microtubule elongation assay
+ free tubulin
GMPCPP-stabilized microtubule seeds immobilized on slide
C
Microtubule elongation rate (nm/sec)
200
150
100
50
0
*
Tubulin alone
+ TOG12
+ TOG12MTbd
+ TOG1-4
+ TOG1-4MTbd
+ XMAP215
+ γ-tubulin
D
Spontaneous tubulin assembly assay
+ free tubulin + 10% glycerol
E
Normalized light scattering at 350 nm
1
0.75
0.5
0.25
0
0.2
0.15
0.1
0.05
1.5 2.5 3.5 4.5
0 5 10 15 20
Time (min)
Tubulin alone
+ TOG12
+ TOG12MTbd
+ TOG1-4
+ TOG1-4MTbd
+ XMAP215
F
Normalized nucleation lag
1.2
1.0
0.8
0.6
0.4
0.2
0.0
TOG12
tubulin alone
TOG12MTbd
TOG1-4
TOG1-4MTbd
γ-tubulin
$f(x) = x^{-0.33}$
XMAP215
0 1 2 3 4 5 6 7 8
Normalized microtubule growth rate

Figure 2.5. The microtubule nucleation activity of XMAP215 correlates strongly with its polymerase activity.

(A) XMAP215 and XMAP215 deletion constructs used in this work. The red box represents the basic MTbd. (B) Schematic of the assay used to measure tip growth rates from immobilized GMPCPP-stabilized microtubule seeds by microscopy. (C) Microtubule elongation rates at 12 μM free αβ-tubulin, with full-length XMAP215 or the indicated deletion constructs added at 40 nM, or with γ-tubulin added at 300 nM. Error bars represent standard deviation (N = 41, 35, 33, 41, 49, 53, 41 microtubules measured for each respective condition). Asterisk represents p<0.0001, two-sided t-test. (D) Schematic of the assay used to measure non-templated tubulin assembly by turbidity. (E) Representative turbidity assay at 15 μM free αβ-tubulin, with XMAP215 or the indicated deletion constructs added at 40 nM. Red dashed line represents 10% of the maximum light scattering. Inset shows the data indicated by the red box re-plotted on a larger scale for clarity. (F) Nucleation activity plotted against polymerase activity. Data for XMAP215 and its deletion constructs, each added at 40 nM, are fit by a power curve with the equation $f(x) = x^{-0.33}$ (see Methods). Normalized microtubule growth rate means ± SEM represent the data from Figure 2.5C normalized to the growth rate of tubulin alone. Relative nucleation activity for each construct is represented by delay between the start of the polymerization reaction and when the turbidity reached 10% of its maximum, divided by the delay measured in controls with αβ-tubulin alone. Normalized nucleation rate means ± SEM represent the continuous turbidity reaction data of experimental conditions normalized to the nucleation lag of tubulin alone (N ≥ 12, 7, 6, 4, 6, 5, and 6 for tubulin alone, 300 nM γ-tubulin, TOG12, TOG12MTbd, TOG1-4, TOG1-4MTbd, and XMAP215, respectively).

We then tested the activity of our XMAP215 constructs in microtubule nucleation. Three of the deletion constructs added at identical concentrations had moderate nucleation activity compared to full-length XMAP215: TOG1-4MTbd, TOG12MTbd, and TOG1-4. Of these, TOG1-4MTbd had the largest effect, reducing the nucleation lag by 31% compared to αβ-tubulin alone (Figure 2.5E). TOG12MTbd and TOG1-4 promoted nucleation similarly; each reduced the nucleation lag by ~25%. Only one of the deletion constructs we tested, TOG12, showed no effect on nucleation. Notably, the activity of the constructs in nucleation was not dependent on the number of TOG domains.

Similarities in the domain requirements for nucleation versus polymerase activity were striking. Deletion of TOG5 and the C-terminus of XMAP215 significantly reduced

both polymerase and nucleation activity. Further reduction of microtubule lattice affinity, by deleting either TOGs 3 and 4 (TOG12MTbd construct) or the basic region following TOG4 (TOG1-4 construct), predictably reduced polymerization activity and likewise reduced nucleation activity. Elimination of microtubule lattice affinity altogether (TOG12) eliminated both activities. Taken together, these results show that elongation activity and nucleation activity both require only TOGs1 and 2 and a lattice binding region. Therefore, the nucleation activity of XMAP215 does not depend on any particular lattice-binding domain or on the number of TOG domains, but rather it correlates directly with microtubule elongation activity.

Plotting the turbidity and tip growth data against one another illustrates their correlation (Figure 2.5F). To fit the data, a power-law function was chosen because it fits the theoretical relationship between microtubule elongation and nucleation. As microtubule growth rate approaches zero, the nucleation lag should increase and approach infinity. In contrast, as microtubule growth rate approaches infinity, the nucleation lag should decrease and approach zero. The curve fit was constrained to go through (1,1) because elongation and nucleation are defined as 1 in the absence of XMAP215 constructs. The resulting power curve fit is $f(x) = x^{-0.33}$. The exponent, -0.33, is negative. Therefore, as elongation rate increases, the nucleation lag decreases. The magnitude of the exponent is less than 1, which indicates that XMAP215 constructs increase elongation rates at growing microtubule tips more potently than they increase addition of tubulin dimers to nucleation intermediates.

γ-tubulin promotes microtubule nucleation without affecting elongation rate

For comparison with XMAP215, it was instructive to also compare the effects of γ-tubulin in the tip growth and turbidity assays. Addition of purified γ-tubulin alone had no effect on plus-end growth rates (Figure 2.5C), which is not surprising since γ-tubulin caps minus ends and does not associate with microtubule plus ends. However, the same concentration of γ-tubulin dramatically reduced the nucleation lag in the turbidity assay, by 50% (Figure 2.4A and Figure 2.5F). These observations confirm that γ-tubulin promotes microtubule nucleation without affecting microtubule plus-end elongation, consistent with its expected role as a minus-end-binding template.

XMAP215 and γ-tubulin function additively during microtubule nucleation

If XMAP215 functions strictly to elongate nucleation intermediates during microtubule formation, then its role should not overlap with γ-tubulin, and thus the effects of XMAP215 and γ-tubulin arrays in the turbidity assay should be additive. In contrast, if XMAP215 and γ-tubulin arrays function synergistically (or redundantly), they should produce a larger (or smaller) effect when combined than the sum of their independent contributions.

Condition	Normalized nucleation lag
Tubulin alone	1
+ 300 nM γ-tubulin	0.507
+ 20 nM XMAP215	0.749

Normalized nucleation lag with 300 nM γ-tubulin alone:	0.507
	x
Normalized nucleation lag with 20 nM XMAP215 alone:	0.749
Predicted additive effect:	0.380

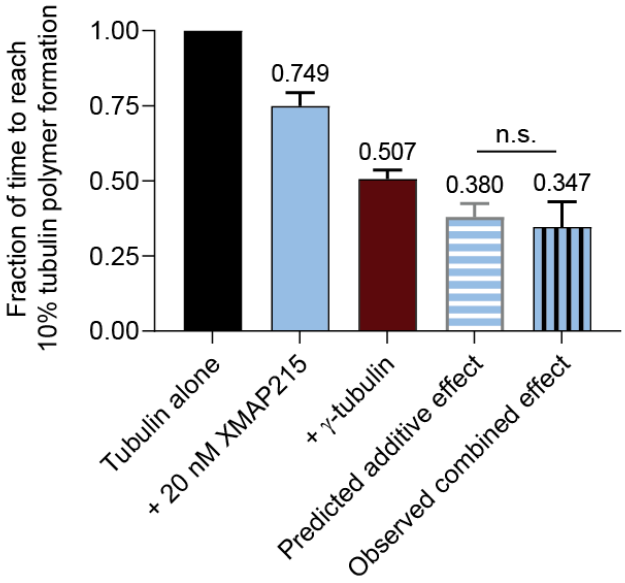

Figure 2.6. Example calculation for predicted additive effect.
Data plotted are mean values ± SEM (N = 12 for tubulin alone, N = 4 for all other conditions). Significance was tested, two-sided t-test.

To distinguish the type of relationship XMAP215 and γ-tubulin arrays display, we calculated the effect on nucleation lag that would occur in a purely additive scenario (Figure 2.6 shows example calculations). Then, over the previously tested concentrations of XMAP215, we measured the combined effects of XMAP215 and γ-tubulin arrays (Figure 2.7A). We compared the observed nucleation lags with the predicted nucleation lags, and found they closely matched across all XMAP215 concentrations (Figure 2.7B).

To further test if XMAP215 and γ-tubulin act in an additive manner, we measured the combined effect of each of our XMAP215 deletion constructs with γ-tubulin. In every case, the nucleation lag observed when the two were combined was not significantly different from the predicted additive value (Figure 2.7C). Thus, the removal of various domains from XMAP215 does not allow for either synergy or redundancy with γ-tubulin. Overall, the close correspondence of the measured nucleation lags with the predicted additive values, across different XMAP215 concentrations and across the different deletion constructs, shows that XMAP215 and γ-tubulin function additively in the absence of other ring complex proteins.

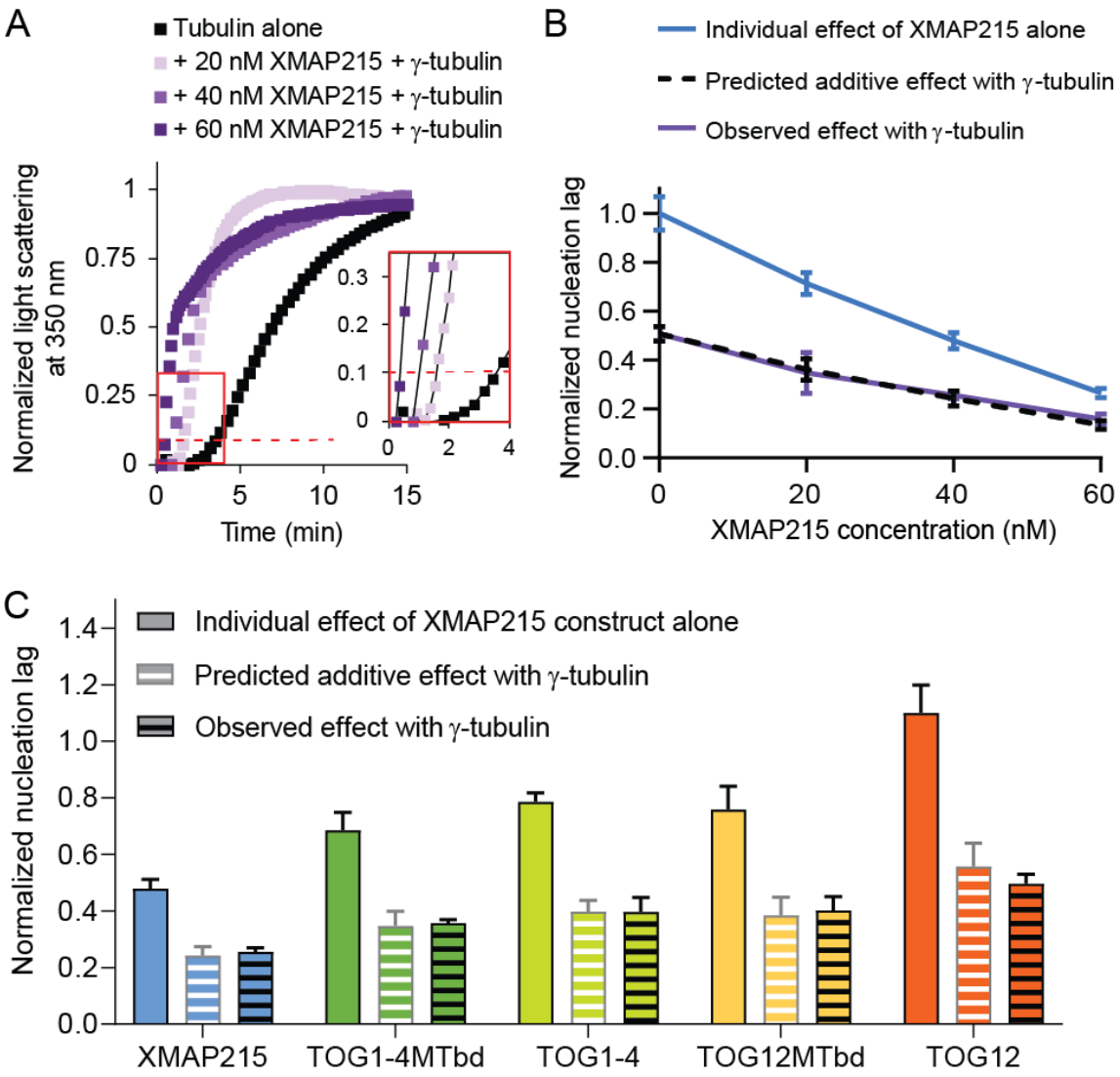

Figure 2.7. XMAP215 and γ-tubulin promote nucleation additively in pure tubulin solutions.

(A) Representative tubulin assembly assay for 20 nM, 40 nM, or 60 nM XMAP215 in combination with 300 nM γ-tubulin with 15 μM free tubulin. Red dashed line represents 10% of the normalized maximum light scattering. Inset shows same data from red box plotted on larger scale for clarity. For 40 nM and 60 nM XMAP215 in combination with 300 nM γ-tubulin, microtubule bundling occurs at later time points, which causes a difference in the shape of the curve of tubulin assembly. See Figure 2.8. (B) XMAP215 functions additively with γ-tubulin at all concentrations measured (see Figure 2.6). Data plotted are mean values ± SEM (N = 12, 4, 6, 4 for 0 nM, 20 nM, 40 nM, and 60 nM XMAP215, respectively; N = 7, 4, 4, and 4 for 0 nM, 20 nM, 40 nM, and 60 nM XMAP215 + γ-tubulin, respectively). (C) XMAP215 deletion constructs all show additive action with γ-tubulin (Figure 2.6). Data plotted for each XMAP215 deletion construct are mean values ± SEM replotted from Figure 2.5F. Data plotted for each XMAP215 deletion construct + γ-tubulin are mean values ± SEM (N = 4 for each condition).

During polymerization, XMAP215 increases the on-rate for tubulin dimers associating with the microtubule tip [101]. Our results suggest that this is its primary contribution during microtubule nucleation as well. XMAP215's effect on microtubule nucleation correlates with its polymerase activity, independent of the domains present. This provides support for a model of independent action by XMAP215 during microtubule nucleation, as suggested previously [43], [94], [102].

Our results also show that γ-tubulin and XMAP215 do not show the synergistic interaction that was previously reported for the full γ-TuRC and XMAP215. Several possibilities could explain this difference. It is thought that the γ-TuRC is activated through a conformational change, and the reported interaction between the unstructured C-terminal tail of XMAP215 and γ-tubulin might be responsible for this. It is also possible that the full γ-TuRC offers higher affinity binding sites for this interaction with XMAP215 than arrays of γ-tubulin alone. Extra molecules of XMAP215 would increase the local concentration of αβ-tubulin near the template and thereby increase the rate of addition of αβ-tubulin. Alternatively, the arrangement of a γ-tubulin template into a ring might activate it for synergistic action by forming better substrates for XMAP215. Laterally associated γ-tubulin arrays and γ-TuRCs both provide templates that should promote lateral interactions between αβ-tubulin dimers. However, the templates are not identical and each might promote a distinct ensemble of nucleation intermediates. According to this model, XMAP215 would act preferentially on nucleation intermediates that form on the 13-member γ-tubulin template provided by the ring complex.

We show here that XMAP215 functions additively with laterally associated arrays of γ-tubulin. That a microtubule polymerase, which promotes elongation, and a template, which promotes lateral interactions, act independently during the early stages of microtubule formation supports early nucleation models that include several rate-limiting steps [56], [57] and a more recent model that proposes microtubules form by progressively faster tubulin accretion [59]. Our results suggest that there must be at least two distinct types of rate-limiting processes in the nucleation pathway. Given the theoretical activities of the template and the polymerase, we propose that two of these processes are (i) the formation of initial lateral αβ-tubulin bonds, which is specifically accelerated by γ-tubulin, and (ii) the formation of subsequent αβ-tubulin bonds, which is specifically accelerated by XMAP215.

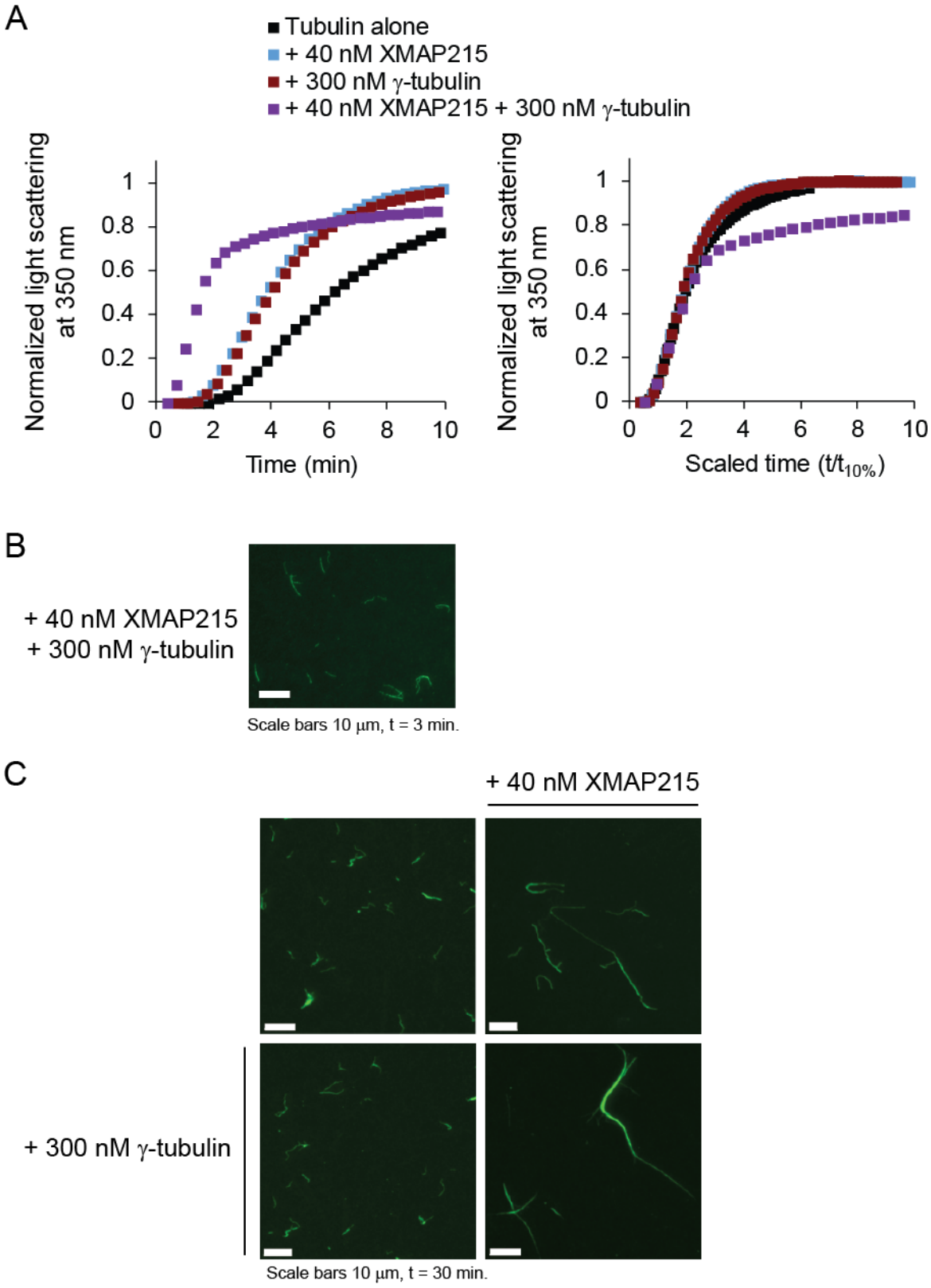

Figure 2.8. XMAP215 and γ-tubulin in combination promote microtubule bundling.

Historically, the mechanism of spontaneous tubulin assembly has been explored using the turbidity data across a range of initial tubulin concentrations [57]. Flyvbjerg and coworkers normalized light scattering to the maximum value at which the data plateaus and normalized time to the time at which turbidity reaches one-tenth its maximum. Finding that the curves were identical following these normalizations, they determined that tubulin follows a single mechanism during assembly, regardless of initial concentration.

We applied this type of analysis to explore the mechanism of assembly in the presence of γ-tubulin and XMAP215. When γ-tubulin is added at 300 nM in combination with XMAP215 at sufficiently high concentration (~40 nM), light scattering increases indefinitely. Normalization of the light scattering of this condition results in a curve with differing shape, specifically with a distinct linear increase in light scattering after turbidity reaches 60% of its maximum value, after approximately 2 min (Figure 2.8A).

To determine if the species of microtubules were different when both γ-tubulin and XMAP215 were present, we performed microtubule pelleting at various time points. By the earliest time point of 3 min, small (≤ 10 microns) microtubule bundles were rare but visible (Figure 2.8B). By the latest time point of 30 min, most microtubules were present in bundles (Figure 2.8C).

The combination of γ-tubulin and XMAP215 in purified solutions promotes bundling of existing microtubules, as noted previously [92]. Comparisons for the effect on nucleation are taken when turbidity reaches 10% of its maximum value, well before bundling occurs. The mechanism for how this bundling occurs is unknown. I would hypothesize that combining the stabilizing activities of γ-tubulin at the minus end in XMAP215 at the plus end promotes general bundling.

2.3 METHODS

Purification of tubulin

αβ-tubulin was purified from fresh bovine brain using a high-concentration PIPES buffer as previously described [103].

γ-tubulin and XMAP215 expression plasmids

A human γ-tubulin construct with a C-terminal myc-His_6 tag was previously described [104]. A construct with XMAP215 with a C-terminal GFP-His_7 tag was previously described [63]. The fragment containing GFP was removed using SalI digestion (pRK009) and QuikChange was performed to produce TOG1-4MTbd (pRK087) and TOG1-4 (pRK031). pPW263, a bacterial expression plasmid containing TOG12 and three K loops with a C-terminal myc-His_6 tag was previously described [100]. QuikChange was performed to produce TOG12MTbd (pRK074) and TOG12 (pRK056).

Purification of γ-tubulin and XMAP215 constructs

γ-tubulin, XMAP215, TOG1-4MTbd, and TOG1-4 were expressed in Sf9 cells using the Bac-to-Bac system from Invitrogen (Thermo Fisher Scientific, Waltham, Massachusetts). Sf9 cells at a density 1-2x10^6 cells/ml were infected with baculovirus. Cell pellets were harvested 48-72 hrs. post-infection. Infections were done both in-house, at the National Cell Culture Center (Minneapolis, MN), or at the Tissue Culture Core Facility, Univ. of Colorado Cancer Center, UCHSC at Fitzsimons (Aurora, CO). TOG12MTbd and TOG12 were expressed in *E. coli* Rosetta 2 cells with plasmid

pRARE. All XMAP215 and TOG constructs were purified as previously described [105], and γ-tubulin was purified as previously described [88].

Spontaneous tubulin assembly assay

The spontaneous assembly of purified bovine brain tubulin was measured by light scattering at 350 nm as described previously [56]. Tubulin was thawed on ice slurry (0°C) and pelleted in a TLA100 rotor at 90,000 rpm for 10 minutes to remove microtubule polymers and/or inactive tubulin. The supernatant was removed, kept at 0°C, and used for the assembly reactions. Experimental reactions were prepared without tubulin in 1.7 mL Eppendorf tubes at 0°C, with 30% glycerol, 1 mM DTT (Millipore Sigma, St. Louis, Missouri), 1 mM GTP (Millipore Sigma) in BRB80 buffer (80 mM potassium PIPES (EMD Chemicals Inc., Gibbstown, New Jersey), 1 mM $MgCl_2$ (Millipore Sigma) and 1 mM EGTA (Millipore Sigma), pH 6.8). Immediately before measuring light scattering, tubulin was added at either 12 μM or 15 μM to experimental reactions at 0°C for a total volume of 150 μL, and then the entire reaction was moved to a pre-warmed cuvettes at 37°C in a DU 800 spectrophotometer (Beckman Coulter Life Sciences, Indianapolis, Indiana). The $A_{350\ nm}$ was recorded every 6-20 seconds on 2-6 samples at a time for greater than 40 minutes. Recording on the spectrophotometer was started prior to tubulin being added to experimental reaction mix. For XMAP215 and γ-tubulin, at least 7 experimental samples per condition were tested, for two independent purifications of each protein. For XMAP215 deletion constructs, at least 4 experimental samples were tested. All conditions were randomized by experiment across multiple days. Scaling analysis was performed by hand.

For data quantification, a tubulin alone control was run simultaneously with each reaction, using the same freshly thawed and cleared tubulin aliquot and the same buffers. Nucleation lag was quantified by comparing time to reach 0.1 maximum polymer, or 10% maximum polymer, between experimental reactions and their corresponding tubulin alone control reaction. The effect of each protein was reproducible, with experimental variation run to run likely due to different tubulin concentrations.

Microtubule growth rate assay

Small flow chambers were constructed by adhering a KOH etched coverslip onto a glass slide with two strips of double-sided tape. Flow chambers were incubated with pre-warmed 1 mg/ml biotin-BSA (Vector Laboratories, Burlingame, California) for 15 minutes at room temperature, then washed with pre-warmed BRB80 (80 mM PIPES (EMD Chemicals Inc., Gibbstown, New Jersey), 120 mM KCl (Hach Company, Loveland, Colorado), 1 mM $MgCl_2$ (Millipore Sigma, St. Louis, Missouri) and 1 mM EGTA (Millipore Sigma), pH 6.8). GMPCPP-stabilized microtubule seeds assembled from a mixture of biotinylated porcine tubulin, 7 or 14% of total, (Cytoskeleton, Inc., Denver, Colorado) and purified bovine tubulin were secured to the glass coverslip surface using 0.25 mg/mL avidin (Vector Laboratories) [106]–[109]. After 5 minutes, microtubule seeds were washed with BRB80 containing 1 mM GTP (Millipore Sigma), 8 mg/mL BSA (Millipore Sigma), and 1 mg/mL K-casein (Millipore Sigma), until reaction mixture was added.

Dynamic microtubule extensions were grown in the absence, or presence, of 40 nM XMAP215 constructs. Reaction mixture consisted of freshly thawed 12 μM purified

bovine brain tubulin in microtubule growth buffer (BRB80, 1 mM GTP (Millipore Sigma), 5 mM DTT (Millipore Sigma), 25 mM glucose (Millipore Sigma), 200 µg/mL glucose oxidase (Millipore Sigma), 35 µg/mL catalase (Millipore Sigma)). Microtubule extensions were imaged by recording video-enhanced differential interference contrast (VE-DIC), which allowed us to visualize the dynamic microtubule tips. A field of view (FOV) was imaged for 15-20 minutes. 4-8 FOVs per flow chamber were analyzed per experiment.

Growing microtubule tips were manually tracked using MTrackJ. X-Y coordinates of the microtubule tips were projected onto a line corresponding to the microtubule long-axis. Projected tip positions were then plotted against time, and during episodes of steady growth were fitted to a line. The slopes of these line-fits were recorded as the growth velocities.

Nucleation lag and elongation rate correlational analysis

Data was plotted and fit using Igor Pro software (WaveMetrics, Portland, Oregon). A power curve was chosen to fit the data, in consideration of the theoretical relationship between microtubule elongation and nucleation. As microtubule growth rate approaches zero, the nucleation lag should increase and approach infinity. In contrast, as microtubule growth rate approaches infinity, the nucleation lag should decrease and approach zero. In accordance with this last point, the horizontal asymptote was constrained to zero. Additionally, the curve was weighted in relation to the SEM for the normalized nucleation lag data.

Electron microscopy and helical reconstructions

γ-tubulin arrays were prepared by diluting pure γ-tubulin to 0.5-1 μM out of 0.5 M KCl-containing buffer to ≤ 100 mM KCl, no GTP. Notably, arrays form at 4ºC and 37ºC, with or without GTP. For negative stained samples, carbon-coated grids were glow-discharged or plasma-cleaned prior to use, followed by application of 3-5 μl of protein solution for 60 secs. Grids were then washed in ddH_2O and stained with filtered 1% uranyl acetate for 30 secs. Images were obtained on a Tecnai20 transmission electron microscope (FEI, Hillsboro, Oregon) at 62,000 magnification and 200kV in low-dose mode with the use of either a 1024x1024 pixel CCD camera or a 4096x4096 pixel CCD camera (Gatan, Pleasanton, California) at -1.3-1.5 μm defocus. For γ-tubulin array reconstructions, individual arrays 300 pixels wide were extracted from the original micrographs using EMAN2 Helixboxer [110], after rotation to vertical along the long array axis. SPIDER [111], [112] was then used to window the arrays along the long axis, shifting by 270 pixels for 90% overlap between adjacent images. The image stacks were then padded by 90 pixels and binned 2x for a final square image size of 195 pixels. Image stacks corresponding to individually picked arrays were aligned in 2D to initially characterize array symmetry. Using a simple rectangular initial reference image based on an unaligned average of the image stacks, 10 rounds of reference-based alignment and averaging were run to calculate a final average image. Three similar, long and well-ordered arrays consisting of 560 overlapping segments were chosen as an initial dataset for 3D reconstruction. A repeat distance of ~ 52 Å was measured from the 2D averages and used as a starting parameter for 3D reconstruction. The IHRSR program was used as the 3D helical alignment algorithm [113]. 50 rounds of refinement

were run for each experiment using a simple cylinder with a diameter similar to the width of the 2D averages of the images. Multiple runs of IHRSR were performed using different initial azimuthal angles. Several different point group symmetries were also applied. The best results were obtained using a 5-fold point group symmetry with a final refined azimuthal angle of 6.5° and a rise of 52.9 Å. The final volume was contoured to an estimated 8.4 MDa and x-ray structures of γ-tubulin trimers [88] were manually fit to the corresponding density.

Microtubule pelleting assay

Experimental reactions were prepared as described in the spontaneous tubulin assembly, and incubated at 37°C for 30 min. The reactions were fixed by 1:4 dilution in 2% glutaraldehyde (Electron Microscopy Services, Hatfield, Pennsylvania), and 2 min incubation at room temperature. Dilution of samples (1:1200) before pelleting was required to differentiate individual microtubules. Pelleting onto coverslips was performed as previously described [114].

To visualize microtubules on coverslip, immunostaining was performed using anti-α-tubulin—FITC antibody (Millipore Sigma, St. Louis, Missouri). The slides were imaged using an AxioObserver Z1 microscope (Zeiss, Jena, Germany) equipped with an ORCA-Flash4.0 camera (Hamamatsu Photonics K.K., Bridgewater, New Jersey) and an α Plan-Apochromat 63X objective (1.46 NA) (Zeiss). Immunostained microtubules were imaged with 0.4 s exposures and were not binned with a final resolution of 2048 x 2048.

2.4 ACKNOWLEDGEMENTS

We thank Albion Baucom and Koji Yonekura for help with reconstructions of the γ-tubulin arrays. We thank Per Widlund for XMAP215 expression plasmids and helpful discussion.

Table 2.1. Plasmids used in this study.

Plasmid name	Protein expressed	Vector	References
γ-tubulin-myc-His	γ-tubulin-myc-His_6	pFastBac	[104]
XMAP215-GFP-His	XMAP215-GFP-His_7	pFastBac	[105]
pRK009	XMAP215-His_7	pFastBac	This study
pRK087	TOG1-4MTbd-His_7	pFastBac	This study
pRK031	TOG1-4-His_7	pFastBac	This study
pPW263	TOG12-3Kloop-myc-His_6	pTrcHis A	[100]
pRK074	TOG12MTbd-His_6	pTrcHis A	This study
pRK056	TOG12-His_6	pTrcHis A	This study

Chapter 3. PLUS-END TRACKING PROTEINS PROMOTE MICROTUBULE NUCLEATION *IN VIVO*

3.1 INTRODUCTION

In budding yeast, MTs are nucleated at spindle pole bodies (SPBs). MTs are capped at their minus ends by the γ-tubulin ring complex (γ-TuRC), which is anchored to the SPB via the coiled-coil protein Spc110 [14]–[16]) (Figure 3.1). MT nucleation from purified SPBs is poor; each SPB in live yeast nucleate 20-25 MTs, but the fraction of purified SPBs that nucleate even 1 MT *in vitro* is 5-10% (unpublished data, Davis lab). Purified γ-tubulin complexes from yeast and other model organisms such as *Drosophila* and *Xenopus* also show poor MT nucleation efficiency [19], [28], [87], [115]–[117].

The failure of purified MTOCs to nucleate is likely due to a lack of understanding of other factors that regulate MT nucleation *in vivo*. These factors are hypothesized to be either post-translational modifications or MT-associated proteins (MAPs). The role of phosphorylation is unclear, with one group reporting that it promotes assembly of the nucleating machinery [21], and another finding it has no effect [118]. The Davis lab, in collaboration with the Agard lab of UCSF, showed that a conformational change in γ-TuRC, induced by engineered cysteine bonds, promotes MT nucleation [29]. This provided evidence for a conformational change promoted by phosphoregulation.

While the role of phosphorylation in MT nucleation is an on-going area of research, my work here focuses on the role of MAPs. MAPs, in general, are proteins that localize to MTs by binding directly to tubulin. Because MT nucleation requires the

oligomerization of tubulin subunits at the SPB, characteristics of nucleation factors likely include an interaction with the SPB and a stabilizing interaction with tubulin intermediates. With this in mind, I chose three candidate MAPs—Stu2, Bim1, and Bik1—that exhibit these characteristics (see below).

Due to the aforementioned poor efficiency of purified MTOCs to nucleate, I investigated these proteins using an *in vivo* approach. Studying MT nucleation in live cells poses its own unique problem, however—MTOCs such as SPBs always have MTs present. This is true even for "brand new" SPBs (the newly duplicated SPB that is created in order for mitosis to occur). This makes it impossible to differentiate between pre-existing MTs and currently nucleating MTs. Therefore the Davis lab developed a novel tool to observe nucleation *de novo* in cells—the Spc110 chimera expression system (Figure 3.1). In cells, the Spc110 chimera nucleates MTs robustly (Figure 3.2). I exploited this system to test the hypotheses that regulatory MAPs promote MT nucleation.

3.2 A NOVEL TOOL RECRUITS THE γ-TUBULIN COMPLEX AND FORMS MICROTUBULE BUNDLES *IN VIVO*

Temporally controlled by an inducible promoter, the Spc110 chimera recruits the γ-tubulin complex to the DNA, rather than the SPB, through lac operator/lac repressor interactions (Figure 3.1). This provides an ectopic site of nucleation that is distinct from the SPB. Interestingly, Spc110 chimera puncta appear to form antiparallel MT arrays with capped minus ends, as revealed by electron tomography (data collected by Janet Meehl, University of Colorado Boulder). While these MT bundles are less organized than mitotic spindles, minus ends appear to cluster (Figure 3.2).

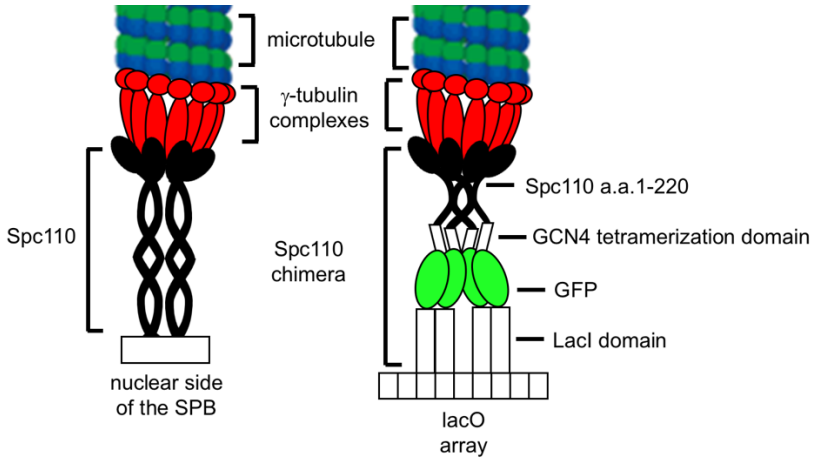

Figure 3.1. The γ-tubulin complex serves as a robust MT nucleation template at the wild-type SPB and the Spc110 chimera system.

(Left) Full-length Spc110 dimerizes via a coiled coil domain and anchors γ-tubulin complexes to the nuclear side of the budding yeast SPB. (Right) The Spc110 chimera is comprised of the N-terminal 220 amino acids of Spc110, a tetramerization domain, a GFP tag, and a lac repressor domain which binds *lacO* arrays integrated into Chromosome XII.

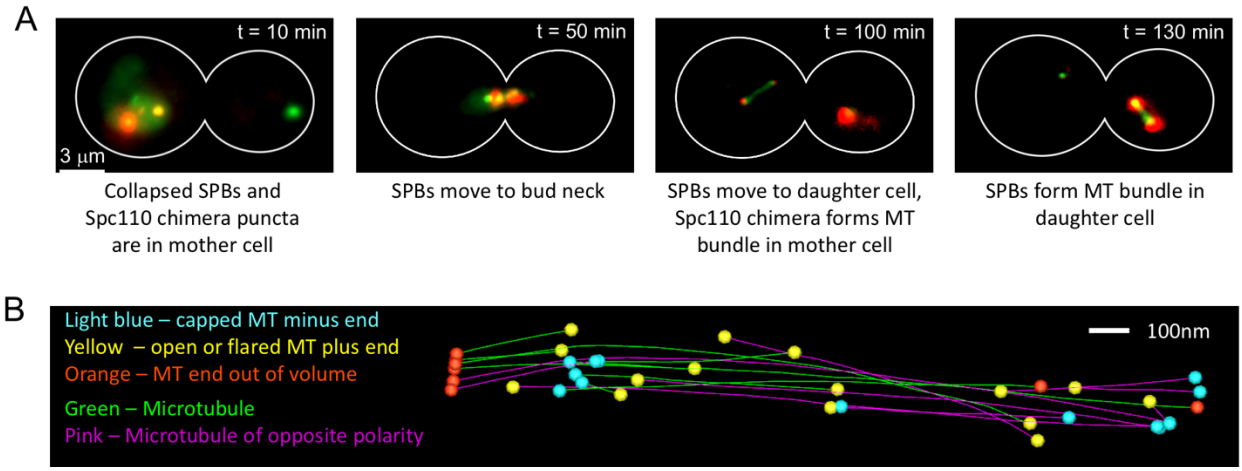

Figure 3.2. Visualization of the Spc110 chimera MT bundles in live cells.

(A) A representative timeline of events following β-estradiol pulse induction of Spc110 chimera. γ-tubulin complexes are visualized using expression of Spc97-mCherry (shown in red), and tubulin is visualized using expression of GFP-Tub1 (shown in green). (B) Electron tomography of MT bundles associated with Spc110 chimera puncta revealed antiparallel MTs with clusters of capped minus ends. Data for this section of the figure collected by Janet Meehl-Fox of the Winey lab.

Work from our lab has shown that constitutive overexpression of the Spc110 chimera in yeast results in excessive MT formation, spindle abnormalities, and eventual lethality (data collected by King Yabut, Davis lab, Figure 3.3).

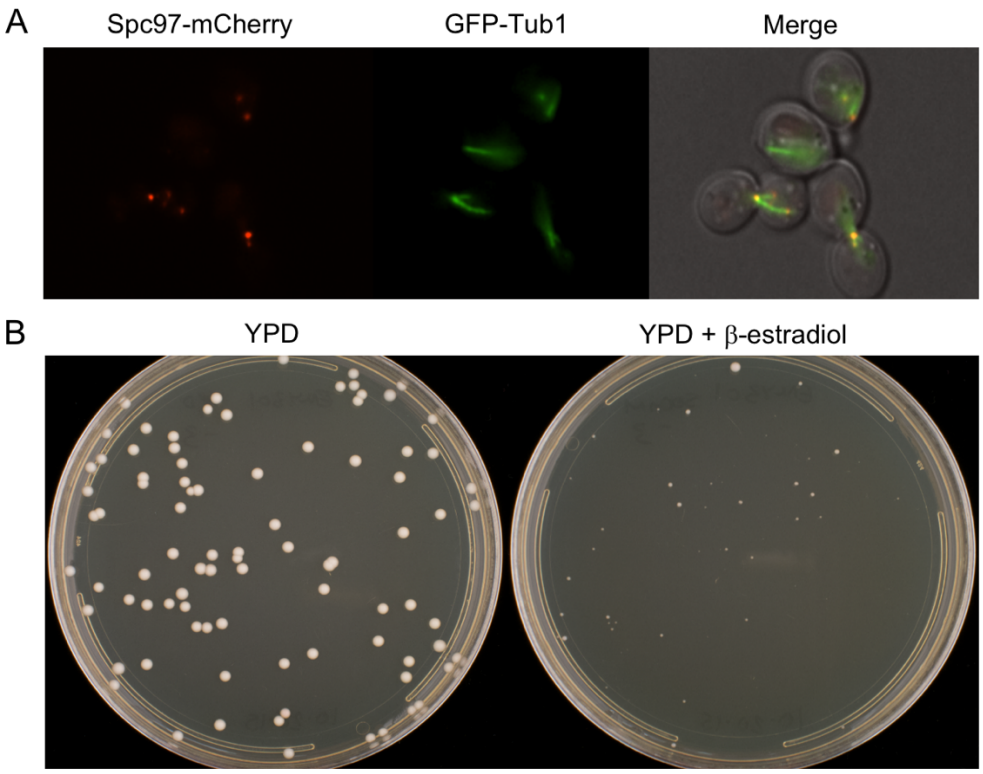

Figure 3.3. Overexpression of the Spc110 chimera results in spindle abnormalities and is toxic.
(A) Spc97-mCherry and GFP-Tub1 localization reveals abnormal or multipolar spindles during Spc110 chimera overexpression. (B) (Left) Strains carrying the Spc110 chimera display normal growth on YPD (left), and reduced growth when the Spc110 chimera is constitutively induced with β-estradiol (right). Data for this figure collected by King Yabut of the Davis lab.

The Spc110 chimera is a novel tool that allows observation of MT nucleation *de novo* and can be used to perform a variety of studies (such as investigation of the effect of Spc110 phosphorylation). For my work, I used the Spc110 chimera to determine the role of candidate MAPs in two essential steps in nucleation, the recruitment of the γ-tubulin complex to Spc110 and the formation of a MT.

3.3 MICROTUBULE PLUS-END TRACKING PROTEINS PROMOTE MICROTUBULE FORMATION FROM THE SPC110 CHIMERA FOLLOWING NOCODAZOLE TREATMENT

Stu2, Bim1, and Bik1 are MT plus-end tracking proteins (+TIPs) but each has been shown to physically associate with components of the SPB [119]–[123]. Further, during nucleation, the MT minus and plus ends are colocalized, so +TIPs may be localized to the site of nucleation.

These three +TIPS are also known to stabilize existing MTs. Deletion of CLIP-170, the human homolog of Bik1, *in vivo* results in decreased rates of rescue [81]. Bim1 inhibits catastrophe, and does so in complex with Bik1 [124]. Stu2 is a member of the XMAP215 family of MT polymerases that promote growth rates [63]. Furthermore, homologs of Stu2 and Bim1 have been shown to promote MT nucleation (separately) *in vivo* and *in vitro* [90]–[92], [125]. The same properties that allow these +TIPs to stabilize MTs may allow them to stabilize the initial nucleus of tubulin dimers.

+TIPs are not required for localization of γ-tubulin complex to the Spc110 chimera

A necessary step in MT nucleation is the recruitment of the γ-tubulin complex to Spc110 at the SPB. The Spc110 chimera recruits the γ-tubulin complex in control strains, even in the presence of the MT depolymerizing drug nocodazole. This allowed me to test the effect of each +TIP on this behavior. The Spc110 chimera was visualized using its GFP tag and the γ-tubulin complex was visualized using Spc97-mCherry. I used the auxin-degradation system to deplete either Stu2, Bim1, or Bik1. I found that none of the candidate +TIPs had an effect on the recruitment of the γ-tubulin complex to the Spc110 chimera during nocodazole treatment (Figure 3.4).

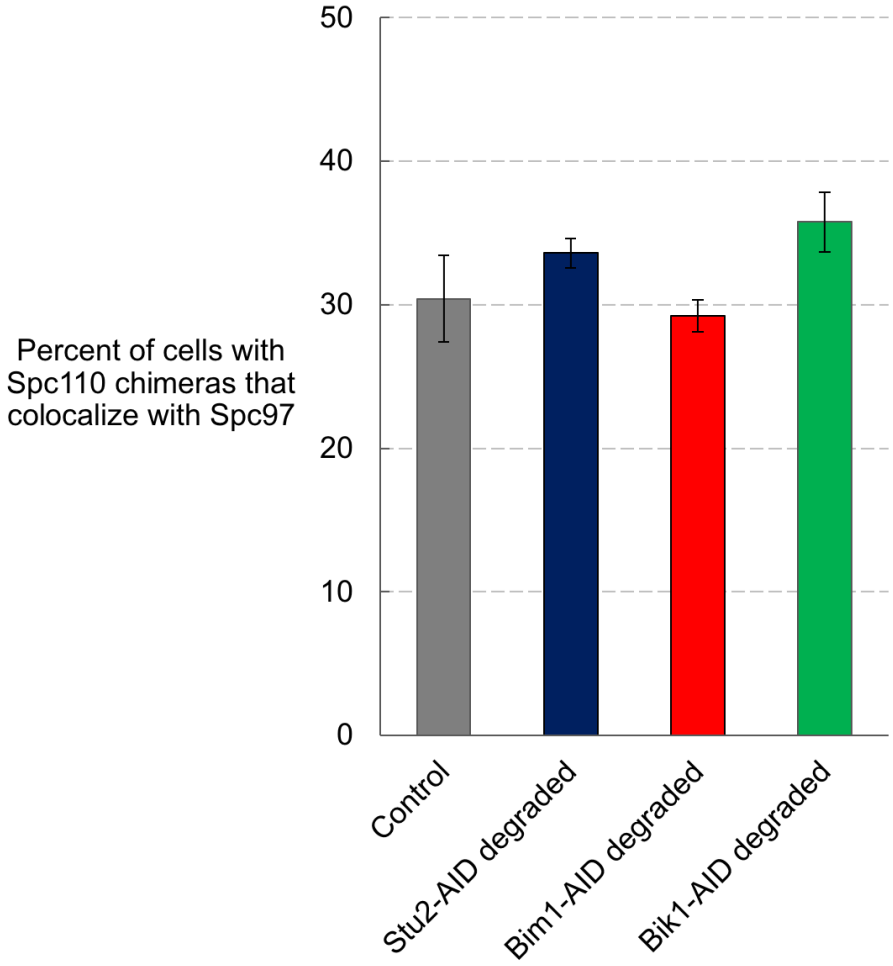

Figure 3.4. +TIPs are not required for γ-tubulin complex localization to the Spc110 chimera.

Depletion of Stu2, BIm, or Bik1 has no effect on the percent of cells in which a measurable amount of γ-tubulin complex is recruited to the Spc110 chimera during nocodazole treatment. Values shown are mean ± S.D., N = 3 experiments and ≥ 100 total cells for each condition.

+TIPs promote MT formation at the Spc110 chimera

Following nocodazole washout, the Spc110 chimera forms MT bundles in control strains (Figure 3.5B). I tested the effect of Stu2, Bim1, and Bik1 on this process. MT bundles were visualized using GFP-Tub1. I found that, under these conditions, Stu2 and Bim1 are required for MT formation from the Spc110 chimera and the SPB (Figure 3.5

and Figure 3.6). Bik1, on the other hand, was required to promote MT formation from the Spc110 chimera, but not the SPB (Figure 3.5 and Figure 3.6).

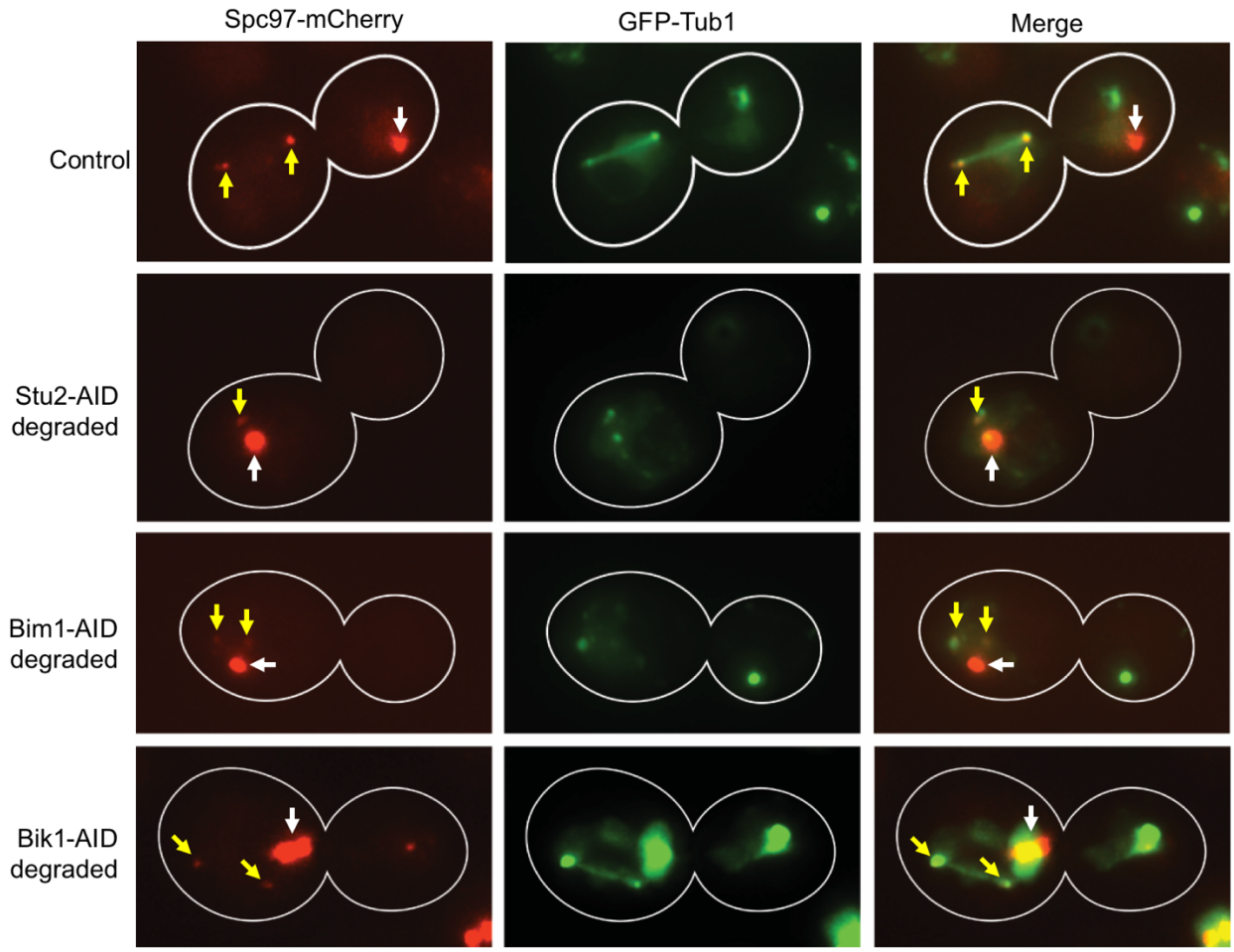

Figure 3.5. +TIPs promote MT nucleation from the Spc110 chimera.
Representative cells show that Stu2, Bim1 and Bik1 each promote MT nucleation from the Spc110 chimera. Control strains are able to form MT bundles, while depletion of Stu2 or Bim1 results in no MT formation. Some Bik1 depleted cells show MT bundle formation. White arrows denote Spc97-mCherry puncta associated with the SPB, and yellow arrows denotes Spc97-mCherry puncta associated with the Spc110 chimera. Spc97-mCherry shown in red and GFP-Tub1 shown in green.

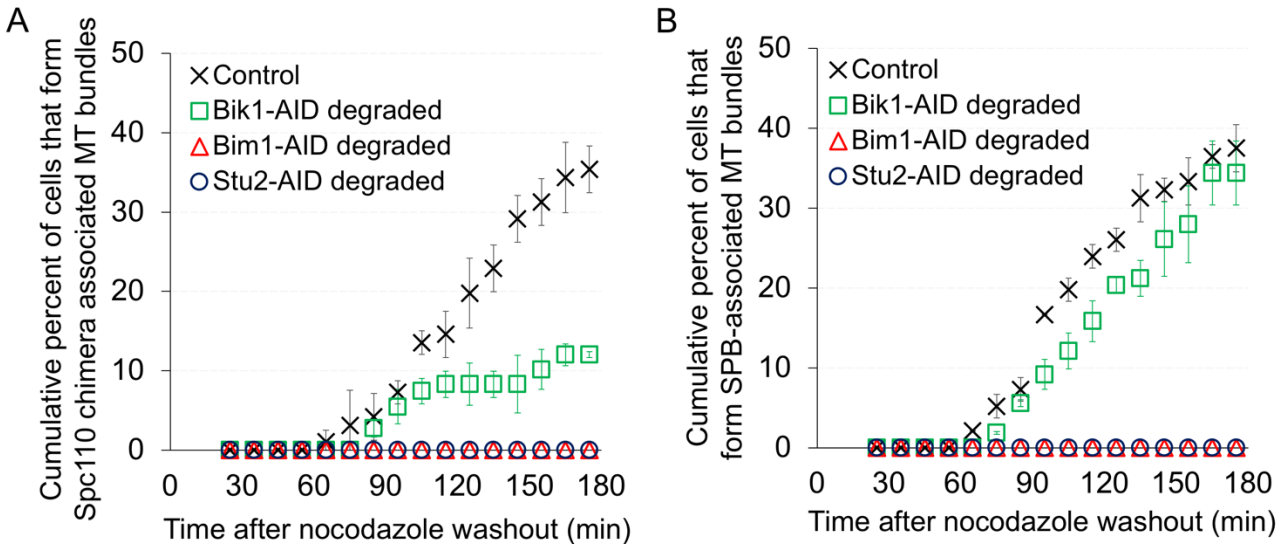

Figure 3.6. +TIPs promote MT nucleation following induction of the Spc110 chimera.

(A) Bik1 promotes MT bundle formation at the Spc110 chimera, while Stu2 and BIm1 each are required. (B) Stu2 and BIm1 each are required for MT bundle formation at the SPB when the Spc110 chimera is expressed. Values shown are mean ± S.D., N = 3 experiments and ≥ 100 total cells for each condition.

Bik1 indirectly promotes microtubule formation from the Spc110 chimera

Bik1 promoted MT formation at the Spc110 chimera, yet had little effect on MT formation at the SPB. Further examination of cells depleted of Bik1 revealed that Bik1 is required for SPB positioning (Figure 3.7A). In strains expressing endogenous Bik1 that has been C-terminally tagged with the auxin-inducible degron (Bik1-AID strains), SPB movement to bud is reduced by ~30%. When Bik1 is depleted by the addition of auxin, SPB movement is reduced an additional ~50%. This is consistent with previous reports of Bik1 being critical for targeting dynein to astral MT plus ends, as part of the dynein-dependent pathway of SPB positioning [126]–[128].

In control cells, SPB movement to the bud correlates with a higher proportion of Spc110 chimera MT formation. Therefore the effect of Bik1 on the Spc110 chimera may be indirect, as Bik1 promotes SPB movement to the bud.

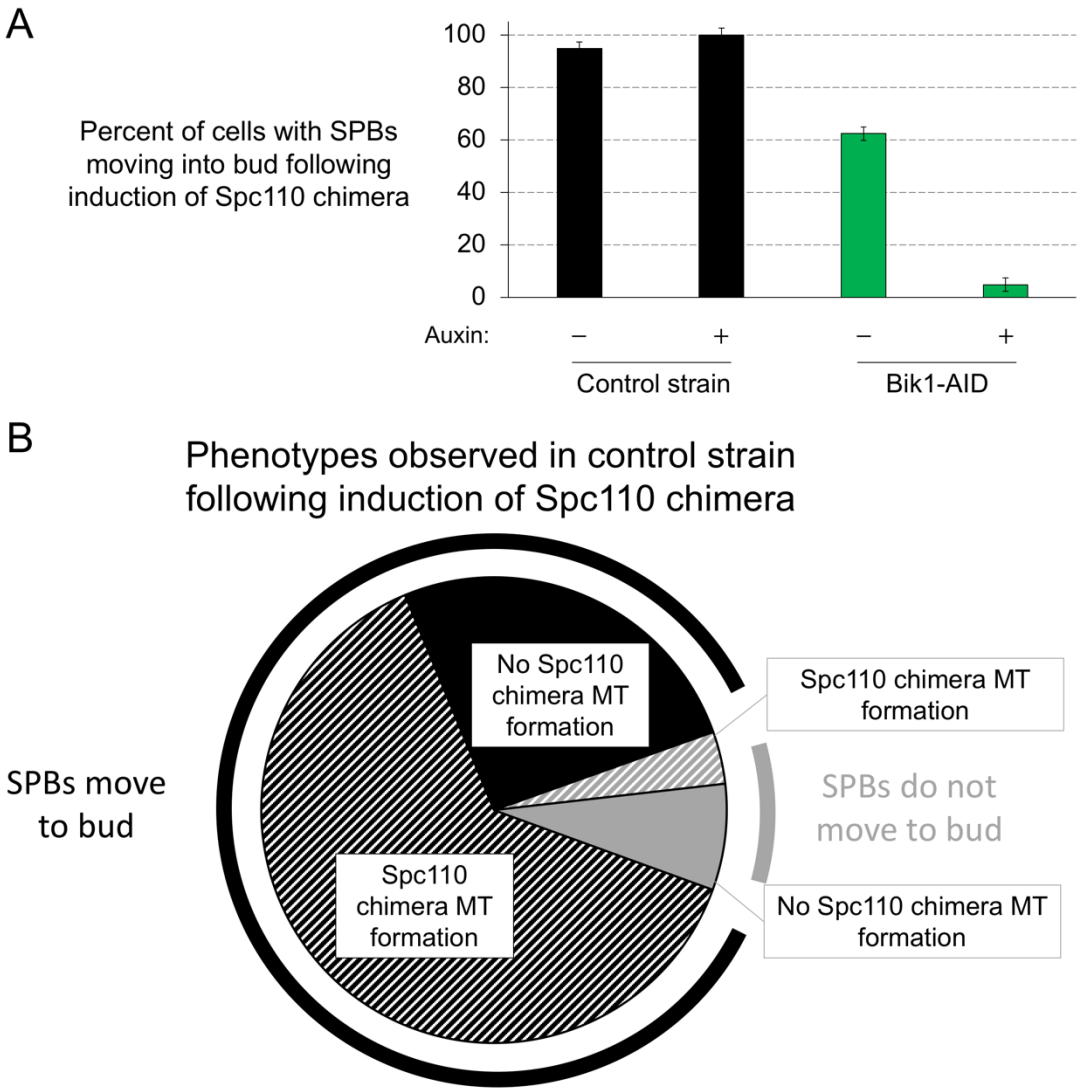

Figure 3.7. Bik1 indirectly promotes MT nucleation at the Spc110 chimera.
(A) Strains with an auxin-inducible degron tag on native Bik1 show decreased SPB movement into buds, and Bik1 depletion reduces SPB movement severely. Values shown are mean ± S.D., N = 3 experiments and ≥ 100 total cells for each condition. (B) In control strains, SPBs and Spc110 chimeras have consistent behavior. The majority of the time, SPBs move into the bud and Spc110 chimeras form a MT bundle in the mother.

The ability of the Spc110 chimera to form MTs correlates with the polymerase activity of Stu2

I have shown that Stu2 is required for MT formation following nocodazole treatment. Here, I found that, through constitutive expression of Stu2 at an exogenous

locus, I could rescue MT formation when native Stu2 was depleted. I hypothesized that I could use this assay to test the effects of mutations in Stu2 on MT formation *in vivo*.

Based on my work studying the relationship between polymerase activity and nucleation activity with XMAP215, I hypothesized that the effect of Stu2 in Spc110 chimera MT formation would correlate with Stu2 polymerase activity. Stu2 polymerase activity can be modulated by inhibiting its ability to bind free tubulin via TOG domains, its ability to localize to the MT lattice via the basic MT binding domain, or its ability to dimerize via the coiled coil domain.

A recent study quantified the polymerase activity of various Stu2 mutants, placing them into three categories: wild-type polymerase activity, moderate polymerase activity, or no activity (Figure 3.8). They found that mutations that block tubulin binding in either TOG1 (R200A, TOG1* mutant) or TOG2 (W519A, TOG2* mutant) resulted in moderate polymerase activity. Mutation of both TOG1 and TOG2 abolished polymerase activity entirely (data from Geyer, et al., [129] reported in Figure 3.8).

The authors found that a Stu2 truncation mutant that maintains the presence of the TOG domains and the MT binding domain but eliminates the dimerization coiled coil domain, Δcc (1-760a.a.), also showed no polymerase activity. Interestingly, polymerase activity of this mutant was partially rescued by alkalifying the MT binding domain by mutating ten uncharged residues to lysine: Δcc-2xbasic (1-760a.a., 10K) showed reduced but measurable polymerase activity. It is thought that the alkalification of the MT binding domain functionally substitutes for the additional MT binding domain that would be present in a Stu2 dimer (data from Geyer, et al., [129] reported in Figure 3.8).

To compare Stu2 mutants with different polymerase activities in my Spc110 chimera assay, I depleted native Stu2 using the auxin-degradation system while constitutively expressing a Stu2 mutant at an exogenous locus. Simultaneous expression of the Spc110 chimera allowed me to compare its activity in the presence of each Stu2 mutant. As predicted, Stu2 polymerase activity correlated with MT formation activity (Figure 3.8).

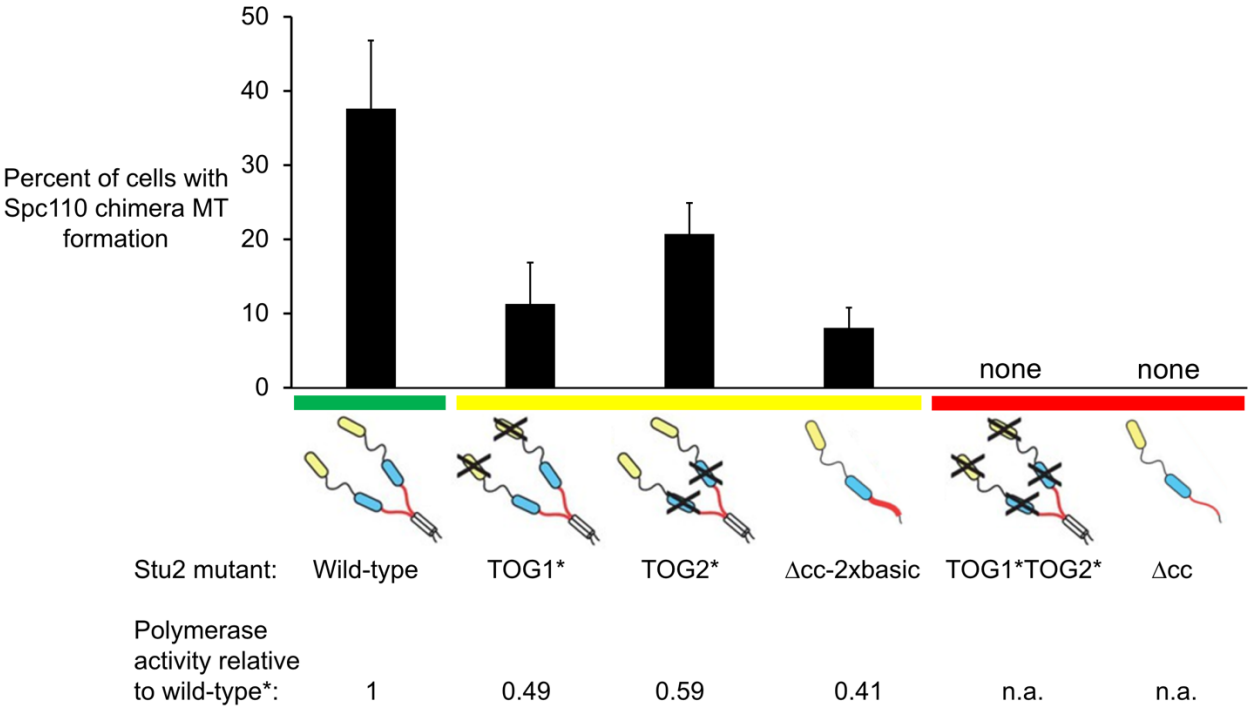

Figure 3.8. Stu2 promotion of MT nucleation at the Spc110 chimera correlates with its reported polymerase activity *in vitro*.

Stu2 mutants fall into categories in their ability to promote MT formation from the Spc110 chimera. These categories are correlated with their polymerase activity *in vitro*. TOG1* contains a single point mutation, R200A, to block free tubulin binding. TOG2* contains a single point mutation, W519A, to block free tubulin binding. Polymerase activity is reported here from Geyer, et al. [129]. MT bundle formation data are mean ± S.D., N ≥ 2 experiments and ≥ 60 total cells for each condition. The percent is the cumulative percent of cells with Spc110 associated MT bundles at the end of a 3 hr period following nocodazole washout.

These results, while in agreement with the principles of my XMAP215 work, also provide a unique information: the biochemical characterizations of polymerase and nucleation activities determined *in vitro* are relevant in cells.

3.4 METHODS

Strain construction

Transformations were performed with a standard lithium acetate method. The Spc110 chimera construct, consisting of Spc110(1-220a.a.)-GCN4-GFP-lacI was integrated at ADE2 with a promoter specific to the transcription factor Z_4EV as previously described [118]. Z_4EV was integrated at CAN1 with a β-estradiol inducible promoter [130]. A 256-lacO repeat was integrated into Chromosome XII as described previously [118]. MAPs were C-terminally tagged with 3-V5 repeat and the auxin-responsive protein IAA7. The ubitiquitin ligase complex protein OsTIR1, necessary for auxin-inducible degradation, was integrated at LEU2. Spc97 was C-terminally tagged with mCherry. Tub1 was N-terminally tagged with GFP.

Electron microscopy

Electron microscopy of MT bundles associated with Spc110 chimera in yeast cells was performed as previously described [131].

γ-tubulin complex recruitment assay

Cells were grown asynchronously in YPD 3xADE at 25°C to 40 Klett, within log phase. Cells were first pulsed with 0.1 μM β-estradiol (Millipore Sigma, St. Louis, Missouri) for 10 minutes and then washed with YPD 3x ADE. Cells were then treated with 15 μg/mL nocodazole (Millipore Sigma) and 1 mM auxin (Millipore Sigma) for 2.5 hours. Cells were pelleted and placed on Lo-Flo agar supplemented with 15 μg/mL nocodazole and

1 mM auxin, as previously described [132]. Cells were imaged using a DeltaVision system (Applied Precision, Issaquah, WA) equipped with IX70 inverted microscope (Olympus, Center Valley, PA), a Coolsnap HQ digital camera (Photometrics, Tucson, AZ), and a U Plan Apo 100X objective (1.35 NA).

For the recruitment assay, the Spc110 chimera was visualized using its integrated GFP and γ-tubulin complexes were visualized with Spc97-mCherry. GFP was imaged with 0.25 s exposures, mCherry was imaged with 0.4 s exposures, and 25 0.2 μm z-sections were taken. Images were binned 2 × 2 with a final resolution of 512 × 512. Recruitment analysis was performed using the Spots colocalization function of Imaris software (Bitplane, Switzerland) (RRID: SCR_007370). Spc110(1-220a.a.)-GCN4-GFP-lacI puncta were located by assigning an XY diameter of 0.4 μm and a Z diameter of 1.3 μm. Spc97-mCherry puncta were located by assigning an XY diameter of 0.4 μm and a Z diameter of 1.8 μm. Quality of spots was manually determined. To exclude background staining of the agar in the total number of puncta, spots were first colocalized to be within 4 μm. These filtered spots were then colocalized within 0.5 μm, and this was the number of recruitment events used for analysis.

MT formation assay

Cells were grown asynchronously in YPD 3xADE at 25°C to 40 Klett, within log phase. Cells were then treated with 15 μg/mL nocodazole for 1 hour. 1 mM auxin was then added and the incubation continued for an additional hour. 0.1 μM β-estradiol was then added and the incubation continued for an additional 1.5 hours. Cells were released from nocodazole and β-estradiol and treated with only 1 mM auxin for 10 minutes. Cells

were pelleted and placed on Lo-Flo agar pads supplemented with auxin. Cells were imaged at 10-minute intervals for 2.5 hours using a DeltaVision system (Applied Precision) equipped with IX70 inverted microscope (Olympus), a Coolsnap HQ digital camera (Photometrics), and a U Plan Apo 100X objective (1.35 NA).

For the MT formation assay, the Spc110 chimera was visualized using its integrated GFP, γ-tubulin complexes were visualized with Spc97-mCherry, and microtubules were visualized using GFP-Tub1. GFP was imaged with 0.25 s exposures, mCherry was imaged with 0.4 s exposures, and 15 0.2 μm z-sections were taken at each time point. Images were binned 2 × 2 with a final resolution of 512 × 512.

MT formation analysis was performed manually using Imaris software (Bitplane).

3.5 ACKNOWLEDGEMENTS

I thank Genevieve Morin, Tamira Vojnar, and Eric Muller for their pioneering work on the Spc110 chimera. I thank Janet Meehl and King Yabut for their work cited in this chapter.

Table 3.2. Strains used in this study.

Strain name	Auxin-inducible degron markers	Spc110 chimera system markers	Other fluorescent markers
RKY7	*STU2-3V5-IAA7::kanMX6/ STU2-3V5-IAA7::kanMX6*	*ade2-1oc/ ADE2::Z4EVpr-SPC110 (1-220a.a.)-GCN4-GFP-lacI*	*SPC97-mCherry::hphMX/ SPC97-mCherry::hphMX*
	LEU2::pDPD1-OsTIR1/ LEU2::pDPD1-OsTIR1	*can1-100/ CAN1::NatMX-ACT1pr-Z4EV*	*URA3::GFP-TUB1/ TUB1*
		ChrXII-R::lacO::TRP1/ ChrXII-R	*NUF2-mTurquoise::HIS3/ NUF2-mTurquoise::HIS3*
RKY14	*STU2-3V5-IAA7::kanMX6/ STU2-3V5-IAA7::kanMX6*	*ade2-1oc/ ADE2::Z4EVpr-SPC110 (1-220a.a.)-GCN4-GFP-lacI*	*SPC97-mCherry::hphMX/ SPC97-mCherry::hphMX*
	LEU2::pDPD1-OsTIR1/ LEU2::pDPD1-OsTIR1	*can1-100/ CAN1::NatMX-ACT1pr-Z4EV*	*NUF2-mTurquoise::HIS3/ NUF2-mTurquoise::HIS3*
		ChrXII-R::lacO::TRP1/ ChrXII-R	
RKY46	*BIM1-3HA-IAA7::kanMX6/ BIM1-3HA-IAA7::kanMX6*	*ADE2::Z4EVpr-SPC110 (1-220a.a.)-GCN4-GFP-lacI/ ade2-1oc*	*SPC97-mCherry::hphMX/ SPC97-mCherry::hphMX*
	LEU2::pDPD1-OsTIR1/ LEU2::pDPD1-OsTIR1	*CAN1::NatMX-ACT1pr-Z4EV/ can1-100*	*URA3::GFP-TUB1/ TUB1*
		ChrXII-R/ ChrXII-R::lacO::TRP1	*NUF2-mTurquoise::HIS3/ NUF2-mTurquoise::HIS3*
RKY47	*BIM1-3HA-IAA7::kanMX6/ BIM1-3HA-IAA7::kanMX6*	*ADE2::Z4EVpr-SPC110 (1-220a.a.)-GCN4-GFP-lacI/ ade2-1oc*	*SPC97-mCherry::hphMX/ SPC97-mCherry::hphMX*
	LEU2::pDPD1-OsTIR1/ LEU2::pDPD1-OsTIR1	*CAN1::NatMX-ACT1pr-Z4EV/ can1-100*	*NUF2-mTurquoise::HIS3/ NUF2-mTurquoise::HIS3*
		ChrXII-R/ ChrXII-R::lacO::TRP1	
RKY36	*BIK1-3HA-IAA7::kanMX6/ BIK1-3HA-IAA7::kanMX6*	*ADE2::Z4EVpr-SPC110 (1-220a.a.)-GCN4-GFP-lacI/ ade2-1oc*	*SPC97-mCherry::hphMX/ SPC97-mCherry::hphMX*
	LEU2::pDPD1-OsTIR1/ LEU2::pDPD1-OsTIR1	*CAN1::NatMX-ACT1pr-Z4EV/ can1-100*	*URA3::GFP-TUB1/ TUB1*
		ChrXII-R/ ChrXII-R::lacO::TRP1	*NUF2-mTurquoise::HIS3/ NUF2-mTurquoise::HIS3*
RKY51	*BIK1-3HA-IAA7::kanMX6/ BIK1-3HA-IAA7::kanMX6*	*ADE2::Z4EVpr-SPC110 (1-220a.a.)-GCN4-GFP-lacI/ ade2-1oc*	*SPC97-mCherry::hphMX/ SPC97-mCherry::hphMX*
	LEU2::pDPD1-OsTIR1/ LEU2::pDPD1-OsTIR1	*CAN1::NatMX-ACT1pr-Z4EV/ can1-100*	*NUF2-mTurquoise::HIS3/ NUF2-mTurquoise::HIS3*
		ChrXII-R/ ChrXII-R::lacO::TRP1	

Blue = Stu2 strains, **Green** = Bim1 strains, **Red** = Bik1 strains

Chapter 4. THE ROLE OF MOTOR PROTEINS IN SPINDLE FORMATION

4.1 INTRODUCTION

High fidelity distribution of genetic material during mitosis requires a dramatic reorganization of MTs: the transition of a disperse cellular MT network into the highly organized bipolar spindle. We know the reorganization of the MT network is dependent on interactions of MT-associated proteins and, specifically, motors. There are several factors that complicate our understanding of these interactions. First, these interactions are often carried out en masse; many copies of a single protein or a protein complex must work together to perform their function efficiently [133]–[138]. Second, proteins involved in assembly can function either redundantly [139]–[143], or antagonistically [139], [144]. Finally, a single protein can have diverse functions [135], [142], [145].

The web of protein interactions during mitotic spindle assembly is clearly complex. The Spc110 chimera, in contrast, offers a simplified system to examine specific roles of motor proteins in bundle assembly. Without SPBs to help structure these MT bundles, the Spc110 chimera may be more sensitive to perturbation relative to the spindle and therefore reveal subtle roles for motor proteins. Following nocodazole washout, the Spc110 chimera forms MT bundles with a distinctive phenotype: capped minus ends and two distinct minus end clusters visible by fluorescent microscopy (Figure 3.2). Here I use the Spc110 chimera to examine the roles of the plus-end directed motor Kip3, and the minus-end direction motor complex protein Vik1, during MT formation and bundle assembly.

4.2 KINESIN-8 MOTOR KIP3 PROMOTES MICROTUBULE BUNDLE FORMATION AND ASSEMBLY AT THE SPC110 CHIMERA

Kip3 is a member of the plus-end directed kinesin-8 family of motors. Kinesin-8 motors have a MT length-dependent effect on MTs: destabilization of long MTs and stabilization of short MTs [70]–[76]. This activity is important for, among other things, controlling metaphase spindle length, as deletion of Kip3 results in longer mitotic spindles [77], [146], [147]. Further, the fission yeast homologs, Klp5 and Klp6, were shown to promote microtubule nucleation *in vivo* [148] and *in vitro* [149].

Knowing this, I asked whether and how Kip3 would affect MT bundle assembly from the Spc110 chimera. I first asked whether Kip3 was required for MT formation by measuring the rate at which MT bundles form at the Spc110 chimera following nocodazole washout. I found that the mutant had a slight delay in bundle formation but, by 3 hours, the Spc110 chimera formed the same number of MT bundles in *kip3Δ/kip3Δ* cells as in control cells (Figure 4.1). This result supports a subtle role for Kip3 in overall MT formation, and potentially MT nucleation, in budding yeast nuclei.

Further observation of these cells revealed a role for Kip3 in MT bundle organization as well. Even at the latest time point observed (t = 3 hr), the MT bundles associated with the Spc110 chimera in *kip3Δ/kip3Δ* cells are less consistently organized, appearing extended compared to control cells (Figure 4.2, panels 1 and 2) and sometimes extending the full length of a large budded cell (Figure 4.2, panel 3).

This result is in agreement with previous reports of Kip3 controlling mitotic spindle length [77], [146], [147].

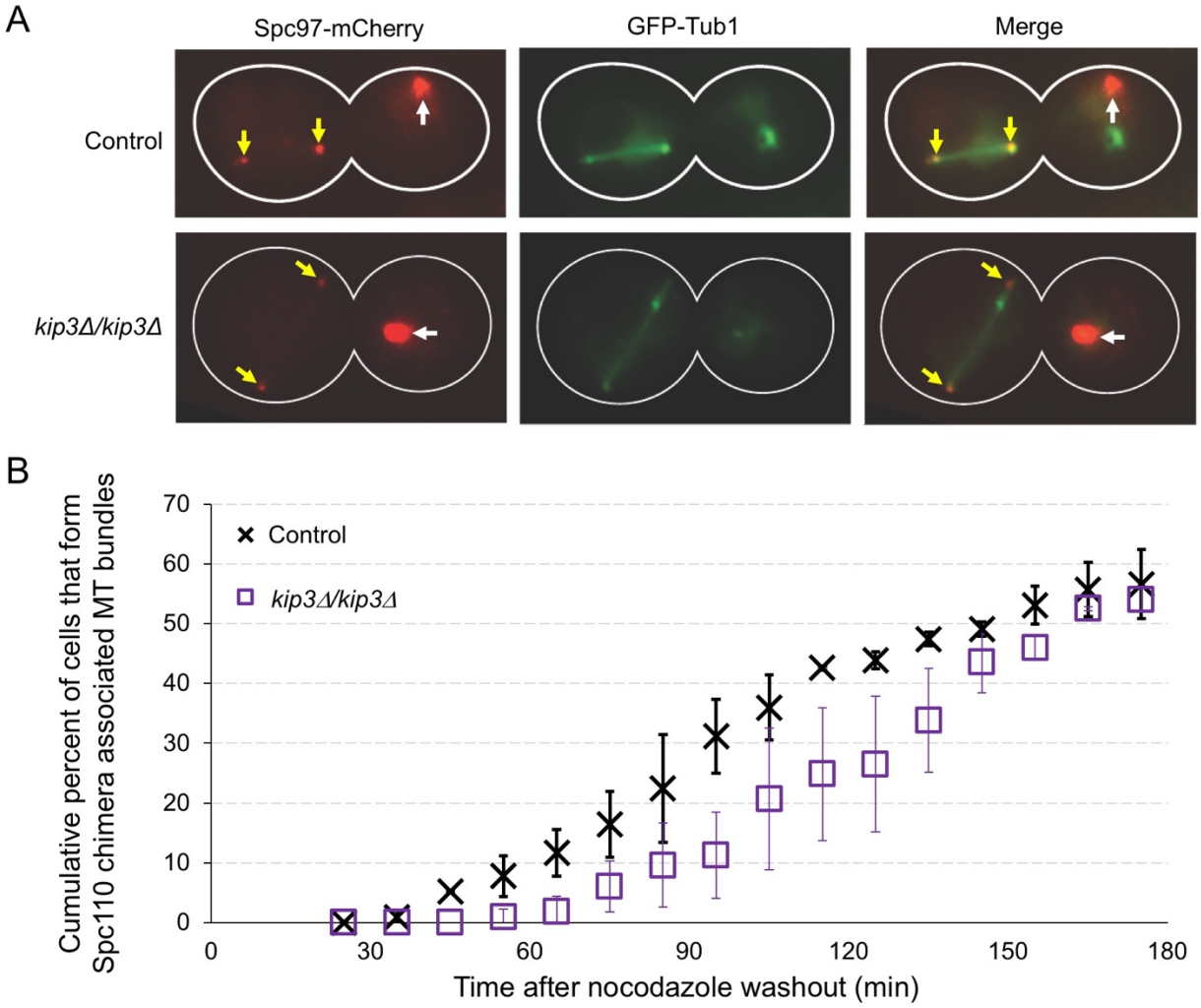

Figure 4.1. Kip3 does not affect MT formation from the Spc110 chimera.
(A) Representative cells show that Kip3 does not affect MT formation from the Spc110 chimera. White arrows denote Spc97-mCherry puncta associated with the SPB, and yellow arrows denotes Spc97-mCherry puncta associated with the Spc110 chimera. (B) *Δkip3/Δkip3* cells form MT bundles between Spc110 chimera puncta similarly to control cells over 2.5 hours. Values shown are mean ± S.D., N = 3 experiments and ≥ 100 total cells for each condition.

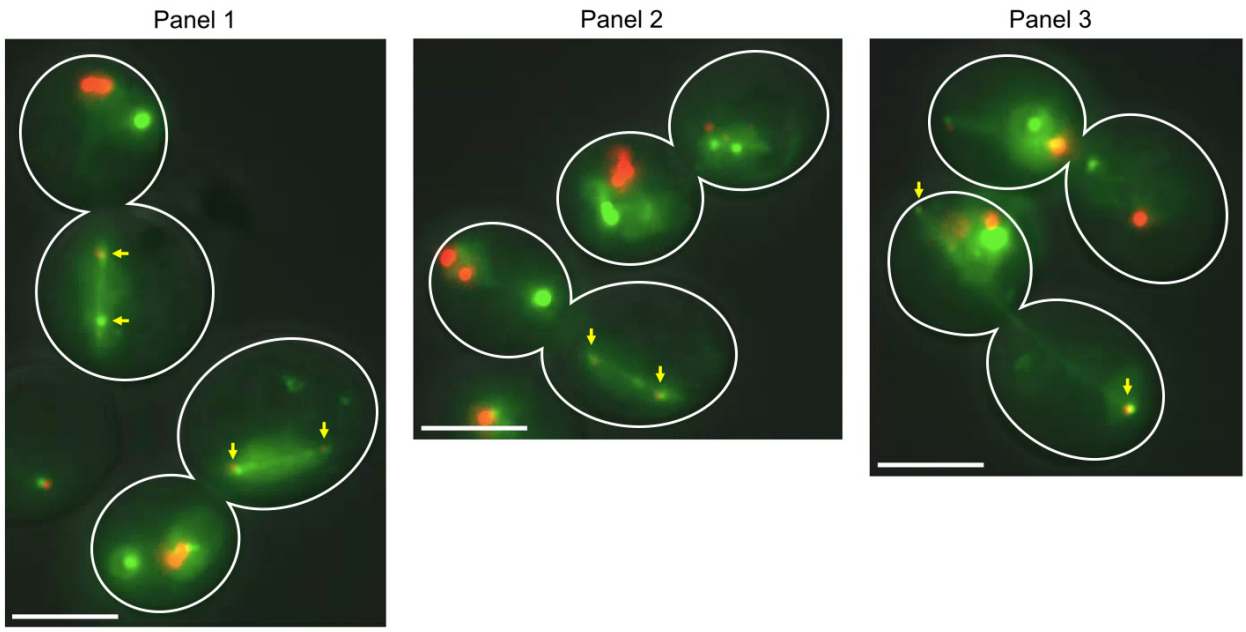

Figure 4.2. Spc110 chimera associated MT bundles are long and extended in *kip3Δ/kip3Δ* cells.

Representative *kip3Δ/kip3Δ* cells show that Spc110 chimera robustly forms MT bundles, many of which are extended. Panel 3 includes a cell in which the MT bundle has extended across the entire large-budded cell, separating the Spc110 chimera and γ-tubulin complex puncta to each side of the cell. Images taken at t = 3 hours. Yellow arrows denote distal Spc97-mCherry puncta associated with the Spc110 chimera. Scale bars are 7.5 μm.

4.3 KINESIN-14 MOTOR COMPLEX PROTEIN VIK1 PROMOTES MICROTUBULE ATTACHMENTS ON THE NUCLEAR FACE OF THE SPINDLE POLE BODY

One family of motors proteins, the kinesin-14 motors, has been implicated in both aspects of spindle assembly: MT nucleation and MT organization. First, kinesin-14 homologs bind directly to the γ-tubulin complex in fission yeast [150]–[152] and in higher eukaryotes [153]. In fission yeast, this interaction was shown to suppress MT nucleation [151]. Second, kinesin-14 homologs play a role in MT minus end focusing in *D.*

melanogaster and *H. sapiens* homologs [154]–[156]. A role for kinesin-14 motors in MT minus end focusing in budding yeast is yet to be determined.

Of the two budding yeast kinesin-14 motor protein complexes, Kar3Vik1 and Kar3Cik1, there is evidence that Kar3Vik1 specifically plays a role in MT nucleation and organization. While there is no evidence that Vik1 interacts with the γ-tubulin complex (unpublished data, Davis lab), it does robustly localize to the poles of the mitotic spindle [123]. Furthermore, the Asbury lab has shown that SPBs depleted of Vik1 have weaker MT attachments compared to wild-type SPBs, indicating a direct or indirect effect of Vik1 on the SPB-MT interface (Figure 4.3, data collected by Krishna Sarangapani and Kim Fong). Additionally, mutations that weaken the binding of the coiled coil protein, Spc110, to either the SPB core, calmodulin, or the γ-tubulin complex are synthetically lethal with Kar3 and Vik1, but not Cik1 [157].

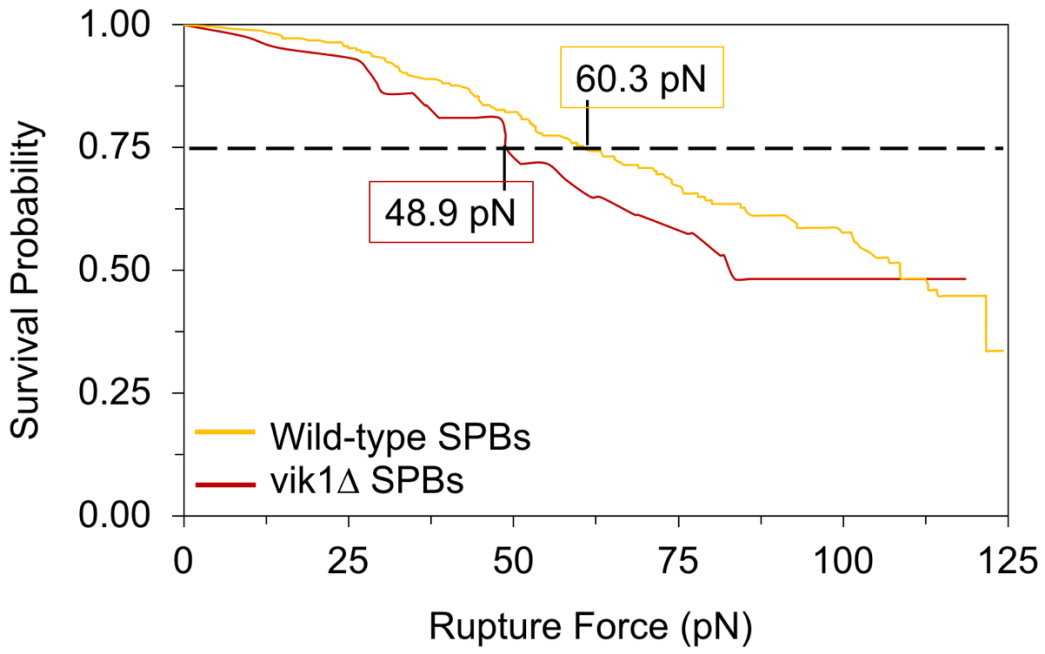

Figure 4.3. Vik1 promotes attachment strength of MTs to SPBs.
SPBs are purified from *S. cerevisiae*, and MT attachment strength is measured using the laser trap. The SPB-MT attachment strength at 75% for wild-type SPBs is ~60 pN (N=95) and ~49 pN for vik1Δ SPBs (N=17). Data collected and analyzed by Krishna Sarangapani and Kim Fong of the Asbury lab.

For these reasons, I asked whether Vik1 affects MT formation or bundle organization at the Spc110 chimera. Using *vik1Δ/vik1Δ* cells, I monitored MT formation from the Spc110 chimera following nocodazole washout and found that loss of Vik1 had no effect on the rate of MT formation (Figure 4.4). Therefore there is no evidence that Vik1 promotes MT nucleation from the Spc110 chimera.

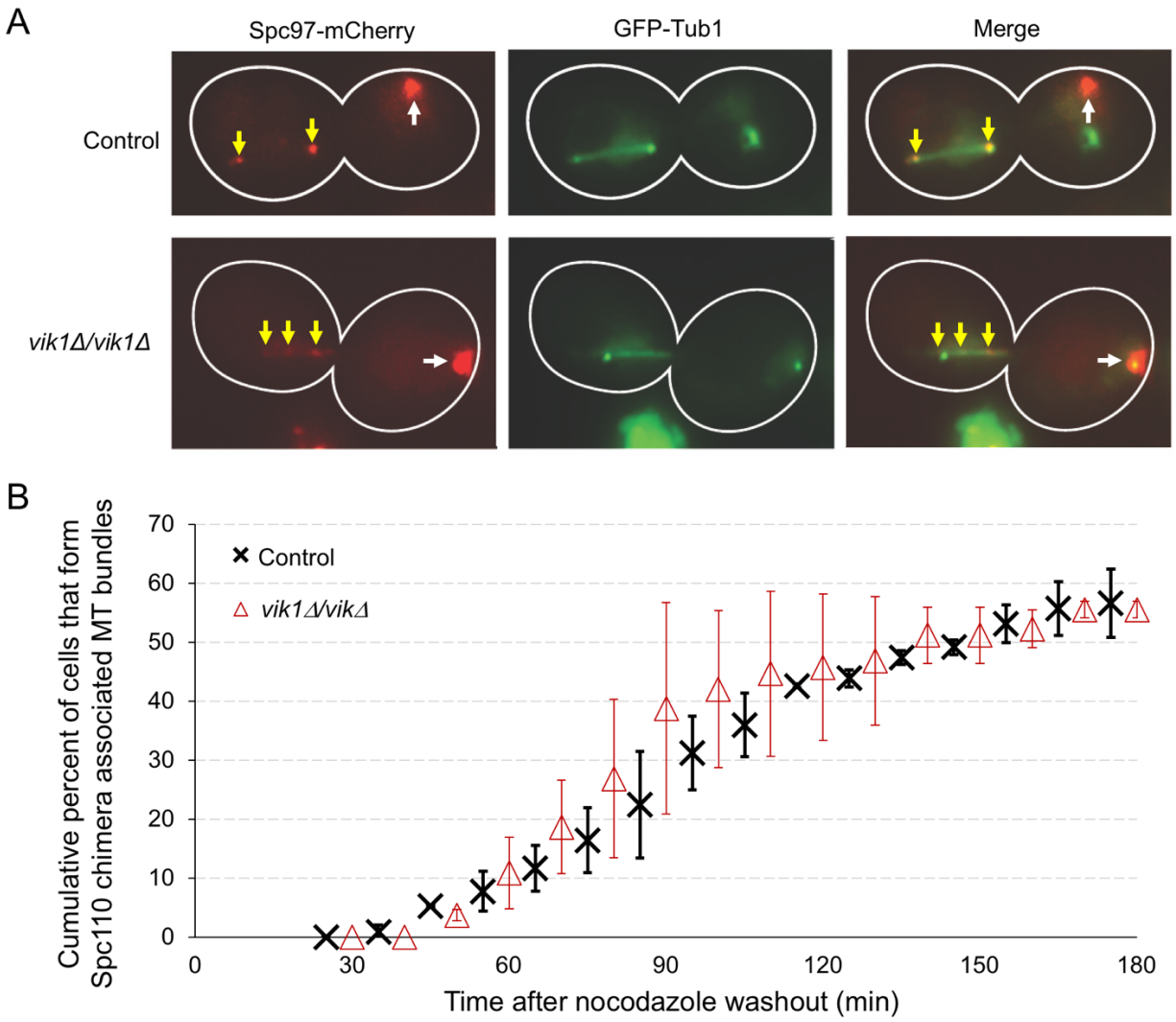

Figure 4.4. Vik1 does not affect MT formation from the Spc110 chimera.
(A) Representative cells show that Vik1 does not affect the rate of MT formation from the Spc110 chimera. White arrows denote Spc97-mCherry puncta associated with the SPB, and yellow arrows denotes Spc97-mCherry puncta associated with the Spc110 chimera. (B) *Δvik1/Δvik1* cells form MT bundles between Spc110 chimera puncta at similar rates to control cells over 3 hours. Values shown are mean ± S.D., N = 3 experiments and ≥ 100 total cells for each condition.

However, Vik1 promotes a distinct morphology of MT bundles associated with the Spc110 chimera: MT minus end clustering on distal sides of the bundle. In *vik1Δ/vik1Δ* cells, the γ-tubulin complex puncta associated with the Spc110 chimera were more disperse along the bundle of MTs, relative to wild-type (Figure 4.5). To

further analyze these phenotypes, I measured the Spc97-mCherry intensity along Spc110 chimera MT bundles in the control and *vik1Δ/vik1Δ* cells and compared their distributions. Specifically, I used the root-mean-square error (Equation 1):

$$RMSE = \sqrt{\frac{1}{n}\sum_{i=1}^{n}(y_i - \hat{y}_i)^2} \quad (4.1)$$

where n = number of Spc110 chimera MT bundles measured, y_i = Spc97-mCherry intensity at a given point, and $\hat{y}_i$ = mean Spc97-mCherry intensity across the MT bundles. When γ-tubulin complexes cluster, the Spc97-mCherry intensity at any given point will be further from the mean Spc97-mCherry intensity of the MT bundle. Using this measure, Vik1 significantly promotes MT minus end clustering ($p < 0.001$, Figure 4.5). This is the first evidence of Vik1 clustering of MT minus ends.

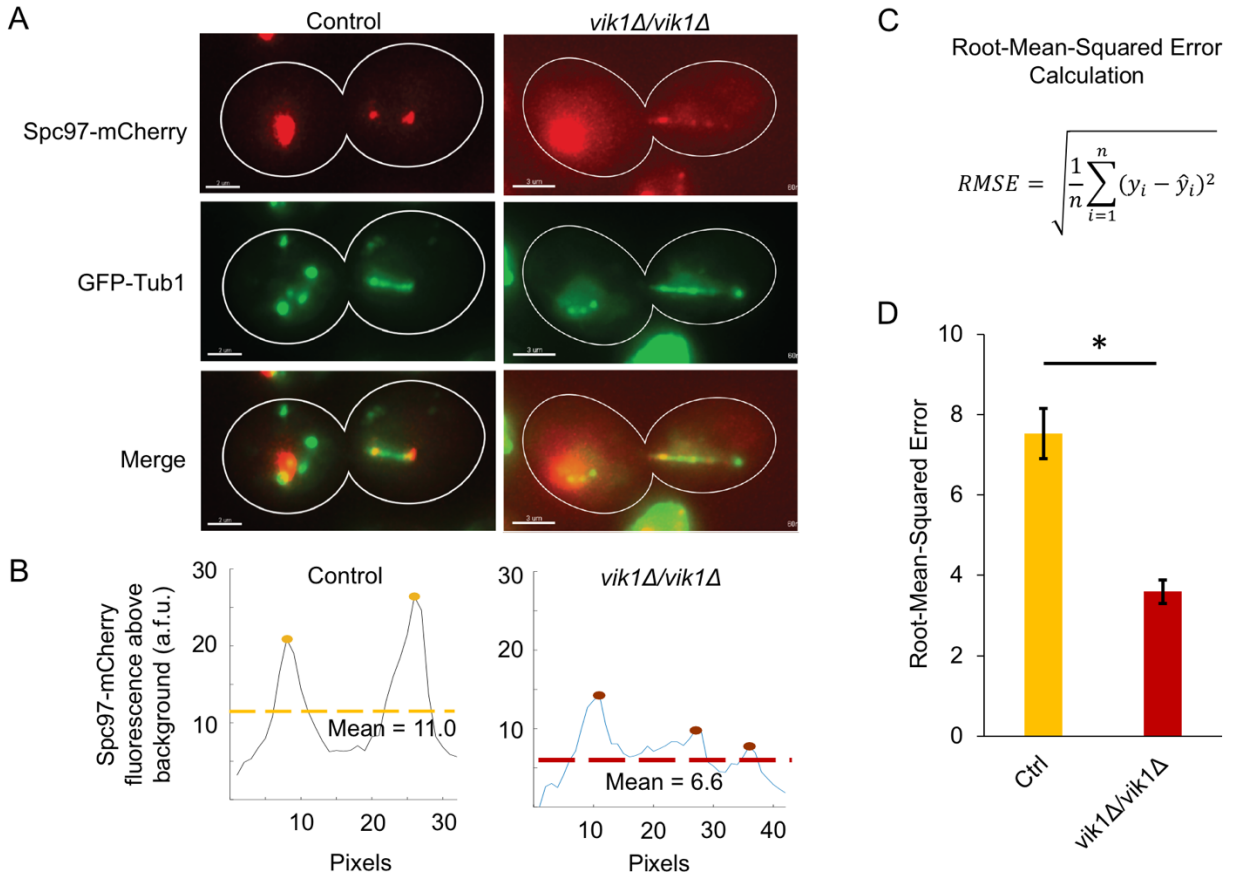

Figure 4.5. Vik1 significantly promotes γ-tubulin complex clustering.
(A) Representative cell shows that (left) the Spc110 chimera characteristically forms MT bundles with distinct γ-tubulin complex puncta at each end. In contrast, (right) in *Δvik1/Δvik1* cells, the Spc110 chimera forms MT bundles that are poorly organized, with disperse γ-tubulin complexes along the bundle rather than forming puncta at each end. Note that the Spc97-mCherry display has been adjusted in these images to see the Spc110 chimera associated γ-tubulin complexes, but that this does not affect the quantification of fluorescence intensity. (B) Line plots of the total Spc97-mCherry intensity at a given pixel along the Spc110 chimera associated MT bundle (data plotted is the sum intensity across a 10-pixel line) in (left) control cells and (right) *Δvik1/Δvik1* cells. (C) Root-mean-squared error calculation, where n = number of Spc110 chimera MT bundles measured, y_i = Spc97-mCherry intensity at a given point, and $\hat{y}_i$ = mean Spc97-mCherry intensity across the MT bundles. (D) Vik1 significantly promotes γ-tubulin complex clustering (*p<0.001). Data plotted are means ± S.D. (control N = 28, *vik1Δ* N = 33).

4.4 METHODS

Strain construction

Transformations were performed with a standard lithium acetate method. The Spc110 chimera construct, consisting of Spc110(1-220a.a.)-GCN4-GFP-lacI was integrated at ADE2 with a promoter specific to the transcription factor Z_4EV as previously described [118]. Z_4EV was integrated at CAN1 with a β-estradiol inducible promoter [130]. A 256-lacO repeat was integrated into Chromosome XII as described previously [118]. Spc97 was C-terminally tagged with mCherry. Tub1 was N-terminally tagged with GFP.

MT formation assay

Cells were grown asynchronously in YPD 3xADE at 25°C to 40 Klett, within log phase. Cells were then treated with 15 μg/mL nocodazole for 2 hours. 0.1 μM β-estradiol was then added and the incubation continued for an additional 1.5 hours. Cells were released from nocodazole and β-estradiol into YPD 3xADE for 10 minutes. Cells were pelleted and placed on Lo-Flo agar pads. Cells were imaged at 10-minute intervals for 2.5 hours using a DeltaVision system (Applied Precision) equipped with IX70 inverted microscope (Olympus), a Coolsnap HQ digital camera (Photometrics), and a U Plan Apo 100X objective (1.35 NA).

The Spc110 chimera was visualized using its integrated GFP, γ-tubulin complexes were visualized with Spc97-mCherry, and microtubules were visualized using GFP-Tub1. GFP was imaged with 0.25 s exposures, mCherry was imaged with 0.4 s exposures,

and 15 0.2 μm z-sections were taken at each time point. Images were binned 2 × 2 with a final resolution of 512 × 512.

MT formation analysis was performed manually using Imaris software (Bitplane).

SPB purification

SPBs were purified exactly as previously described [158].

Laser trapping assay

MTs were nucleated from SPBs and attachment strength was measured using the laser trap exactly as previously described [159].

4.5 ACKNOWLEDGEMENTS

I thank Genevieve Morin, Tamira Vojnar, and Eric Muller for their pioneering work on the Spc110 chimera. I thank Kim Fong and Krishna Sarangapani for their work cited in this chapter.

Table 4.3. Strains used in this study.

Strain name	Deletion	Spc110 chimera system markers	Other fluorescent markers
RKY10	*VIK1Δ::NatMX/ VIK1Δ::NatMX*	*ADE2::Z4EVpr-SPC110 (1-220a.a.)-GCN4-GFP-lacI/ ade2-1oc*	*SPC97-mCherry::hphMX/ SPC97-mCherry::hphMX*
		CAN1::NatMX-ACT1pr-Z4EV/ can1-100	*URA3::GFP-TUB1/ TUB1*
		ChrXII-R::lacO::TRP1/ ChrXII-R	*NUF2-mTurquoise::HIS3/ NUF2-mTurquoise::HIS3*
RKY49	*KIP3Δ::HIS3/ KIP3Δ::HIS3*	*ADE2::Z4EVpr-SPC110 (1-220a.a.)-GCN4-GFP-lacI/ ade2-1oc*	*SPC97-mCherry::hphMX/ SPC97-mCherry::hphMX*
		can1-100/ CAN1::NatMX-ACT1pr-Z4EV	*TUB1/ URA3::GFP-TUB1*
		ChrXII-R::lacO::TRP1/ ChrXII-R	

Green = *vik1Δ* strains, Purple = *kip3Δ* strains.

Chapter 5. CONCLUSIONS

The highly organized microtubule network of the mitotic spindle is formed both by targeted nucleation of new MTs and by the transport and regulation of existing MTs [160]–[163]. During my tenure as a graduate student, I investigated both MT nucleation and MT bundle organization. In my studies of MT bundle assembly, I characterized roles for Bik1, Kip3, and Vik1 that provide new evidence for their respective roles previously characterized in other systems or other organisms. In my studies of MT nucleation, I first report a new role for Bim1, the yeast homolog of the end-binding (EB) family. Then I investigate the role of the chTOG/XMAP215 family of MT polymerases, both *in vitro* and *in vivo*.

5.1 MICROTUBULE ORGANIZATION

The ectopic MTOC developed in the Davis lab has proven an invaluable tool for studying MT bundle organization, fortifying previous results showing the involvement of Bik1 in SPB positioning and elucidating new roles for Kip3 and Vik1 in MT nucleation and minus end clustering, respectively.

In >90% of cells expressing an ectopic MTOC, the SPB initially moves to the bud but SPBs eventually form a bipolar spindle and separate, one to the mother cell and one to the bud. In >30% of mother cells, the ectopic MTOC recruits the γ-tubulin complex and a MT array forms between two focused clusters of γ-tubulin complexes. I have found that Bik1, Kip3, and Vik1 promote different steps of this process.

Bik1 is a member of the CLIP170 family proteins, characterized by their plus-end localization and their interactions with other microtubule-associated proteins.

Specifically, Bik1 participates in SPB positioning, via the dynein-dependent pathway and the Kar9-dependent pathway. Bik1, among other proteins, promotes the localization of dynein and Kar9 to the plus-ends of astral MTs [126], [134], [164]. There, cellular cortex protein complexes act to exert force on astral MTs which helps position the SPBs and the mitotic spindle at the bud neck for transition to anaphase. My results with the ectopic MTOC reinforce this role for Bik1 in SPB positioning. Notably, the percent of cells in which SPBs formed a bipolar spindle was unaffected by depletion of Bik1, despite a previous report that Bik1 is required for SPB separation following duplication [165].

Kip3 is a member of the plus-end directed kinesin-8 family of motors that function as length-dependent MT destabilizers. This family regulates MT lengths, specifically by reducing the length of metaphase spindles [77], [146], [147]. My results reinforce this role, as deletion of Kip3 resulted in abnormal, extended MT arrays between ectopic MTOCs, sometimes extending the entire length of the mother and bud.

The kinesin-8 motors in fission yeast have been shown to promote nucleation [148], [149], but no such role had been determined for Kip3 in budding yeast. My results provide the unique finding that Kip3 promotes *de novo* MT formation in cells, as deletion of Kip3 resulted in a delay associated with MT formation. The mechanism of kinesin 8's role in MT nucleation is unknown in either budding or fission yeast.

Vik1 participates in one of the two kinesin-14 motor complexes in budding yeast. In higher eukaryotes, kinesin-14 motors promote MT minus end focusing [154]–[156], which is required for pole integrity during mitosis. My work with the ectopic MTOC shows that Vik1 performs a similar function in budding yeast, by promoting γ-tubulin

complex clustering. It is not clear whether Vik1 functions to transport minus ends of MTs in a poleward direction, or if it functions to stabilize interactions between MT minus ends that have been clustered by some other mechanism. Unpublished data from the Asbury lab showing that Vik1 promotes SPB-MT attachment strength argues for the latter case, as does the finding that Vik1 is synthetically lethal with Spc110 mutations that weaken binding interfaces of the SPB [157].

The ectopic MTOC has revealed roles for Kip3 and Vik1 that may have been too subtle to be detected in the context of the mitotic spindle. The assay is likely robust enough to test for phenotypes associated with mutations in these proteins and provides a unique yet relevant system in which to study MT array organization.

MICROTUBULE NUCLEATION

Bim1 promotes microtubule formation

Bim1 is a member of the functionally divergent EB family. Whether EB proteins perform the same function in purified systems and in cells is unclear. While EB proteins have been shown to suppress catastrophes in cells [166], [167], in cell extract [168], and *in vitro* [125], they have also been found to promote catastrophe in purified systems [125], [166].

Members of this family have been shown to promote MT nucleation. Human EB1 and EB3 promote spontaneous tubulin assembly [125], and fission yeast Mal3 has been shown to promote MT from interpolar MTOCs [167], an organelle that is unique to fission yeast. It has been hypothesized that EB family members promote MT nucleation by stabilizing interactions between tubulin dimers, as they are known to bind the MT lattice between tubulin dimers [169], [170].

My results show that Bim1 promotes *de novo* MT formation in cells, as it is required for MT formation at both the SPBs and at ectopic MTOCs. How Bim1 promotes MT formation is not clear. I have shown that it does not promote recruitment of the γ-tubulin complex to the ectopic MTOC, nor is it required for recruitment.

Based on the previously reported actions of EB proteins, it is possible that Bim1 promotes MT formation either directly by stabilizing lateral dimer-dimer interfaces in nucleation intermediates or through interactions with any of the many other microtubule-associated proteins with which Bim1 associates [171]. Domain analysis on Bim1 has established the presence of an N-terminal calponin homology domain (approximately a.a. 32-100) [170], and a C-terminal region (a.a. 145-344) that interacts with other microtubule-associated proteins such as Stu2 and Bik1 [172] and contains a coiled coil through which Bim1 dimerizes [172]. To determine if the essential role Bim1 plays in MT nucleation at the Spc110 is through an interaction with tubulin, domain analysis targeting these various functions could be tested for efficiency at the Spc110 chimera.

If Bim1's interactions with tubulin and microtubules specifically are required for MT nucleation at the Spc110 chimera, what is the mechanism? As mentioned above, EB proteins uniquely bind the MT lattice across protofilaments [169], [170], and human EB1 and EB3 promote tubulin sheet closure into a MT *in vitro* [125]. These activities suggest a possible role in the stabilization of lateral interactions between tubulin dimers.

This promotion of lateral contacts is also the theorized role for γ-tubulin, the MT template. Future researchers could test for overlapping function *in vivo* by testing for

synthetic lethality between γ-TuRC and EB proteins[5]. Redundancy of function *in vivo* could be tested by analyzing the phenotype when γ-tubulin expression is reduced or depleted while the EB protein of choice is overexpressed (and/or vice versa) [173]. Similarly, redundancy of function can be tested using the classical light scattering assay, much as I tested for synergy between XMAP215 and γ-tubulin.

The XMAP215 family as nucleators

For many years, XMAP215 was thought to promote nucleation through its ability to promote the addition of tubulin dimers to MT nucleation intermediates. Recently, this hypothesis was modified based on new evidence that the C-terminus of XMAP215 binds to γ-tubulin [92]. Under this new model, XMAP215 binds γ-tubulin directly to promote MT nucleation synergistically.

The C-terminus of chTOG/XMAP215 family members is an unstructured region that promotes its ability to diffuse on the MT lattice. Now reported to bind γ-tubulin, the C-terminal tail binds many other proteins promiscuously, having been reported to interact with the cytoplasmic linker protein (CLIP170) family [174], the end-binding (EB) family [175], the transforming acidic coiled coil (TACC) protein family [176], [177], kinesin-8 Kip3 [178], kinesin-14 Kar9 [179], SPB outer plaque component Spc72 [120], [180], outer kinetochore proteins such as Ndc80 [181], and the degradation pathway proteins SUMO and Ubc9 [182].

[5] Deletion of Bim1 has been shown to be synthetic lethal with γ-tubulin mutants that perturb MT dynamics, Y445D and Δdsyl [173].

For my work, I asked whether the binding interaction between γ-tubulin and XMAP215 was sufficient to promote synergistic action during MT nucleation. Across various concentrations of XMAP215 and across XMAP215 mutants of varying polymerase activities, I found no functional synergy with γ-tubulin filaments.

My work shows that the polymerase activity of XMAP215 correlates with its ability to nucleate, regardless of the number of TOGs or the presence of the C-terminal tail. Further each XMAP215 construct shows additive action with γ-tubulin, again regardless of the number of TOGs or the presence of the C-terminal tail. These results show that XMAP215 largely functions to promote tubulin addition to nucleation intermediates, independently of γ-tubulin.

Therefore the previously reported synergy between XMAP215 and γ-tubulin must be unique to the γ-TuRC. XMAP215 may in fact interact with the additional exterior proteins of the γ-TuRC (GCP2-6, MZT1, or MZT2). Ideally, the light scattering experiments could be performed comparing XMAP215 with *X. laevis* γ-TuRC.[6]

It may be that XMAP215 does not bind to the γ-TuRC for functional synergy, but rather specifically promotes growth of nucleation intermediates that are associated with the γ-TuRC. The XMAP215 family localizes to plus ends (growing or shrinking) [183], [184]. The intermediates that form on the γ-TuRC may more closely resemble a MT plus end compared to those that form on laterally associated γ-tubulin filaments.

Regardless, my work shows that XMAP215 promotes MT nucleation and that this ability correlates with its polymerase activity. Some would argue that, knowing this,

[6] Our collaborators that provided the γ-tubulin (Agard lab of UCSF) are not able to purify γ-TuRC, and other labs that purify γ-TuRC struggle to purify enough protein for their own purposes.

XMAP215 is not a nucleator at all; some define a nucleator by whether it alters the nucleation pathway/intermediates, and it is not clear whether a polymerase would do so or whether it would increase the flux through the existing pathway.

When considering these results in the context of the cell, I define a nucleator as a factor that promotes *de novo* formation of MTs. Under this designation, my work defines XMAP215 as a nucleator, as do the studies that show that XMAP215 homologs promote MT formation from templates including the γ-TuRC, isolated centrosomes, and GMPCPP-stabilized seeds [42], [43], [90]–[93].

If polymerase activity correlates directly with promotion of MT nucleation *in vitro*, does it correlate with promotion of MT nucleation *in vivo*? Due to the experimental ease of studying live *S. cerevisiae*, I investigated this question using the budding yeast chTOG/XMAP215 homolog, Stu2. I hypothesized that the polymerase activity of Stu2 would correlate with its effect on MT formation in the nucleus. The polymerase activities of various Stu2 mutants were recently reported [129]. and fell broadly into three categories: full activity (full-length Stu2), moderate (TOG1*, TOG2*, Δcc-2xbasic), and no activity (TOG1*TOG2*, Δcc). Stu2 is essential for cell viability, and depletion of Stu2 in asynchronous cells results in metaphase arrest. Therefore, to investigate the effect of Stu2 *in vivo* in a novel way, I used an ectopic MTOC. I found that higher polymerase activity of Stu2 mutants correlates with higher levels of *de novo* MT formation at ectopic MTOCs. It is not clear how Stu2 promotes MT formation. Based on my XMAP215 results, I hypothesize that Stu2 promotes early stages of tubulin polymer formation, and that polymerase activity is required for this role.

Looking forward, the field of MT nucleation has reached an interesting era of research. We are questioning even the basic definition of nucleation. For years, it was thought that the MT must have some defined nucleus, as actin does. This nucleus was thought to contain a certain number of tubulin dimers, on the order of 10 [56], [57]. This so-called “critical nucleus” would represent the transition from nucleation to elongation. Yet no model could fully parameterize the nucleation model to fit the kinetic data of tubulin assembly light scattering experiments.

Recently it was proposed that perhaps a single nucleus does not exist, but that the process of MT formation happens through accretion instead [59]. That is, tubulin dimers associate to form polymers in huge variety of different arrangements, and that as the polymer grows, the more likely it is to continue to grow. This of course complicates the nucleation model mathematically, and yet it is does not mean that it is impossible to model. The authors of the accretion model offer new parameters not considered in previous models and show their model closely matches the kinetic data, and yet their fit is still not perfect.

The authors of the accretion model begin by parameterizing the dissociation constants of tubulin dimer-dimer interactions, such as lateral interactions, longitudinal interactions, and interactions on both surfaces simultaneously (so-called “corner interactions.”), They go on to include a variation on the pathway of nucleation intermediates, in which tubulin dimers are added in pairs in addition to being added individually. They also modify the model to include a penalty when three or more tubulin dimers interact laterally, that represents the strain of the center tubulin(s) to straighten. Likely there are still more parameters to consider. I would hypothesize that the

“straightening penalty,” represented as a single value in their model, may vary depending on the size of the tubulin oligomer.

Whether we can fully parameterize MT nucleation would seem to be limited only by technology, logic, and creativity. If it is possible, the experimental impact would be invaluable. We could first consider the role that a specific MT nucleators plays. Does it promote lateral interactions? Longitudinal? Does it promote conformational changes that occur to tubulin as it is incorporated into a lattice? Does it promote tubulin sheet closure? By altering that parameter of the model, we could predict the experimental data and compare it to observations. Perhaps most importantly, an accurate, tunable model would reflect a perfect understanding of the process, which is the ultimate goal.

Chapter 6. REFERENCES

[1] "Zellsubstanz, Kern und Zelltheilung (1882 edition) | Open Library." [Online]. Available: https://openlibrary.org/books/OL20780192M/Zellsubstanz_Kern_und_Zelltheilung. [Accessed: 13-Apr-2020].

[2] "Chromosomal Abnormalities: Aneuploidies | Learn Science at Scitable." [Online]. Available: https://www-nature-com.offcampus.lib.washington.edu/scitable/topicpage/chromosomal-abnormalities-aneuploidies-290/. [Accessed: 13-Apr-2020].

[3] S. L. Thompson and D. A. Compton, "Proliferation of aneuploid human cells is limited by a p53-dependent mechanism," *J. Cell Biol.*, vol. 188, no. 3, pp. 369–381, Feb. 2010, doi: 10.1083/jcb.200905057.

[4] B. R. Williams *et al.*, "Aneuploidy Affects Proliferation and Spontaneous Immortalization in Mammalian Cells Downloaded from," *Science (80-.).*, vol. 322, no. 5902, pp. 703–709, 2008.

[5] K. Jeganathan, L. Malureanu, D. J. Baker, S. C. Abraham, and J. M. Van Deursen, "Bub1 mediates cell death in response to chromosome missegregation and acts to suppress spontaneous tumorigenesis," *J. Cell Biol.*, vol. 179, no. 2, pp. 255–267, Oct. 2007, doi: 10.1083/jcb.200706015.

[6] G. J. P. L. Kops, D. R. Foltz, and D. W. Cleveland, "Lethality to human cancer cells through massive chromosome loss by inhibition of the mitotic checkpoint," *Proc. Natl. Acad. Sci. U. S. A.*, vol. 101, no. 23, pp. 8699–8704, Jun. 2004, doi: 10.1073/pnas.0401142101.

[7] M. Li *et al.*, "The ATM-p53 pathway suppresses aneuploidy-induced tumorigenesis," *Proc. Natl. Acad. Sci. U. S. A.*, vol. 107, no. 32, pp. 14188–14193, Aug. 2010, doi: 10.1073/pnas.1005960107.

[8] A. D. Silk, L. M. Zasadil, A. J. Holland, B. Vitre, D. W. Cleveland, and B. A. Weaver, "Chromosome missegregation rate predicts whether aneuploidy will promote or suppress tumors," *Proc. Natl. Acad. Sci. U. S. A.*, vol. 110, no. 44, pp. E4134-41, Oct. 2013, doi: 10.1073/pnas.1317042110.

[9] R. M. Naylor and J. M. van Deursen, "Aneuploidy in Cancer and Aging," *Annu. Rev. Genet.*, vol. 50, no. 1, pp. 45–66, Nov. 2016, doi: 10.1146/annurev-genet-120215-035303.

[10] S. L. Jaspersen and M. Winey, "THE BUDDING YEAST SPINDLE POLE BODY: Structure, Duplication, and Function," *Annu. Rev. Cell Dev. Biol*, vol. 20, pp. 1–28, 2004, doi: 10.1146/annurev.cellbio.20.022003.114106.

[11] J. V. Kilmartin, "Lessons from yeast: The spindle pole body and the centrosome," *Philos. Trans. R. Soc. B Biol. Sci.*, vol. 369, no. 1650, 2014, doi: 10.1098/rstb.2013.0456.

[12] J. V. Kilmartin and A. E. M. Adams, "Structural rearrangements of tubulin and actin during the cell cycle of the yeast Saccharomyces," *J. Cell Biol.*, vol. 98, no. 3, pp. 922–933, Mar. 1984, doi: 10.1083/jcb.98.3.922.

[13] A. M. Cavanaugh and S. L. Jaspersen, "Big Lessons from Little Yeast: Budding and Fission Yeast Centrosome Structure, Duplication, and Function," *Annu. Rev. Genet.*, vol. 51, no. 1, pp. 361–383, Nov. 2017, doi: 10.1146/annurev-genet-120116-024733.

[14] J. V Kilmartin, S. L. Dyos, D. Kershaw, and J. T. Finch, "3," *J. Cell Biol.*, vol. 123, no. 5, pp. 1175–1184, 1993, doi: 10.1083/jcb.123.5.1175.

[15] A. Spang, K. Grein, and E. Schiebel, “The spacer protein Spc110p targets calmodulin to the central plaque of the yeast spindle pole body,” *J. Cell Sci.*, vol. 109, no. 9, 1996.

[16] J. R. Geiser, H. A. Sundberg, B. H. Chang, E. G. Muller, and T. N. Davis, “The essential mitotic target of calmodulin is the 110-kilodalton component of the spindle pole body in Saccharomyces cerevisiae.,” *Mol. Cell. Biol.*, vol. 13, no. 12, pp. 7913–24, 1993, doi: 10.1128/MCB.13.12.7913.Updated.

[17] H. A. Sundberg and T. N. Davis, “A mutational analysis identifies three functional regions of the spindle pole component Spc110p in Saccharomyces cerevisiae.,” *Mol. Biol. Cell*, vol. 8, no. 12, pp. 2575–90, 1997.

[18] T. Nguyen, D. B. N. Vinh, D. K. Crawford, and T. N. Davis, “A genetic analysis of interactions with Spc110p reveals distinct functions of Spc97p and Spc98p, components of the yeast γ-tubulin complex,” *Mol. Biol. Cell*, vol. 9, no. 8, pp. 2201–2216, 1998, doi: 10.1091/mbc.9.8.2201.

[19] J. M. Kollman, J. K. Polka, A. Zelter, T. N. Davis, and D. a Agard, “Microtubule nucleating gamma-TuSC assembles structures with 13-fold microtubule-like symmetry.,” *Nature*, vol. 466, no. 7308, pp. 879–882, 2010, doi: 10.1038/nature09207.

[20] A. S. Lyon *et al.*, “Higher-order oligomerization of Spc110p drives γ-Tubulin ring complex assembly,” *Mol. Biol. Cell*, vol. 27, no. 14, pp. 2245–2258, Jul. 2016, doi: 10.1091/mbc.E16-02-0072.

[21] T. C. Lin, A. Neuner, Y. Schlosser, A. Scharf, L. Weber, and E. Schiebel, “Cell-cycle dependent phosphorylation of yeast pericentrin regulates γ-TUSC-mediated microtubule nucleation,” *Elife*, vol. 2014, no. 3, 2014, doi: 10.7554/eLife.02208.

[22] D. B. Friedman, H. A. Sundberg, E. Y. Huang, and T. N. Davis, “The 110-kD spindle pole body component of Saccharomyces cerevisiae is a phosphoprotein that is modified in a cell cycle-dependent manner,” *J. Cell Biol.*, vol. 132, no. 5, pp. 903–914, Mar. 1996, doi: 10.1083/jcb.132.5.903.

[23] D. B. Friedman *et al.*, “Yeast Mps1p Phosphorylates the Spindle Pole Component Spc110p in the N-terminal Domain,” *J. Biol. Chem.*, vol. 276, no. 21, pp. 17958–17967, 2001, doi: 10.1074/jbc.M010461200.

[24] D. A. Stirling and M. J. R. Stark, “The Phosphorylation State of the 110 kDa Component of the Yeast Spindle Pole Body Shows Cell Cycle Dependent Regulation,” *Biochem. Biophys. Res. Commun.*, vol. 222, no. 2, pp. 236–242, 1996.

[25] S. M. Huisman, M. F. M. a Smeets, and M. Segal, “Phosphorylation of Spc110p by Cdc28p-Clb5p kinase contributes to correct spindle morphogenesis in S. cerevisiae.,” *J. Cell Sci.*, vol. 120, no. Pt 3, pp. 435–46, 2007, doi: 10.1242/jcs.03342.

[26] J. Keck *et al.*, “A Cell Cycle Phosphoproteome of the Yeast Centrosome,” *Science (80-.).*, vol. 332, pp. 1557–1561, 2011.

[27] M. Knop and E. Schiebel, “Spc98p and Spc97p of the yeast gamma-tubulin complex mediate binding to the spindle pole body via their interaction with Spc110p.,” *EMBO J.*, vol. 16, no. 23, pp. 6985–95, Dec. 1997, doi: 10.1093/emboj/16.23.6985.

[28] K. Oegema *et al.*, “Characterization of two related Drosophila ??-tubulin complexes that differ in their ability to nucleate microtubules,” *J. Cell Biol.*, vol. 144, no. 4, pp. 721–733, 1999, doi: 10.1083/jcb.144.4.721.

[29] J. M. Kollman *et al.*, “Ring closure activates yeast γTuRC for species-specific microtubule nucleation,” *Nat. Struct. Mol. Biol.*, vol. 22, no. 2, pp. 132–139, 2015, doi: 10.1038/nsmb.2953.

[30] B. R. Oakley, C. E. Oakley, Y. Yoon, and M. K. Jung, “γ-tubulin is a component of the spindle pole body that is essential for microtubule function in Aspergillus nidulans,” *Cell*, vol. 61, no. 7, pp. 1289–1301, Jun. 1990, doi: 10.1016/0092-8674(90)90693-9.

[31] S. G. Sobel and M. Snyder, “A Highly Divergent γ-Tubulin Gene Is Essential for Cell Growth and Proper Microtubule Organization in Saccharomyces cerevisiae,” *J. Cell Biol.*, vol. 131, no. 6, pp. 1775–1788, 1995, doi: 10.1083/jcb.131.6.1775.

[32] H. C. Joshi, M. J. Palacios, L. McNamara, and D. W. Cleveland, “γ-Tubulin is a centrosomal protein required for cell cycle-dependent microtubule nucleation,” *Nature*, vol. 356, no. 6364, pp. 80–83, Mar. 1992, doi: 10.1038/356080a0.

[33] T. Stearns, L. Evans, and M. Kirschner, “γ-Tubulin is a highly conserved component of the centrosome,” *Cell*, vol. 65, no. 5, pp. 825–836, May 1991, doi: 10.1016/0092-8674(91)90390-K.

[34] L. G. Marschall, R. L. Jeng, J. Mulholland, and T. Stearns, “Analysis of Tub4p, a yeast γ-tubulin-like protein: Implications for microtubule-organizing center function,” *J. Cell Biol.*, vol. 134, no. 2, pp. 443–454, Jul. 1996, doi: 10.1083/jcb.134.2.443.

[35] C. E. Oakley and B. R. Oakley, “Identification of γ-tubulin, a new member of the tubulin superfamily encoded by mipA gene of Aspergillus nidulans,” *Nature*, vol. 338, no. 6217, pp. 662–664, 1989, doi: 10.1038/338662a0.

[36] T. Horio, S. Uzawa, M. K. Jung, B. R. Oakley, K. Tanaka, and M. Yanagida, “The fission yeast γ-tubulin is essential for mitosis and is localized at microtubule organizing centres,” *J. Cell Sci.*, vol. 99, no. 4, pp. 693–700, 1991.

[37] Y. Zheng, M. K. Jung, and B. R. Oakley, “γ-Tubulin Is Present in Drosophila melanogaster and Homo sapiens and Is Associated with the Centrosome,” *Cell*, vol. 65, no. 5, pp. 817–823, May 1991, doi: 10.1016/0092-8674(91)90389-G.

[38] T. J. Keating and G. G. Borisy, “Immunostructural evidence for the template mechanism of microtubule nucleation,” *Nat. Cell Biol.*, vol. 2, no. 6, pp. 352–357, 2000, doi: 10.1038/35014045.

[39] M. Moritz, M. B. Braunfeld, V. Guénebaut, J. Heuser, and D. A. Agard, “Structure of the γ-tubulin ring complex: A template for microtubule nucleation,” *Nat. Cell Biol.*, vol. 2, no. 6, pp. 365–370, 2000, doi: 10.1038/35014058.

[40] C. Wiese and Y. Zheng, “A new function for the γ-tubulin ring complex as a microtubule minus-end cap,” *Nat. Cell Biol.*, vol. 2, no. 6, pp. 358–364, 2000, doi: 10.1038/35014051.

[41] Y.-K. Choi, P. Liu, S. K. Sze, C. Dai, and R. Z. Qi, “CDK5RAP2 stimulates microtubule nucleation by the γ-tubulin ring complex,” *J. Cell Biol.*, vol. 191, no. 6, pp. 1089–1095, 2010, doi: 10.1083/jcb.201007030.

[42] T. Consolati *et al.*, “Microtubule Nucleation by Single Human γTuRC in a Partly Open Asymmetric Conformation,” *bioRxiv*, p. 853218, 2019, doi: 10.1101/853218.

[43] A. Thawani, H. A. Stone, J. W. Shaevitz, and S. Petry, “Molecular mechanism of microtubule nucleation from gamma-tubulin ring complex,” *bioRxiv*, p. 853010, 2019, doi: 10.1101/853010.

[44] T. C. Lin *et al.*, “MOZ ART1 and γ-tubulin complex receptors are both required to turn γ-TuSC into an active microtubule nucleation template,” *J. Cell Biol.*, vol. 215, no. 6, pp. 823–840, Dec. 2016, doi: 10.1083/jcb.201606092.

[45] D. K. Dhani *et al.*, “Mzt1/Tam4, a fission yeast MOZART1 homologue, is an essential component of the γ-tubulin complex and directly interacts with GCP3Alp6,” *Mol. Biol. Cell*, vol. 24, no. 21, pp. 3337–3349, Nov. 2013, doi: 10.1091/mbc.E13-05-0253.

[46] H. Masuda, R. Mori, M. Yukawa, and T. Toda, “Fission yeast MOZART1/Mzt1 is an essential γ-tubulin complex component required for complex recruitment to the microtubule organizing center, but not its assembly,” *Mol. Biol. Cell*, vol. 24, no. 18, pp. 2894–2906, Sep. 2013, doi: 10.1091/mbc.E13-05-0235.

[47] R. R. Cota *et al.*, “MZT1 regulates microtubule nucleation by linking γTuRC assembly to adapter-mediated targeting and activation,” *J. Cell Sci.*, vol. 130, no. 2, pp. 406–419, 2017, doi: 10.1242/jcs.195321.

[48] N. Teixidó-Travesa *et al.*, “The γTuRC revisited: A comparative analysis of interphase and mitotic human γTuRC redefines the set of core components and identifies the novel subunit GCP8,” *Mol. Biol. Cell*, vol. 21, no. 22, pp. 3963–3972, Nov. 2010, doi: 10.1091/mbc.E10-05-0408.

[49] M. Wieczorek, L. Urnavicius, S.-C. Ti, K. R. Molloy, B. T. Chait, and T. M. Kapoor, “Asymmetric molecular architecture of the human γ-tubulin ring complex,” *bioRxiv*, p. 820142, Oct. 2019, doi: 10.1101/820142.

[50] J. C. Fox, A. E. Howard, J. D. Currie, S. L. Rogers, and K. C. Slep, “The XMAP215 family drives microtubule polymerization using a structurally diverse TOG array,” *Mol. Biol. Cell*, vol. 25, no. 16, pp. 2375–2392, 2014, doi: 10.1091/mbc.E13-08-0501.

[51] P. Liu *et al.*, “Insights into the assembly and activation of the microtubule nucleator γ-TuRC.,” *Nature*, Dec. 2019, doi: 10.1038/s41586-019-1896-6.

[52] S. Bustin, “Sixth Edition; ISBN: 9780815344643; and Molecular Biology of the Cell, Sixth Edition, The Problems Book,” *B. Rev. Mol. Biol. Cell*, vol. 16, pp. 28123–28125, 2015, doi: 10.3390/ijms161226074.

[53] T. Mitchison and M. Kirschner, “Dynamic instability of microtubule growth,” *Nature*, vol. 312, pp. 237–242, 1984.

[54] T. Kobayashi, “Dephosphorylation of tubulin-bound guanosine triphosphate during microtubule assembly.,” *J. Biochem.*, vol. 77, no. 6, pp. 1193–7, Jun. 1975.

[55] S. W. Manka and C. A. Moores, “Microtubule structure by cryo-EM: Snapshots of dynamic instability,” *Essays in Biochemistry*, vol. 62, no. 6. Portland Press Ltd, pp. 737–751, 07-Dec-2018, doi: 10.1042/EBC20180031.

[56] W. Voter and H. Erickson, “The kinetics of microtubule assembly. Evidence for a two-stage mechanism,” *J. Biol. Chem.*, vol. 259, no. 16, pp. 10430–43, 1984.

[57] H. Flyvbjerg, E. Jobs, and S. Leibler, “Kinetics of self-assembling microtubules: An ‘inverse problem’ in biochemistry,” *Proc. Natl. Acad. Sci. U. S. A.*, vol. 93, no. 12, pp. 5975–5979, 1996, doi: 10.1073/pnas.93.12.5975.

[58] D. Kuchnir Fygenson, H. Flyvbjerg, K. Sneppen, A. Libchaber, and S. Leibler, “Spontaneous nucleation of microtubules,” *Phys. Rev. E*, vol. 51, no. 5, pp. 5058–5063, 1995, doi: 10.1103/physreve.51.5058.

[59] L. Rice, M. Moritz, and D. A. Agard, “Microtubules form by progressively faster tubulin accretion, not by nucleation-elongation,” *bioRxiv*, p. 545236, 2019, doi: 10.1101/545236.

[60] M. Moritz, Y. Zheng, B. M. Alberts, and K. Oegema, “Recruitment of the γ-tubulin ring complex to Drosophila salt-stripped centrosome scaffolds,” *J. Cell Biol.*, vol. 142, no. 3, pp. 775–786, Aug. 1998, doi: 10.1083/jcb.142.3.775.

[61] B. Buendia, G. Draetta, and E. Karsenti, “Regulation of the Microtubule Nucleating Activity of Centrosomes in Xenopus Egg Extracts : Role of Cyclin A-Associated Protein Kinase,” *J. Cell Biol.*, vol. 116, no. 6, pp. 1431–1442, 1992.

[62] J. Helenius, G. Brouhard, Y. Kalaidzidis, S. Diez, and J. Howard, “The depolymerizing

kinesin MCAK uses lattice diffusion to rapidly target microtubule ends," *Nature*, vol. 441, no. 1, pp. 115–119, May 2006, doi: 10.1038/nature04736.

[63] G. J. Brouhard *et al.*, "XMAP215 Is a Processive Microtubule Polymerase," *Cell*, vol. 132, no. 1, pp. 79–88, 2008, doi: 10.1016/j.cell.2007.11.043.

[64] P. Bieling *et al.*, "Reconstitution of a microtubule plus-end tracking system in vitro," *Nature*, vol. 450, no. 7172, pp. 1100–1105, Dec. 2007, doi: 10.1038/nature06386.

[65] K. A. Dragestein *et al.*, "Dynamic behavior of GFP-CLIP-170 reveals fast protein turnover on microtubule plus ends," *J. Cell Biol.*, vol. 180, no. 4, pp. 729–737, Feb. 2008, doi: 10.1083/jcb.200707203.

[66] L. K. Su *et al.*, "APC Binds to the Novel Protein EB," *Cancer Res.*, vol. 55, no. 14, pp. 2972–2977, Jul. 1995.

[67] H. Browning, D. D. Hackney, and P. Nurse, "Targeted movement of cell end factors in fission yeast," *Nat. Cell Biol.*, vol. 5, no. 9, pp. 812–818, Sep. 2003, doi: 10.1038/ncb1034.

[68] Y. Mimori-Kiyosue *et al.*, "CLASP1 and CLASP2 bind to EB1 and regulate microtubule plus-end dynamics at the cell cortex," *J. Cell Biol.*, vol. 168, no. 1, pp. 141–153, Jan. 2005, doi: 10.1083/jcb.200405094.

[69] P. Niethammer, I. Kronja, S. Kandels-Lewis, S. Rybina, P. Bastiaens, and E. Karsenti, "Discrete States of a Protein Interaction Network Govern Interphase and Mitotic Microtubule Dynamics," *PLoS Biol.*, vol. 5, no. 2, p. e29, Jan. 2007, doi: 10.1371/journal.pbio.0050029.

[70] A. Melbinger, L. Reese, and E. Frey, "Microtubule Length Regulation by Molecular Motors," 2012, doi: 10.1103/PhysRevLett.108.258104.

[71] L. Reese, A. Melbinger, and E. Frey, "Crowding of molecular motors determines microtubule depolymerization," *Biophys. J.*, vol. 101, no. 9, pp. 2190–2200, Nov. 2011, doi: 10.1016/j.bpj.2011.09.009.

[72] X. Su, W. Qiu, M. L. Gupta, J. B. Pereira-Leal, S. L. Reck-Peterson, and D. Pellman, "Mechanisms Underlying the Dual-Mode Regulation of Microtubule Dynamics by Kip3/Kinesin-8," *Mol. Cell*, vol. 43, no. 5, pp. 751–763, Sep. 2011, doi: 10.1016/j.molcel.2011.06.027.

[73] C. Tischer, D. Brunner, and M. Dogterom, "Force- and kinesin-8-dependent effects in the spatial regulation of fission yeast microtubule dynamics," *Mol. Syst. Biol.*, vol. 5, p. 250, Jan. 2009, doi: 10.1038/msb.2009.5.

[74] M. L. Gupta, P. Carvalho, D. M. Roof, and D. Pellman, "Plus end-specific depolymerase activity of Kip3, a kinesin-8 protein, explains its role in positioning the yeast mitotic spindle.," *Nat. Cell Biol.*, vol. 8, no. 9, pp. 913–923, 2006, doi: 10.1038/ncb1457.

[75] M. K. Gardner, M. Zanic, C. Gell, V. Bormuth, and J. Howard, "Depolymerizing kinesins Kip3 and MCAK shape cellular microtubule architecture by differential control of catastrophe," *Cell*, vol. 147, no. 5, pp. 1092–1103, Nov. 2011, doi: 10.1016/j.cell.2011.10.037.

[76] V. Varga, J. Helenius, K. Tanaka, A. A. Hyman, T. U. Tanaka, and J. Howard, "Yeast kinesin-8 depolymerizes microtubules in a length-dependent manner," *Nat. Cell Biol.*, vol. 8, no. 9, 2006, doi: 10.1038/ncb1462.

[77] Y. Fukuda, A. Luchniak, E. R. Murphy, and M. L. Gupta, "Spatial control of microtubule length and lifetime by opposing stabilizing and destabilizing functions of kinesin-8," *Curr. Biol.*, vol. 24, no. 16, pp. 1826–1835, Aug. 2014, doi: 10.1016/j.cub.2014.06.069.

[78] J. Stumpff *et al.*, "A Tethering Mechanism Controls the Processivity and Kinetochore-Microtubule Plus-End Enrichment of the Kinesin-8 Kif18A," *Mol. Cell*, vol. 43, no. 5, pp. 764–775, Sep. 2011, doi: 10.1016/j.molcel.2011.07.022.

[79] J. Stumpff, G. von Dassow, M. Wagenbach, C. Asbury, and L. Wordeman, "The Kinesin-8 Motor Kif18A Suppresses Kinetochore Movements to Control Mitotic Chromosome Alignment," *Dev. Cell*, vol. 14, no. 2, pp. 252–262, Feb. 2008, doi: 10.1016/j.devcel.2007.11.014.

[80] V. Varga, C. Leduc, V. Bormuth, S. Diez, and J. Howard, "Kinesin-8 Motors Act Cooperatively to Mediate Length-Dependent Microtubule Depolymerization," *Cell*, vol. 138, no. 6, pp. 1174–1183, Sep. 2009, doi: 10.1016/j.cell.2009.07.032.

[81] Y. A. Komarova, A. S. Akhmanova, S. I. Kojima, N. Galjart, and G. G. Borisy, "Cytoplasmic linker proteins promote microtubule rescue in vivo," *J. Cell Biol.*, vol. 159, no. 4, pp. 589–599, Nov. 2002, doi: 10.1083/jcb.200208058.

[82] J. Al-Bassam, M. Van Breugel, S. C. Harrison, and A. Hyman, "Stu2p binds tubulin and undergoes an open-to-closed conformational change," *J. Cell Biol.*, vol. 172, no. 7, pp. 1009–1022, 2006, doi: 10.1083/jcb.200511010.

[83] D. L. Gard and M. W. Kirschner, "A microtubule-associated protein from Xenopus eggs that specifically promotes assembly at the plus-end," *J. Cell Biol.*, vol. 105, no. 5, pp. 2203–2215, 1987, doi: 10.1083/jcb.105.5.2203.

[84] M. Srayko, A. Kaya, J. Stamford, and A. A. Hyman, "Identification and characterization of factors required for microtubule growth and nucleation in the early C. elegans embryo," *Dev. Cell*, vol. 9, no. 2, pp. 223–236, Aug. 2005, doi: 10.1016/j.devcel.2005.07.003.

[85] R. Tournebize *et al.*, "Control of microtubule dynamics by the antagonistic activities of XMAP215 and XKCM1 in Xenopus egg extracts," *Nat. Cell Biol.*, vol. 2, no. 1, pp. 13–19, Jan. 2000, doi: 10.1038/71330.

[86] R. J. Vasquez, D. L. Gard, and L. Cassimeris, "XMAP from Xenopus Eggs Promotes Rapid Plus End Assembly of Microtubules and Rapid Microtubule Polymer Turnover," *J Cell Biol*, vol. 127, no. 4, pp. 985–993, 1994.

[87] C. Wiese and Y. Zheng, "A new function for the gamma-tubulin ring complex as a microtubule minus-end cap.," *Nat. Cell Biol.*, vol. 2, no. 6, pp. 358–364, 2000, doi: 10.1038/35014051.

[88] H. Aldaz, L. M. Rice, T. Stearns, and D. A. Agard, "Insights into microtubule nucleation from the crystal structure of human γ-tubulin," *Nature*, vol. 435, no. 7041, pp. 523–527, May 2005, doi: 10.1038/nature03586.

[89] C. Klotz, M.-C. Dabauvalle, M. Paintrand, T. Weber, M. Bornens, and E. Karsenti, "Parthenogenesis in Xenopus Eggs Requires Centrosomal Integrity," *J. Cell Biol.*, vol. 110, no. 2, pp. 405–415, 1990.

[90] A. V. Popov, F. Severin, and E. Karsenti, "XMAP215 is required for the microtubule-nucleating activity of centrosomes," *Curr. Biol.*, vol. 12, no. 15, pp. 1326–1330, Aug. 2002, doi: 10.1016/S0960-9822(02)01033-3.

[91] M. Wieczorek, S. Bechstedt, S. Chaaban, and G. J. Brouhard, "Microtubule-associated proteins control the kinetics of microtubule nucleation," *Nat. Cell Biol.*, vol. 17, no. 7, pp. 907–918, 2015, doi: 10.1038/ncb3188.

[92] A. Thawani, R. S. Kadzik, and S. Petry, "XMAP215 is a microtubule nucleation factor that functions synergistically with the γ-tubulin ring complex," *Nat. Cell Biol.*, vol. 20, no. 5, pp. 575–585, May 2018, doi: 10.1038/s41556-018-0091-6.

[93] I. Flor-Parra, A. B. Iglesias-Romero, and F. Chang, "The XMAP215 Ortholog Alp14 Promotes Microtubule Nucleation in Fission Yeast," *Curr. Biol.*, vol. 28, no. 11, pp. 1681-1691.e4, Jun. 2018, doi: 10.1016/j.cub.2018.04.008.

[94] J. Roostalu, N. I. Cade, and T. Surrey, "Complementary activities of TPX2 and chTOG constitute an efficient importin-regulated microtubule nucleation module," *Nat. Cell Biol.*, vol. 17, no. 11, pp. 1422–1434, Nov. 2015, doi: 10.1038/ncb3241.

[95] F. Hussmann, D. R. Drummond, D. R. Peet, D. S. Martin, and R. A. Cross, "Alp7/TACC-Alp14/TOG generates long-lived, fast-growing MTs by an unconventional mechanism," *Sci. Rep.*, vol. 6, Feb. 2016, doi: 10.1038/srep20653.

[96] J. B. Woodruff, B. Ferreira Gomes, P. O. Widlund, J. Mahamid, A. Honigmann, and A. A. Hyman, "The Centrosome Is a Selective Condensate that Nucleates Microtubules by Concentrating Tubulin," *Cell*, vol. 169, no. 6, pp. 1066–1077, 2017, doi: 10.1016/j.cell.2017.05.028.

[97] K. C. Slep and R. D. Vale, "Structural Basis of Microtubule Plus End Tracking by XMAP215, CLIP-170, and EB1," *Mol. Cell*, vol. 27, no. 6, pp. 976–991, Sep. 2007, doi: 10.1016/j.molcel.2007.07.023.

[98] F. Gaskin, C. R. Cantor, and M. L. Shelanski, "Turbidimetric studies of the in vitro assembly and disassembly of porcine neurotubules," *J. Mol. Biol.*, vol. 89, no. 4, Nov. 1974, doi: 10.1016/0022-2836(74)90048-5.

[99] A. Wegner and J. Engel, "Kinetics of the cooperative association of actin to actin filament," *Biophys. Chem.*, vol. 3, no. 3, pp. 215–225, 1975, doi: 10.1016/0301-4622(75)80013-5.

[100] P. O. Widlund *et al.*, "XMAP215 polymerase activity is built by combining multiple tubulin-binding TOG domains and a basic lattice-binding region," *PNAS*, vol. 108, no. 7, pp. 2741–2746, 2011, doi: 10.1073/pnas.1016498108/-/DCSupplemental.

[101] P. Ayaz *et al.*, "A tethered delivery mechanism explains the catalytic action of a microtubule polymerase.," *Elife*, vol. 3, p. e03069, 2014, doi: 10.7554/eLife.03069.

[102] T. A. Reid *et al.*, "Suppression of microtubule assembly kinetics by the mitotic protein TPX2," *J. Cell Sci.*, vol. 129, no. 7, pp. 1319–1328, Apr. 2016, doi: 10.1242/jcs.178806.

[103] M. Castoldi and A. V. Popov, "Purification of brain tubulin through two cycles of polymerization- depolymerization in a high-molarity buffer," *Protein Expr. Purif.*, vol. 32, no. 1, pp. 83–88, 2003, doi: 10.1016/S1046-5928(03)00218-3.

[104] S. M. Murphy, L. Urbani, and T. Stearns, "The mammalian γ-tubulin complex contains homologues of the yeast spindle pole body components Spc97p and Spc98p," *J. Cell Biol.*, vol. 141, no. 3, pp. 663–674, May 1998, doi: 10.1083/jcb.141.3.663.

[105] G. J. Brouhard *et al.*, "XMAP215 is a processive microtubule polymerase.," *Cell*, vol. 132, no. 1, pp. 79–88, 2008, doi: 10.1016/j.cell.2007.11.043.

[106] B. Akiyoshi *et al.*, "Tension directly stabilizes reconstituted kinetochore-microtubule attachments," *Nature*, vol. 468, no. 7323, pp. 576–579, Nov. 2010, doi: 10.1038/nature09594.

[107] A. D. Franck, A. F. Powers, D. R. Gestaut, T. N. Davis, and C. L. Asbury, "Direct physical study of kinetochore-microtubule interactions by reconstitution and interrogation with an optical force clamp," *Methods*, vol. 51, no. 2, pp. 242–250, Jun. 2010, doi: 10.1016/j.ymeth.2010.01.020.

[108] A. F. Powers *et al.*, "The Ndc80 Kinetochore Complex Forms Load-Bearing Attachments to Dynamic Microtubule Tips via Biased Diffusion," *Cell*, vol. 136, no. 5, pp. 865–875,

Mar. 2009, doi: 10.1016/j.cell.2008.12.045.
[109] A. D. Franck, A. F. Powers, D. R. Gestaut, T. Gonen, T. N. Davis, and C. L. Asbury, "Tension applied through the Dam1 complex promotes microtubule elongation providing a direct mechanism for length control in mitosis," *Nat. Cell Biol.*, vol. 9, no. 7, pp. 832–837, Jul. 2007, doi: 10.1038/ncb1609.
[110] G. Tang *et al.*, "EMAN2: An extensible image processing suite for electron microscopy," *J. Struct. Biol.*, vol. 157, no. 1, pp. 38–46, Jan. 2007, doi: 10.1016/j.jsb.2006.05.009.
[111] J. Frank *et al.*, "SPIDER and WEB: Processing and visualization of images in 3D electron microscopy and related fields," *J. Struct. Biol.*, vol. 116, no. 1, pp. 190–199, 1996, doi: 10.1006/jsbi.1996.0030.
[112] C. Sachse, J. Z. Chen, P. D. Coureux, M. E. Stroupe, M. Fändrich, and N. Grigorieff, "High-resolution Electron Microscopy of Helical Specimens: A Fresh Look at Tobacco Mosaic Virus," *J. Mol. Biol.*, vol. 371, no. 3, pp. 812–835, Aug. 2007, doi: 10.1016/j.jmb.2007.05.088.
[113] E. H. Egelman, "Reconstruction of helical filaments and tubes," in *Methods in Enzymology*, vol. 482, no. C, Academic Press Inc., 2010, pp. 167–183.
[114] B. Graczyk and T. N. Davis, "An assay to measure the affinity of proteins for microtubules by quantitative fluorescent microscopy," *Anal. Biochem.*, vol. 410, no. 2, pp. 313–315, 2011, doi: 10.1016/j.ab.2010.12.009.
[115] D. B. N. Vinh, J. W. Kern, W. O. Hancock, J. Howard, and T. N. Davis, "Reconstitution and characterization of budding yeast gamma-tubulin complex.," *Mol. Biol. Cell*, vol. 13, no. 4, pp. 1144–57, 2002, doi: 10.1091/mbc.02-01-0607.
[116] R. N. Gunawardane *et al.*, "Characterization and reconstitution of Drosophila ??-tubulin ring complex subunits," *J. Cell Biol.*, vol. 151, no. 7, pp. 1513–1523, 2000, doi: 10.1083/jcb.151.7.1513.
[117] Y. Zheng, M. L. Wong, B. Alberts, and T. Mitchison, "Nucleation of microtubule assembly by a gamma-tubulin-containing ring complex.," *Nature*, vol. 378, no. 6557, pp. 578–83, 1995, doi: 10.1038/378578a0.
[118] A. S. Lyon *et al.*, "Higher-order oligomerization of Spc110p drives -tubulin ring complex assembly," *Mol. Biol. Cell*, vol. 27, no. 14, pp. 2245–2258, 2016, doi: 10.1091/mbc.E16-02-0072.
[119] P. A. Wigge, O. N. Jensen, S. Holmes, S. Soues, M. Mann, and J. V Kilmartin, "Analysis of the Saccharomyces spindle pole by matrix-assisted laser desorption/ionization (MALDI) mass spectrometry.," *J Cell Biol*, vol. 141, no. 4, pp. 967–977, 1998.
[120] T. Usui, H. Maekawa, G. Pereira, and E. Schiebel, "The XMAP215 homologue Stu2 at yeast spindle pole bodies regulates microtubule dynamics and anchorage," *EMBO J.*, vol. 22, no. 18, pp. 4779–4793, 2003, doi: 10.1093/emboj/cdg459.
[121] J. R. Newman, E. Wolf, and P. S. Kim, "A computationally directed screen identifying interacting coiled coils from Saccharomyces cerevisiae," *Proc. Natl. Acad. Sci. U. S. A.*, vol. 97, no. 24, pp. 13203–13208, 2000, doi: 10.1073/pnas.97.24.13203.
[122] Y. Wang *et al.*, "Coiled-coil networking shapes cell molecular machinery," *Mol. Biol. Cell*, vol. 23, no. 19, pp. 3911–3922, 2012, doi: 10.1091/mbc.E12-05-0396.
[123] B. D. Manning, J. G. Barrett, J. A. Wallace, H. Granok, and M. Snyder, "Differential regulation of the Kar3p kinesin-related protein by two associated proteins, Cik1p and Vik1p," *J. Cell Biol.*, vol. 144, no. 6, pp. 1219–1233, 1999, doi: 10.1083/jcb.144.6.1219.
[124] K. Blake-Hodek, L. Cassimeris, and T. C. Huffaker, "Regulation of microtubule dynamics

by Bim1 and Bik1, the budding yeast members of the EB1 and CLIP-170 families of plus-end tracking proteins.," *Mol. Biol. Cell*, vol. 21, no. 12, pp. 2013–23, 2010, doi: 10.1091/mbc.E10-02-0083.

[125] B. Vitre, F. M. Coquelle, C. Heichette, C. Garnier, D. Chrétien, and I. Arnal, "EB1 regulates microtubule dynamics and tubulin sheet closure in vitro.," *Nat. Cell Biol.*, vol. 10, no. 4, pp. 415–421, 2008, doi: 10.1038/ncb1703.

[126] P. Carvalho, M. L. Gupta, M. A. Hoyt, and D. Pellman, "Cell cycle control of kinesin-mediated transport of Bik1 (CLIP-170) regulates microtubule stability and dynein activation," *Dev. Cell*, vol. 6, no. 6, pp. 815–829, 2004, doi: 10.1016/j.devcel.2004.05.001.

[127] F. Caudron, A. Andrieux, D. Job, and C. Boscheron, "A new role for kinesin-directed transport of Bik1p (CLIP-170) in Saccharomyces cerevisiae," *J. Cell Sci.*, vol. 121, no. 9, pp. 1506–1513, May 2008, doi: 10.1242/jcs.023374.

[128] F. J. McNally, "Mechanisms of spindle positioning," *Journal of Cell Biology*, vol. 200, no. 2. The Rockefeller University Press, pp. 131–140, 21-Jan-2013, doi: 10.1083/jcb.201210007.

[129] E. A. Geyer, M. P. Miller, C. A. Brautigam, S. Biggins, and L. M. Rice, "Design principles of a microtubule polymerase," *Elife*, vol. 7, Jun. 2018, doi: 10.7554/eLife.34574.

[130] R. S. McIsaac, B. L. Oakes, X. Wang, K. A. Dummit, D. Botstein, and M. B. Noyes, "Synthetic gene expression perturbation systems with rapid, tunable, single-gene specificity in yeast," *Nucleic Acids Res.*, vol. 41, no. 4, pp. 1–10, 2013, doi: 10.1093/nar/gks1313.

[131] E. T. O'Toole, M. Winey, J. R. McIntosh, and D. N. Mastronarde, "Electron tomography of yeast cells.," *Methods Enzymol.*, vol. 351, pp. 81–95, 2002, doi: 10.1016/s0076-6879(02)51842-5.

[132] E. G. D. Muller *et al.*, "The organization of the core proteins of the yeast spindle pole body.," *Mol. Biol. Cell*, vol. 16, no. 7, pp. 3341–52, 2005, doi: 10.1091/mbc.E05-03-0214.

[133] B. D. Page, L. L. Satterwhite, M. D. Rose, and M. Snyder, "Localization of the Kar3 kinesin heavy chain-related protein requires the Cik1 interacting protein," *J. Cell Biol.*, vol. 124, no. 4, pp. 507–519, Feb. 1994, doi: 10.1083/jcb.124.4.507.

[134] R. K. Miller *et al.*, "The kinesin-related proteins, Kip2p and Kip3p, function differently in nuclear migration in yeast," *Mol. Biol. Cell*, vol. 9, no. 8, pp. 2051–2068, Aug. 1998, doi: 10.1091/mbc.9.8.2051.

[135] J. R. Geiser *et al.*, "Saccharomyces cerevisiae genes required in the absence of the CIN8-encoded spindle motor act in functionally diverse mitotic pathways," *Mol. Biol. Cell*, vol. 8, no. 6, pp. 1035–1050, Jun. 1997, doi: 10.1091/mbc.8.6.1035.

[136] R. K. Miller, S.-C. Cheng, and M. D. Rose, "Bim1p/Yeb1p Mediates the Kar9p-dependent Cortical Attachment of Cytoplasmic Microtubules," *Mol. Biol. Cell*, vol. 11, pp. 2949–2959, 2000, doi: 10.1091/mbc.11.9.2949.

[137] K. Furuta, A. Furuta, Y. Y. Toyoshima, M. Amino, K. Oiwa, and H. Kojima, "Measuring collective transport by defined numbers of processive and nonprocessive kinesin motors," *Proc. Natl. Acad. Sci. U. S. A.*, vol. 110, no. 2, pp. 501–506, Jan. 2013, doi: 10.1073/pnas.1201390110.

[138] N. D. Derr, B. S. Goodman, R. Jungmann, A. E. Leschziner, W. M. Shih, and S. L. Reck-Peterson, "Tug-of-war in motor protein ensembles revealed with a programmable DNA

origami scaffold," *Science (80-.).*, vol. 338, no. 6107, pp. 662–665, Nov. 2012, doi: 10.1126/science.1226734.

[139] M. J. O'Connell, P. B. Meluh, M. D. Rose, and N. R. Morris, "Suppression of the bimC4 mitotic spindle defect by deletion of klpA, a gene encoding a KAR3-related kinesin-like protein in Aspergillus nidulans," *J. Cell Biol.*, vol. 120, no. 1, pp. 153–162, Jan. 1993, doi: 10.1083/jcb.120.1.153.

[140] M. A. Hoyt, L. He, K. K. Loo, and W. S. Saunders, "Two Saccharomyces cerevisiae kinesin-related gene products required for mitotic spindle assembly," *J. Cell Biol.*, vol. 118, no. 1, pp. 109–120, 1992, doi: 10.1083/jcb.118.1.109.

[141] D. M. Roof, P. B. Meluh, and M. D. Rose, "Kinesin-related proteins required for assembly of the mitotic spindle," *J. Cell Biol.*, vol. 118, no. 1, pp. 95–108, 1992, doi: 10.1083/jcb.118.1.95.

[142] F. R. Cottingham, L. Gheber, D. L. Miller, and M. A. Hoyt, "Novel roles for Saccharomyces cerevisiae mitotic spindle motors," *J. Cell Biol.*, vol. 147, no. 2, pp. 335–349, Oct. 1999, doi: 10.1083/jcb.147.2.335.

[143] T. M. DeZwaan, E. Ellingson, D. Pellman, and D. M. Roof, "Kinesin-related KIP3 of Saccharomyces cerevisiae is required for a distinct step in nuclear migration," *J. Cell Biol.*, vol. 138, no. 5, pp. 1023–1040, Sep. 1997, doi: 10.1083/jcb.138.5.1023.

[144] W. Saunders, V. Lengyel, and M. A. Hoyt, "Mitotic spindle function in Saccharomyces cerevisiae requires a balance between different types of kinesin-related motors," *Mol. Biol. Cell*, vol. 8, no. 6, pp. 1025–1033, Jun. 1997, doi: 10.1091/mbc.8.6.1025.

[145] E. A. Vallen, M. A. Hiller, T. Y. Scherson, and M. D. Rose, "Separate domains of KAR1 mediate distinct functions in mitosis and nuclear fusion," *J. Cell Biol.*, vol. 117, no. 6, pp. 1277–1287, Jun. 1992, doi: 10.1083/jcb.117.6.1277.

[146] M. K. Gardner *et al.*, "Chromosome Congression by Kinesin-5 Motor-Mediated Disassembly of Longer Kinetochore Microtubules," *Cell*, vol. 135, no. 5, pp. 894–906, Nov. 2008, doi: 10.1016/j.cell.2008.09.046.

[147] A. F. Straight, J. W. Sedat, and A. W. Murray, "Time-lapse microscopy reveals unique roles for kinesins during anaphase in budding yeast," *J. Cell Biol.*, vol. 143, no. 3, pp. 687–694, Nov. 1998, doi: 10.1083/jcb.143.3.687.

[148] R. R. West and J. R. McIntosh, "Novel interactions of fission yeast kinesin 8 revealed through in vivo expression of truncation alleles," *Cell Motil. Cytoskeleton*, vol. 65, no. 8, pp. 626–640, Aug. 2008, doi: 10.1002/cm.20289.

[149] M. Erent, D. R. Drummond, and R. A. Cross, "S. pombe kinesins-8 promote both nucleation and catastrophe of microtubules," *PLoS One*, vol. 7, no. 2, 2012, doi: 10.1371/journal.pone.0030738.

[150] A. S. Rodriguez *et al.*, "Protein complexes at the microtubule organizing center regulate bipolar spindle assembly," *Cell Cycle*, vol. 7, no. 9, pp. 1246–1253, May 2008, doi: 10.4161/cc.7.9.5808.

[151] Z. T. Olmsted, A. G. Colliver, T. D. Riehlman, and J. L. Paluh, "Kinesin-14 and kinesin-5 antagonistically regulate microtubule nucleation by γ-TuRC in yeast and human cells," *Nat. Commun.*, vol. 5, no. 1, pp. 1–15, Oct. 2014, doi: 10.1038/ncomms6339.

[152] Z. T. Olmsted, T. D. Riehlman, C. N. Branca, A. G. Colliver, L. O. Cruz, and J. L. Paluh, "Kinesin-14 Pkl1 targets γ-tubulin for release from the γ-tubulin ring complex (γ-TuRC)," *Cell Cycle*, vol. 12, no. 5, pp. 842–848, Mar. 2013, doi: 10.4161/cc.23822.

[153] S. Cai, L. N. Weaver, S. C. Ems-McClung, and C. E. Walczak, "Proper Organization of

Microtubule Minus Ends Is Needed for Midzone Stability and Cytokinesis," *Curr. Biol.*, vol. 20, no. 9, pp. 880–885, May 2010, doi: 10.1016/j.cub.2010.03.067.

[154] N. Lecland and J. Lüders, "The dynamics of microtubule minus ends in the human mitotic spindle," *Nat. Cell Biol.*, vol. 16, no. 8, 2014, doi: 10.1038/ncb2996.

[155] S. A. Endow and D. J. Komma, "Assembly and dynamics of an anastral:astral spindle: the meiosis II spindle of Drosophila oocytes.," *J. Cell Sci.*, vol. 111, pp. 2487–2495, 1998.

[156] M. Kwon *et al.*, "Mechanisms to suppress multipolar divisions in cancer cells with extra centrosomes," *Genes Dev.*, vol. 22, no. 16, pp. 2189–2203, Aug. 2008, doi: 10.1101/gad.1700908.

[157] K. B. Greenland, H. Ding, M. Costanzo, C. Boone, and T. N. Davis, "Identification of Saccharomyces cerevisiae Spindle Pole Body Remodeling Factors," *PLoS One*, vol. 5, no. 11, p. e15426, Nov. 2010, doi: 10.1371/journal.pone.0015426.

[158] K. K. Fong, B. Graczyk, and T. N. Davis, "Purification of fluorescently labeled Saccharomyces cerevisiae Spindle Pole Bodies," *Methods Mol. Biol. (Clifton, NJ)*, pp. 189–195, 2016, doi: 10.1016/B978-0-12-394447-4.20062-X.

[159] K. K. Fong *et al.*, "Direct measurement of the strength of microtubule attachment to yeast centrosomes," *Mol. Biol. Cell*, vol. 28, no. 14, pp. 1853–1861, Jul. 2017, doi: 10.1091/mbc.E17-01-0034.

[160] F. J. McNally and A. Roll-Mecak, "Microtubule-severing enzymes: From cellular functions to molecular mechanism," *Journal of Cell Biology*, vol. 217, no. 12. Rockefeller University Press, pp. 4057–4069, 01-Dec-2018, doi: 10.1083/jcb.201612104.

[161] A. Akhmanova and M. O. Steinmetz, "Microtubule minus-end regulation at a glance," *Journal of cell science*, vol. 132, no. 11. NLM (Medline), 07-Jun-2019, doi: 10.1242/jcs.227850.

[162] S. Petry, "Mechanisms of Mitotic Spindle Assembly," *Annu. Rev. Biochem.*, vol. 85, no. 1, pp. 659–683, Jun. 2016, doi: 10.1146/annurev-biochem-060815-014528.

[163] J. Brugués, V. Nuzzo, E. Mazur, and D. J. Needleman, "Nucleation and transport organize microtubules in metaphase spindles," *Cell*, vol. 149, no. 3, pp. 554–564, Apr. 2012, doi: 10.1016/j.cell.2012.03.027.

[164] J. K. Moore, S. D'Silva, and R. K. Miller, "The CLIP-170 homologue Bik1p promotes the phosphorylation and asymmetric localization of Kar9p.," *Mol. Biol. Cell*, vol. 17, no. 1, pp. 178–91, Jan. 2006, doi: 10.1091/mbc.e05-06-0565.

[165] L. A. Strawn and H. L. True, "Deletion of RNQ1 gene reveals novel functional relationship between divergently transcribed Bik1p/CLIP-170 and SW1p in spindle pole body separation," *Curr Genet*, vol. 50, pp. 347–366, 2006, doi: 10.1007/s00294-006-0098-6.

[166] Y. Komarova *et al.*, "Mammalian end binding proteins control persistent microtubule growth," *J. Cell Biol.*, vol. 184, no. 5, pp. 691–706, Mar. 2009, doi: 10.1083/jcb.200807179.

[167] K. E. Busch and D. Brunner, "The microtubule plus end-tracking proteins mal3p and tip1p cooperate for cell-end targeting of interphase microtubules," *Curr. Biol.*, vol. 14, no. 7, pp. 548–559, Apr. 2004, doi: 10.1016/j.cub.2004.03.029.

[168] J. S. Tirnauer, G. Alushin, E. D. Salmon, and T. J. Mitchison, "EB1–Microtubule Interactions in Xenopus Egg Extracts: Role of EB1 in Microtubule Stabilization and Mechanisms of Targeting to Microtubules," *Mol. Biol. Cell*, vol. 14, no. May, pp. 2559–2569, 2003, doi: 10.1091/mbc.E02.

[169] L. Sandblad, K. E. Busch, P. Tittmann, H. Gross, D. Brunner, and A. Hoenger, "The Schizosaccharomyces pombe EB1 homolog Mal3p binds and stabilizes the microtubule lattice seam.," *Cell*, vol. 127, no. 7, pp. 1415–24, 2006, doi: 10.1016/j.cell.2006.11.025.
[170] S. C. Howes *et al.*, "Structural differences between yeast and mammalian microtubules revealed by cryo-EM," *J. Cell Biol.*, vol. 216, no. 9, pp. 2669–2677, Sep. 2017, doi: 10.1083/jcb.201612195.
[171] A. H. Y. Tong *et al.*, "Systematic genetic analysis with ordered arrays of yeast deletion mutants," *Science (80-.).*, vol. 294, no. 5550, pp. 2364–2368, Dec. 2001, doi: 10.1126/science.1065810.
[172] M. J. Wolyniak, K. Blake-Hodek, K. Kosco, E. Hwang, L. You, and T. C. Huffaker, "The regulation of microtubule dynamics in Saccharomyces cerevisiae by three interacting plus-end tracking proteins," *Mol. Biol. Cell*, vol. 17, no. 6, pp. 2789–2798, Jun. 2006, doi: 10.1091/mbc.E05-09-0892.
[173] L. Cuschieri, R. Miller, and J. Vogel, "γ-tubulin is required for proper recruitment and assembly of Kar9-Bim1 complexes in budding yeast," *Mol. Biol. Cell*, vol. 17, no. 10, pp. 4420–4434, Oct. 2006, doi: 10.1091/mbc.E06-03-0245.
[174] M. M. Stangier, A. Kumar, X. Chen, A. M. Farcas, Y. Barral, and M. O. Steinmetz, "Structure-Function Relationship of the Bik1-Bim1 Complex," *Structure*, vol. 26, no. 4, pp. 607-618.e4, Apr. 2018, doi: 10.1016/j.str.2018.03.003.
[175] Y. Matsuo *et al.*, "An unconventional interaction between Dis1/TOG and Mal3/EB1 in fission yeast promotes the fidelity of chromosome segregation," *J. Cell Sci.*, vol. 129, no. 24, pp. 4592–4606, 2016, doi: 10.1242/jcs.197533.
[176] M. Sato, L. Vardy, M. A. Garcia, N. Koonrugsa, and T. Toda, "Interdependency of Fission Yeast Alp14/TOG and Coiled Coil Protein Alp7 in Microtubule Localization and Bipolar Spindle Formation," *Mol. Biol. Cell*, vol. 15, no. 4, pp. 1609–1622, Apr. 2004, doi: 10.1091/mbc.E03-11-0837.
[177] J. M. Bellanger and P. Gönczy, "TAC-1 and ZYG-9 form a complex that promotes microtubule assembly in C. elegans embryos," *Curr. Biol.*, vol. 13, no. 17, pp. 1488–1498, Sep. 2003, doi: 10.1016/S0960-9822(03)00582-7.
[178] S. R. Gandhi *et al.*, "Kinetochore-dependent microtubule rescue ensures their efficient and sustained interactions in early mitosis," *Dev. Cell*, vol. 21, no. 5, pp. 920–933, Nov. 2011, doi: 10.1016/j.devcel.2011.09.006.
[179] R. K. Miller, S. C. Cheng, and M. D. Rose, "Bim1p/Yeb1p mediates the Kar9p-dependent cortical attachment of cytoplasmic microtubules," *Mol. Biol. Cell*, vol. 11, no. 9, pp. 2949–2959, Sep. 2000, doi: 10.1091/mbc.11.9.2949.
[180] J. Gunzelmann *et al.*, "The microtubule polymerase Stu2 promotes oligomerization of the γ-TuSC for cytoplasmic microtubule nucleation," *Elife*, vol. 7, Sep. 2018, doi: 10.7554/eLife.39932.
[181] M. P. Miller *et al.*, "Kinetochore-associated Stu2 promotes chromosome biorientation in vivo," *PLoS Genet.*, vol. 15, no. 10, 2019, doi: 10.1371/journal.pgen.1008423.
[182] M. Greenlee *et al.*, "The TOG protein Stu2/XMAP215 interacts covalently and noncovalently with SUMO," *Cytoskeleton*, vol. 75, no. 7, pp. 290–306, Jul. 2018, doi: 10.1002/cm.21449.
[183] M. Zanic, P. O. Widlund, A. A. Hyman, and J. Howard, "Synergy between XMAP215 and EB1 increases microtubule growth rates to physiological levels," *Nat. Cell Biol.*, vol. 15, no. 6, pp. 688–693, Jun. 2013, doi: 10.1038/ncb2744.

[184] S. P. Maurer, N. I. Cade, G. Bohner, N. Gustafsson, E. Boutant, and T. Surrey, “EB1 accelerates two conformational transitions important for microtubule maturation and dynamics,” *Curr. Biol.*, vol. 24, no. 4, pp. 372–384, 2014, doi: 10.1016/j.cub.2013.12.042.
[185] S. K. Rehen *et al.*, “Constitutional aneuploidy in the normal human brain,” *J. Neurosci.*, vol. 25, no. 9, pp. 2176–2180, Mar. 2005, doi: 10.1523/JNEUROSCI.4560-04.2005.
[186] S. K. Rehen, M. J. McConnell, D. Kaushal, M. A. Kingsbury, A. H. Yang, and J. Chun, “Chromosomal variation in neurons of the developing and adult mammalian nervous system,” *Proc. Natl. Acad. Sci. U. S. A.*, vol. 98, no. 23, pp. 13361–13366, Nov. 2001, doi: 10.1073/pnas.231487398.
[187] D. Chretien and R. H. Wade, “New data on the microtubule surface lattice,” *Biol Cell*, vol. 71, pp. 161–174, 1991.

VITA

EDUCATION

Doctor of Philosophy in Biochemistry (June 2020). University of Washington. Seattle, WA.

Bachelor of Science in Biology, with minor in Chemistry, magna cum laude (May 2014). Truman State University. Kirksville, MO.

Valedictorian (May 2010). Trenton Senior High School. Trenton, MO.

RESEARCH EXPERIENCE

Thesis work. Davis lab, Department of Biochemistry, University of Washington, Seattle, WA. 2014-present. Established collaborations and directed their research in relation to my project. Led an independent research project by mastering laboratory techniques, especially: 1) Genetically engineering yeast strains and performing live cell imaging using fluorescent microscopy, 2) Designing mutant protein constructs and expressing them in bacteria and insect tissue culture for use in biochemical assays, 3) Purifying proteins using FPLC (fast protein liquid chromatography), and 4) Developing a bulk assay measuring polymer assembly using spectrophotometry.

Internship research. Jensen lab, Huntsman Cancer Institute, Salt Lake City, UT. June 2013-September 2013. Investigated novel drug delivery for malignant glioma treatment in rats, specifically 1) Performing immunohistochemical staining of rat brain slices, and 2) Injecting tumor cells into rat brains and carrying out subsequent treatment injections

PUBLICATIONS

- **King BR**, Moritz M, Kim H, Agard DA, Asbury, CL, Davis TN. “XMAP215 and g-tubulin function additively in purified solutions.” Manuscript submitted.
- Gillespie DL, Aguirre MT, Ravichandran S, Leishman LL, Berrondo C, Gamboa JT, Wang L, **King R**, Wang X, Tan M, Malamas A, Lu ZR, Jensen RL. “RNA interference targeting hypoxia-inducible factor 1α via a novel multifunctional surfactant attenuates glioma growth in an intracranial mouse model.” *Journal of Neurosurgery.* 2015 February.

AWARDS

Cellular and Molecular Biology Training Grant 2016-2018.

National Science Foundation Graduate Research Fellowship Honorable Mention 2015.

General John J. Pershing Scholarship 2010-2014.